Evaluation of Seismicity Relevant to the Proposed Siting of a Superconducting Supercollider (SSC) in Tooele County, Utah

by
W.J. Arabasz, J.C. Pechmann, and E.D. Brown
University of Utah Seismograph Stations

JANUARY 1989

Utah Geological and Mineral Survey
Miscellaneous Publication 89-1

EVALUATION OF SEISMICITY RELEVANT TO THE PROPOSED SITING OF A SUPERCONDUCTING SUPERCOLLIDER (SSC) IN TOOELE COUNTY, UTAH

by

W.J. Arabasz, J.C. Pechmann, and E.D. Brown
University of Utah Seismograph Stations
Department of Geology and Geophysics
University of Utah
Salt Lake City, Utah 84112

Technical Report to

the
DAMES & MOORE
UTAH SSC PROPOSAL TEAM
Salt Lake City, Utah

Contract Monitors

Larry T. Murdock and Eric J. McHuron

Principal Investigator: Walter J. Arabasz
Award Period: May 15-June 15, 1987

June 1987

(Revised August 1987)

Disclaimer

The views and conclusions in this document are those of the authors and should not be interpreted as representing the official policies, either expressed or implied, of the state of Utah.

SUMMARY

This report presents (1) a characterization of seismicity within 160 km (100 miles) of two alternative sites proposed for a Superconducting Supercollider (SSC) facility in Tooele County, Utah; and (2) an evaluation of implications for earthquake-induced ground motions and other seismic hazards at the proposed sites. The candidate sites lie on the western periphery of the northerly-trending Intermountain seismic belt and are marginal to areas of primary concern for seismic hazards in Utah. The site locations are 75 km or more west of the Wasatch fault and within a domain of continuing Basin-Range extension characterized by (1) a low rate of seismicity, and (2) late Quaternary surface faulting with recurrence intervals for individual faults probably exceeding ten thousand years.

Two types of seismic source zones have the potential of producing damaging ground motions at the sites. These include background seismicity below the threshold of surface faulting of magnitude 6.0-6.5, and larger surface-faulting earthquakes of up to magnitude 7.5±0.2 on major mapped faults within 100 km. Within a circle of 50-km radius around the center of each proposed site, we estimate an average return period of 45 years for earthquakes of magnitude (M_L) 4.0 or greater and 200 years for earthquakes of M_L 5.0 and greater. Only one earthquake of $M_L \geq 4.0$ is known to have occurred in either of these circular areas since 1850--an earthquake of estimated magnitude 4-5 in 1915.

Probabilistic estimates of earthquake ground-shaking hazard made by Algermissen et al. (1982) indicate that, for a point in the general location of the proposed sites, a peak horizontal acceleration of 0.1-0.2 g has a 90% probability of nonexceedance over a 50-year time period. For this study, we performed some preliminary site-specific calculations of the ground-shaking hazard using newly-developed information on seismic source zones, seismicity parameters, and attenuation. Our preferred estimate for the peak horizontal acceleration with a 90% probability of nonexceedance in 50 years along a ring of radius 13 km (the average radius of the proposed SSC alignment) is 0.14 g. This acceleration value is sensitive to the functional relationship used to predict peak horizontal acceleration as a function of magnitude and distance. Our calculations are preliminary, but they do take into account the large size of the proposed SSC ring, which causes probabilistic estimates of ground-shaking hazard for this facility to differ from estimates of hazard at a point.

CONTENTS

1. INTRODUCTION

1.1 Background

In April 1987, seismologists at the University of Utah were contacted by the "Utah SSC Proposal Team" regarding the characterization of seismicity relevant to the proposed siting of a Superconducting Supercollider (SSC) in Utah. The University of Utah operates a regional center for the recording and analysis of seismic activity in Utah and surrounding parts of the Intermountain region—and it has an expert earthquake research group.

In order to meet the needs of the state of Utah's proposal team for up-to-date and comprehensive earthquake information required for site characterization, a contractual arrangement was made for preparation of this technical report by the University of Utah Seismograph Stations.

1.2 Purpose and Scope of This Report

Specifications outlined by the U.S. Department of Energy for proposed SSC sites, under the heading "Seismicity and Faulting" (RFP section 2.2.3.1.4.), require a characterization of site seismicity, an estimate of site-specific maximum ground acceleration, and the identification of active faults in the site vicinity.

The basic purpose of this report is to present: (1) an accurate characterization of seismicity in the region surrounding two alternative sites proposed for an SSC facility in the desert region of Tooele County, Utah (see Figure 1.1); and (2) an expert evaluation of existing information having any implications for earthquake-induced ground motions or other seismic hazards at the proposed SSC sites.

This report is intended to provide the "Utah SSC Proposal Team" with parts—but not all—of the basic information required to complete the site characterization of "Seismicity and Faulting." Its primary focus is on seismicity and potential earthquake ground motion. The identification and evaluation of active faults in the immediate site vicinity was *not* included as a task given to the authors of this report. That investigative task is being handled separately by geologists of Dames & Moore, Salt Lake City. Nevertheless, discussion of active faulting based primarily on published sources is included in this effort as part of an evaluation of the seismotectonics of the region surrounding the proposed SSC sites and as part of an evaluation of potential seismic sources.

Specific tasks given to the authors of this report by the "Utah SSC Proposal Team" included the following:

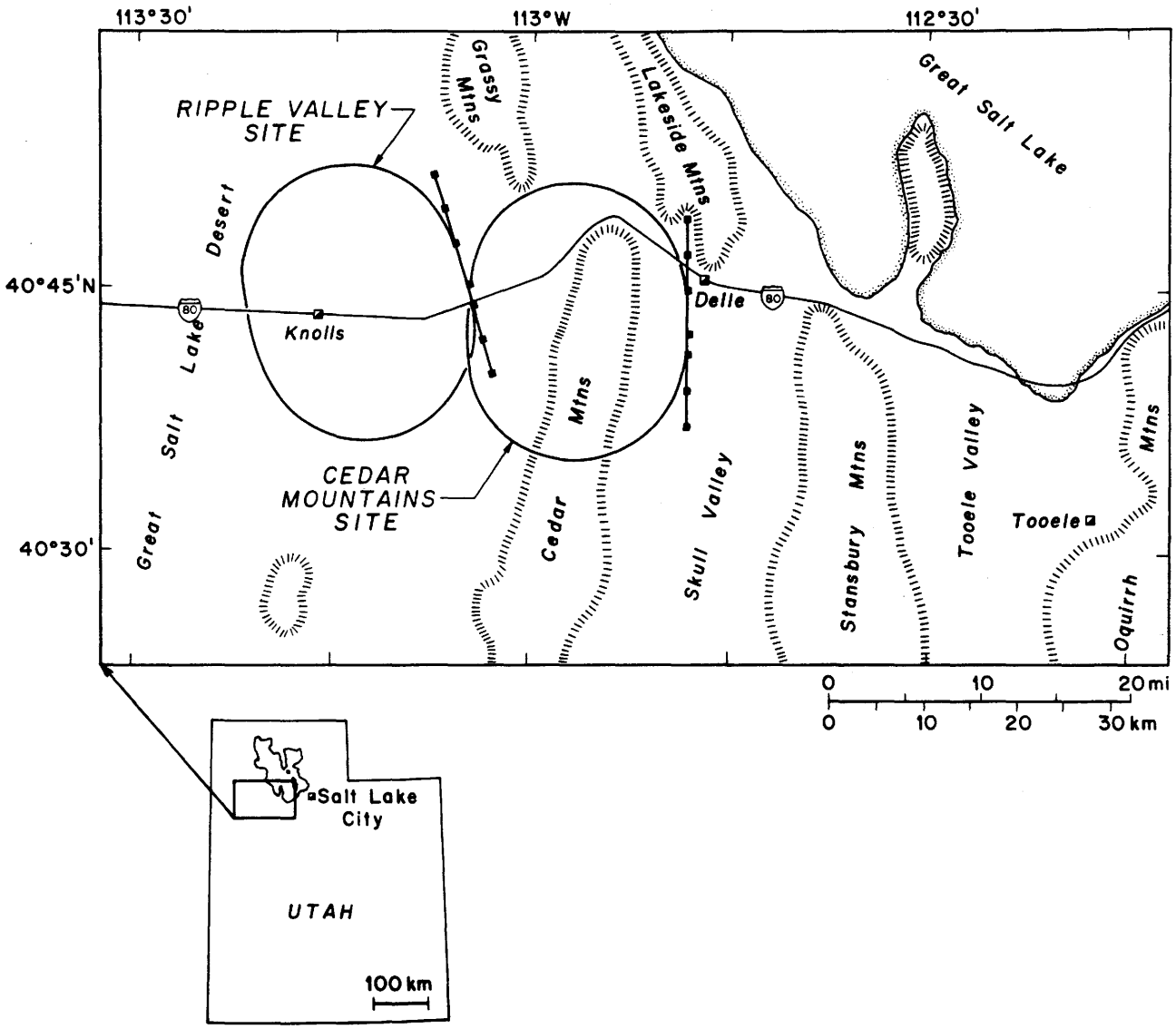

Figure 1.1 Location map of the alternative Ripple Valley and Cedar Mountains candidate sites for the proposed siting of a Superconducting Supercollider (SSC) in western Utah.

(a) General description of the regional seismotectonic framework relevant to proposed SSC alignments in Ripple Valley and at the northern end of the Cedar Mountains (Figure 1.1).

(b) Compilation of historical and instrumental seismicity above magnitude 3 within 160 km of the two SSC alignments, and of microseismicity within 60 km of the two alignments.

(c) Special investigation of seismic events included in the earthquake compilation, and located in the near vicinity of the proposed SSC sites, for discrimination of artificial events (e.g., events attributable to local blasting rather than genuine earthquake activity).

(d) Evaluation and interpretation of historical/instrumental seismicity relevant to the SSC candidate sites—including all seismicity in the near vicinity of the two alignments and sources of moderate-to-large earthquakes at greater distance that could have significant effects at the alignments. (This includes estimation of the maximum credible events at these sources and the probability of such events occurring.)

(e) Identification and description of earthquake-related hazards that might represent adverse risk factors for the proposed SSC facilities.

The remaining sections of this report have been structured to present results systematically keyed to the tasks outlined above. Section 2, "Regional Seismotectonic Framework" addresses task (a). Section 3, "Historical and Instrumental Earthquake Record," presents the results of task (b); subsection 3.3 ("Blast Discrimination") describes the special discrimination of artificial seismic events required for task (c). Section 4, "Evaluation and Interpretation of Historical/Instrumental Seismicity," addresses task (d). Finally, the results of task (e) are discussed in section 4, "Considerations of Earthquake Hazards at the Proposed SSC Sites in Tooele County."

1.3 Acknowledgments

Several individuals provided information and perspective that was extremely helpful in preparing this report. We thank D. Veneziano of the Massachusetts Institute of Technology; T.P. Barnhard and R.C. Bucknam of the U.S. Geological Survey, Golden, Colorado; R.B. Smith of the University of Utah; R.R. Youngs of Geomatrix Consultants, Inc., San Francisco; and R.A. Martin of the U.S. Bureau of Reclamation, Denver, Colorado. The authors assume full responsibility for any errors in interpretation or application.

We thank R. Foott and E. McHuron, Roger Foott Associates, Inc., San Francisco, and L.T. Murdock, Dames & Moore, Salt Lake City, for facilitation of this work. Also, we thank J.A. Barlow, L.B. Burnett, and J.E. Shemeta for substantial help in the report preparation.

2. REGIONAL SEISMOTECTONIC FRAMEWORK

2.1 General Setting of the Proposed SSC Sites

The candidate sites proposed for an SSC facility in western Utah lie near the eastern margin of the Basin and Range province (see Figure 2.1), a region of alluviated valleys and northerly-trending mountain blocks reflecting broad extensional deformation during mid to late Cenozoic time. G.K. Gilbert (1875, 1928) was among the first to recognize that most of these mountain ranges are bounded by normal fault zones and that the topography of the Basin and Range Province is the result of episodic movements on these fault zones that continues to the present. The physiographic boundary between the Basin and Range province and the Middle Rocky Mountains lies about 75 km to the east of the SSC sites and coincides with the Wasatch fault. The latter is a 370-km-long active normal-fault zone along which young mountain blocks have been uplifted to form a prominent west-facing topographic escarpment—the "Wasatch Front"—from central Utah to just north of the Utah-Idaho border.

The eastern margin of the the Basin and Range province roughly follows a northerly-trending zone of crustal weakness and differential movement that has been persistent from late Precambrian time to the present—the so-called "Wasatch Line" (Stokes, 1986). In late Quaternary and modern time, crustal deformation along this zone has been notably reflected by recurrent surface faulting and uplift along the Wasatch fault and by seismic strain release (e.g., see Figure 2.3).

Seismotectonic deformation affects a broad region along the eastern margin of the Basin and Range province, but the locus of relatively higher deformation qualitatively lies within the eastern half of the domain of seismic zone 3 of the Uniform Building Code (UBC) shown in Figure 2.1. Both the Ripple Valley and the Cedar Mountains candidate sites lie within UBC seismic zone 3. In subsequent sections of this report, we quantify the seismic characterization of the candidate SSC sites, but a consistent theme is that—despite their location within UBC seismic zone 3—the sites are marginal to, and on the west of, areas of primary concern for seismic hazards in Utah's main seismic belt.

2.2 Intermountain Seismic Belt (ISB)

2.2.1 General Remarks

Figure 2.2 shows the location of the candidate SSC sites with respect to the Intermountain seismic belt (ISB)—an extensive zone of intraplate deformation within the western United States—as depicted by Arabasz and Smith (1981) on the basis of various seismotectonic studies. It should be emphasized that the western boundary of the ISB in the vicinity of the SSC sites is not well defined. We return to this point in section 4 after presenting detailed information on seismicity and active faulting in the vicinity of the proposed sites.

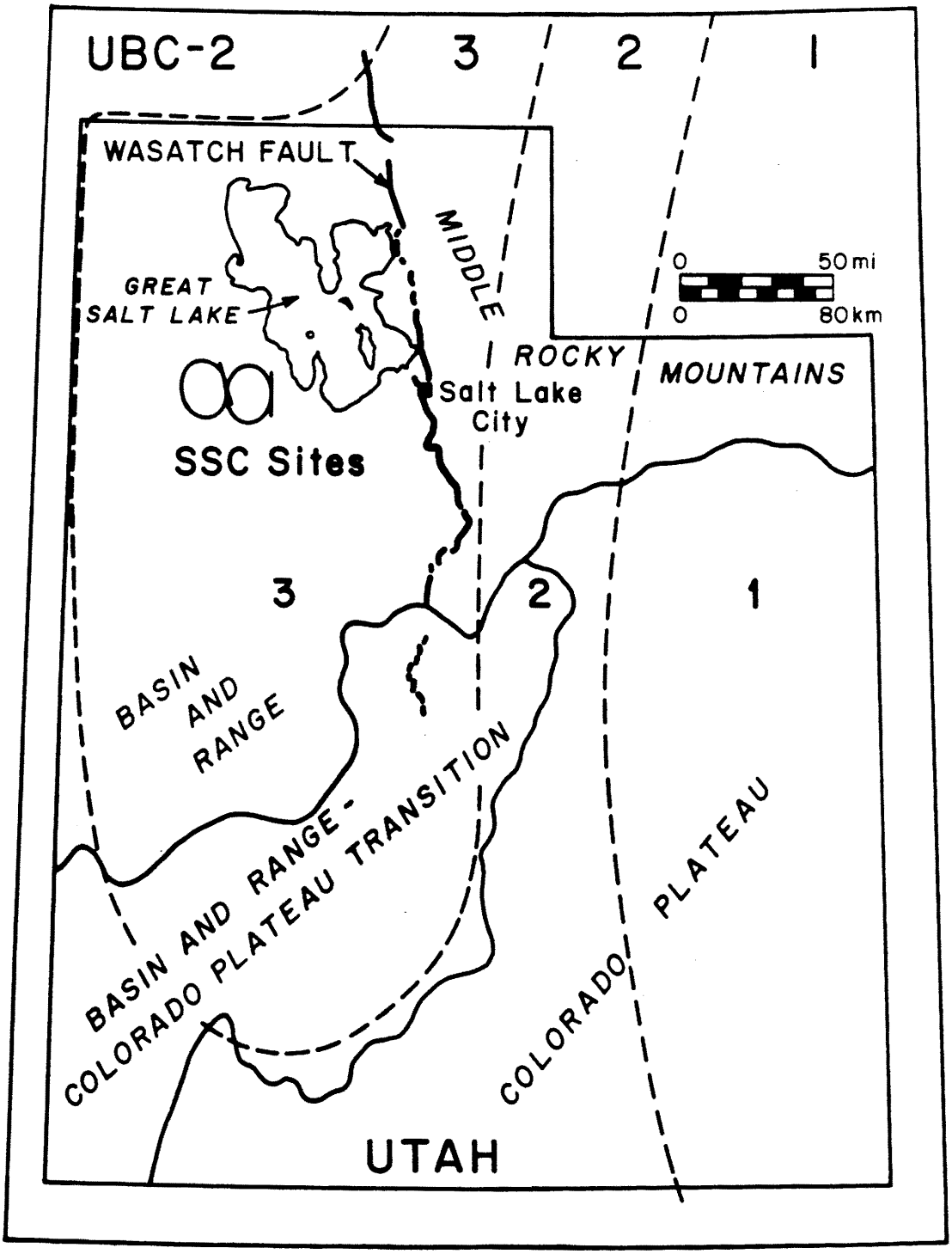

Figure 2.1 Map of the Utah region showing proposed SSC sites with respect to the Wasatch fault, physiographic provinces of Utah (after Stokes, 1977), and seismic zones of the 1985 edition of the Uniform Building Code (UBC).

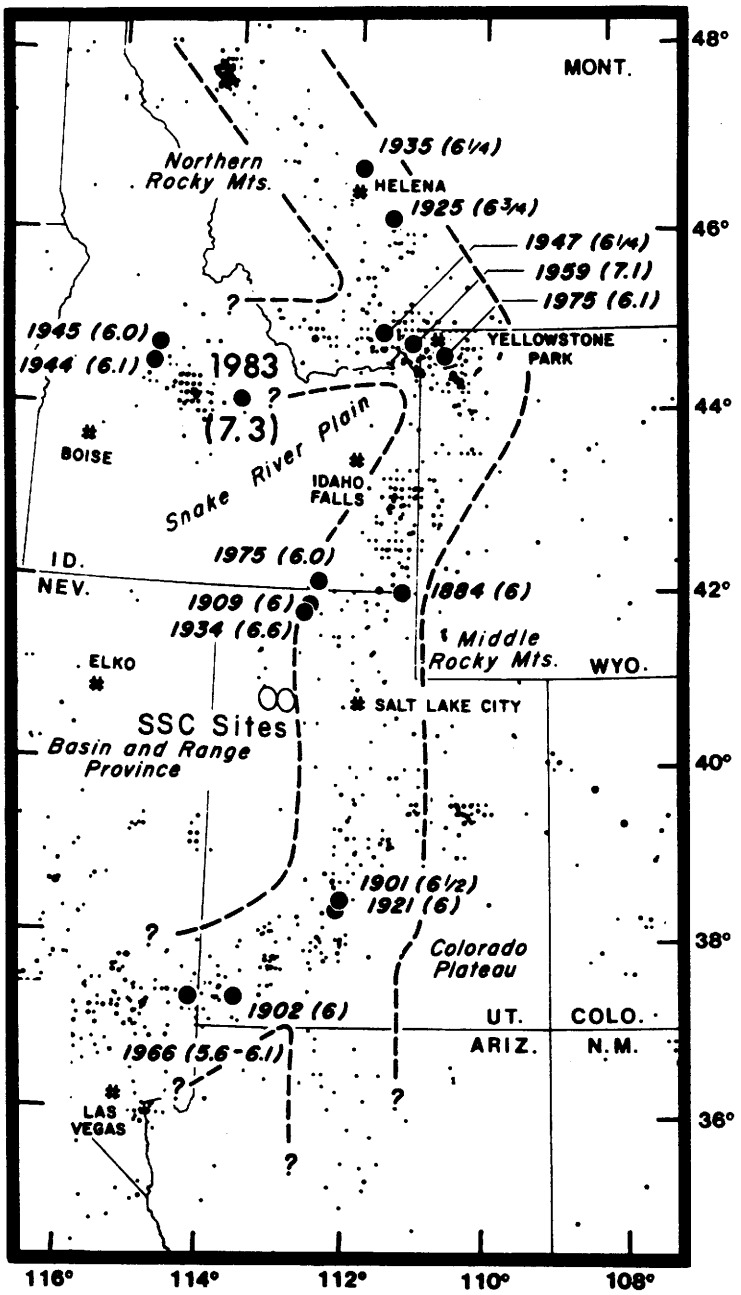

Figure 2.2 Map of the Intermountain seismic belt from Arabasz and Smith (1981) showing location of proposed SSC sites with respect to NOAA epicenters for the period 1950-1976 (small dots) and historic earthquakes of magnitude 6.0 and greater (large dots). The epicenter of the M_S 7.3 Borah Peak, Idaho, earthquake of 1983 has been added. Magnitude of the 1959 Hebgen Lake, Montana, earthquake is now estimated as M_S 7.5 (Abe, 1981).

The ISB is a coherent belt of earthquake activity extending more than 1,300 km from southern Nevada and northern Arizona to northwestern Montana (see Smith and Sbar, 1974; Smith, 1978; Stickney and Bartholomew, 1987). In general, the ISB is characterized by late Quaternary normal faulting, diffuse shallow seismicity (focal depths < 15-20 km), and episodic scarp-forming earthquakes (M~6.5-7.7) associated with the complex interaction of subplates within the western North American plate (e.g., Smith and Sbar, 1974; Smith, 1978). The ISB follows the boundary between relatively thin crust and lithosphere of the Basin and Range province and thicker more stable crust and lithosphere of the Middle Rocky Mountain and Colorado Plateau provinces. Crustal thickness beneath the candidate SSC sites is approximately 30±5 km.

Since 1850, at least 16 independent earthquakes (aftershocks excluded) of magnitude 6.0 or greater have occurred within the ISB. Their locations and sizes are shown in Figure 2.2. Three of these historical earthquakes were associated with documented surface faulting. Normal fault scarps with maximum surface displacements of 5.5±0.3 m, 0.5 m, and 2.7 m, respectively, were produced by the M_S7.5 Hebgen Lake, Montana, earthquake of August 1959 (Bonilla et al., 1984;), the M_S6.6 Hansel Valley, Utah, earthquake of March 1934 (Shenon, 1936;), and the M_S7.3 Borah Peak, Idaho, earthquake of October 1983 (Crone et. al., 1987). Other large historical normal-faulting earthquakes have occurred in the western part of the Basin and Range province in Nevada and California (Slemmons, 1980; Ryall and Van Wormer, 1980; Richter, 1958).

Figure 2.3 shows the location of the proposed SSC sites with respect to the distribution of all historical main shocks of estimated Richter magnitude 4.0 or greater (or maximum Modified Mercalli intensity V or greater) in the Utah region. The historical sample includes at least fifteen independent main shocks that have had an estimated Richter magnitude of 5.5 or greater (or a Modified Mercalli intensity of VII or greater). These earthquakes are listed in Table 2.1 and their epicenters are shown as solid circles in Figure 2.3. Figure 2.3 illustrates the marginal location of the SSC sites with respect to the main belt of historical seismicity. Also, it illustrates that the Wasatch fault is but one break, albeit the longest and most prominent, within a broad zone of deformation. We elaborate in sections 3 and 4 on the seismicity and active faulting surrounding the proposed SSC sites.

2.2.2 Characteristics of the ISB within the Utah Region

Arabasz et al. (1980; see also Arabasz, 1984, and Arabasz and Julander, 1986) and Zoback (1983) have published detailed descriptions of the seismicity and Cenozoic tectonics, respectively, of the Wasatch Front area of north-central Utah encompassing the locations of the candidate SSC sites. Also, Smith (1978), Arabasz and Smith (1981), and Smith and Bruhn (1984) discuss key aspects of the regional seismotectonics of the ISB.

The ISB within the Utah region is notably characterized by: (1) a general predominance of normal faulting, reflecting an extensional stress regime; (2) moderate background seismicity, which is lower by a factor of 4 to 6 than that along the western North American plate boundary (see Arabasz and Smith , 1981); (3) diffuse seismicity having weak correlation with major

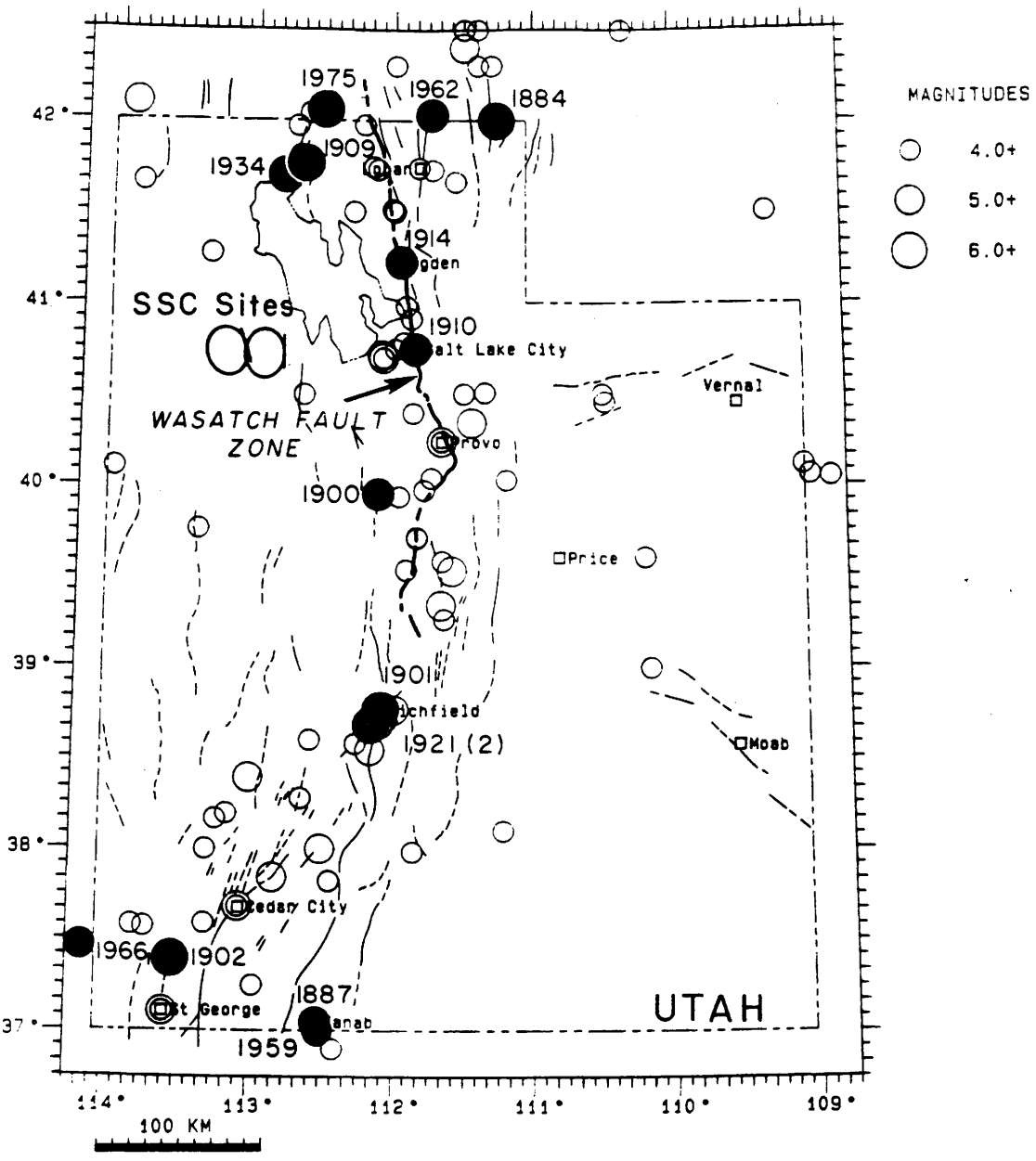

Figure 2.3 Epicenter map of the Utah region showing all independent mainshocks of M_L 4.0 or greater (or Intensity V or greater), 1850-1986. Earthquakes of estimated M_L 5.5 or greater specially labeled. Data from University of Utah Seismograph Stations. Proposed SSC sites shown for reference. Base map of young faults (from Arabasz et al., 1979) is superseded by the compilation of this study, shown in Figure 2.5.

Table 2.1 Largest Earthquakes in the Utah Region

1850 through June 1987[1]
(modified from Arabasz et al., 1979)

Local Date	*Lat(°N)*	*Long(°W)*	*Location*	Intensity *(MM)*	Magnitude *(M_L)*	Moment[3] *($x10^{24}$ dyne-cm)*
1884 Nov 10	42.0	111.3	Bear Lake Valley	8	(6)	
1887 Dec 05	37.1	112.5	Kanab	7	(5½)	
1900 Aug 01	40.0	112.1	Eureka	7	(5½)	
1901 Nov 13	38.8	112.1	Richfield	9	(6½+)	
1902 Nov 17	37.4	113.5	Pine Valley	8	(6)	
1909 Oct 05	41.8	112.7	Hansel Valley	8	(6)	
1910 May 22	40.8	111.9	Salt Lake City	7	(5½)	
1914 May 13	41.2	112.0	Ogden	7	(5½)	
1921 Sep 29	38.7	112.2	Elsinore	8	(6)	
1921 Oct 01	38.7	112.2	Elsinore	8	(6)	
1934 Mar 12	41.7	112.8	Hansel Valley	9	6.6[2]	77.0
1959 Jul 21	37.0	112.5	Utah-Arizona border	6	5.5+	
1962 Aug 30	42.04	111.74	Cache Valley	7	5.7	7.0
1966 Aug 16	37.46	114.15	Nevada-Utah border	6	5.6	1.1
1975 Mar 27	42.10	112.52	Pocatello Valley	8	6.0	18.6

---

[1]Table includes earthquakes of maximum Modified Mercalli intensity of VII or greater, or of Richter magnitude 5.5 or greater. Magnitudes in parentheses are estimated from intensity. Sample area: 36°45'N - 42°30'N, 108°45'W - 114°15'W. Aftershocks excluded.

[2]Richter (1935, p. 24) estimated an M_L value of 7.0. The value of 6.6 comes from Gutenberg and Richter (1954) and appears to be a surface-wave magnitude.

[3]Doser and Smith (1982).

active faults, and with focal depths almost exclusively shallower than 15-20 km; (4) relatively long (1,000 yrs or more) average recurrence intervals for surface faulting on individual faults or fault segments (e.g., Schwartz and Coppersmith, 1984); (5) the historical absence of any surface-faulting earthquake larger than the M_S6.6 Hansel Valley earthquake of 1934—despite abundant late Quaternary and Holocene fault scarps; and (6) relatively low rates of crustal strain (~2 x 10^{-16} sec^{-1}; Eddington et al., 1987).

2.3 Late Quaternary and Historical Surface Faulting in the ISB and Basin and Range Province

2.3.1 General Pattern of Late Quaternary Faulting

It is well accepted that the historical earthquake record provides an inadequate guide to assessing seismic potential in the western United States—and indeed in most seismically active regions of the world—and that information from late Quaternary faulting is essential to consider (e.g., Allen, 1974, 1986; Wallace, 1981). In section 4 we will consider in detail the distribution of late Quaternary faults in the vicinity of the proposed SSC sites. Here we give a general perspective.

Figure 2.4a from Bucknam et al. (1980) and reproduced from Wallace (1981) gives an overview of young faulting in western Utah based on fault scarp data. The Wasatch fault zone, with abundant evidence of recurrent surface faulting during Holocene time (the last 10,000 years) dominates the neotectonics of the area. There is clear evidence of surface faulting during late Quaternary time (approximately the last 500,000 years; Wallace, 1981) throughout parts of the Basin and Range province to the west of the Wasatch fault. However, there appear to be domains in which there is evidence of late Quaternary but no Holocene faulting, and significantly large areas of the Basin and Range province in which late Quaternary faulting is absent. Eastern Nevada and parts of western Utah are thus characterized (Figure 2.4a,b; see also Howard et al., 1978).

The location of the proposed SSC sites superposed on Figure 2.4a suggests that the sites lie within a domain where some Holocene faulting has occurred. We examine this point in more detail in section 4.2.2. It should be emphasized that the map of Figure 2.4a was not intended to show all active or potentially active faults (Bucknam et al., 1980). According to R.C. Bucknam (personal communication, 1987), many of the fault traces shown on that map represent single-event scarps, and, in his judgment, there is no reason to believe that other range-front faults could not produce surface-faulting earthquakes in the future. Implicitly, the recurrence interval for such faulting on an individual fault or fault segment would exceed several thousand years and could be much longer.

There currently exists no definitive map of known and suspected active faults in the Utah region, so efforts were made to compile a base map of late Quaternary faulting for a regional study area extending 160 km (100 miles) from the candidate SSC sites. The resulting map shown in Figure 2.5, which relies chiefly on published sources, includes the traces of fault displacements of Holocene (less than 10,000 yrs B.P.) and late Pleistocene (10,000 to about

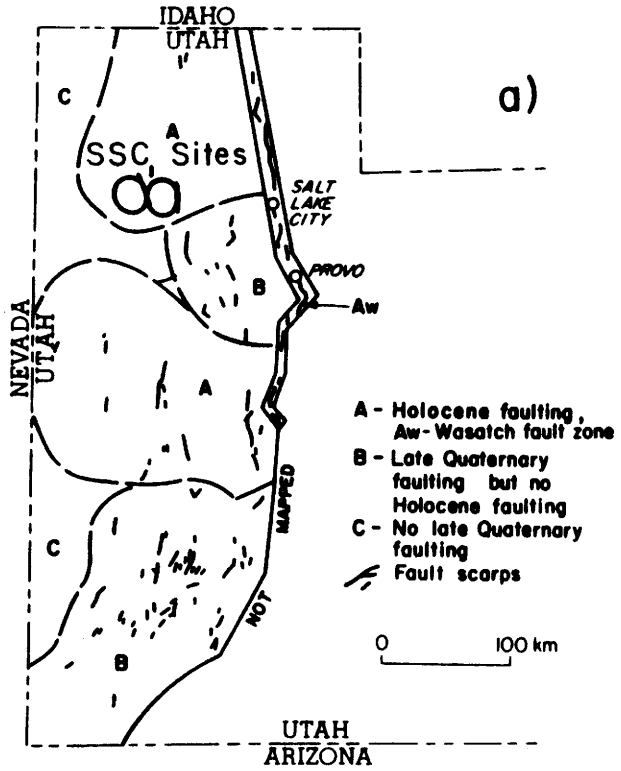

Map of western Utah showing zones of various histories of faulting based on fault scarp data (from Bucknam and others, 1980).

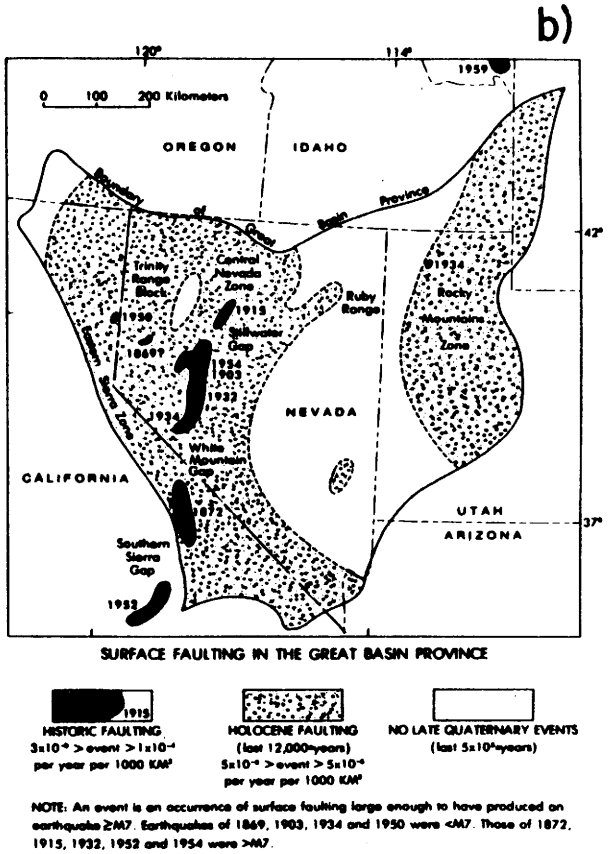

Map of the Great Basin province showing zones of various rates of surface faulting based primarily on fault scarp data. See figure 4 for subdivisions derived for western Utah.

Figure 2.4 Overview of young faulting in the Basin and Range province (from Wallace, 1981).

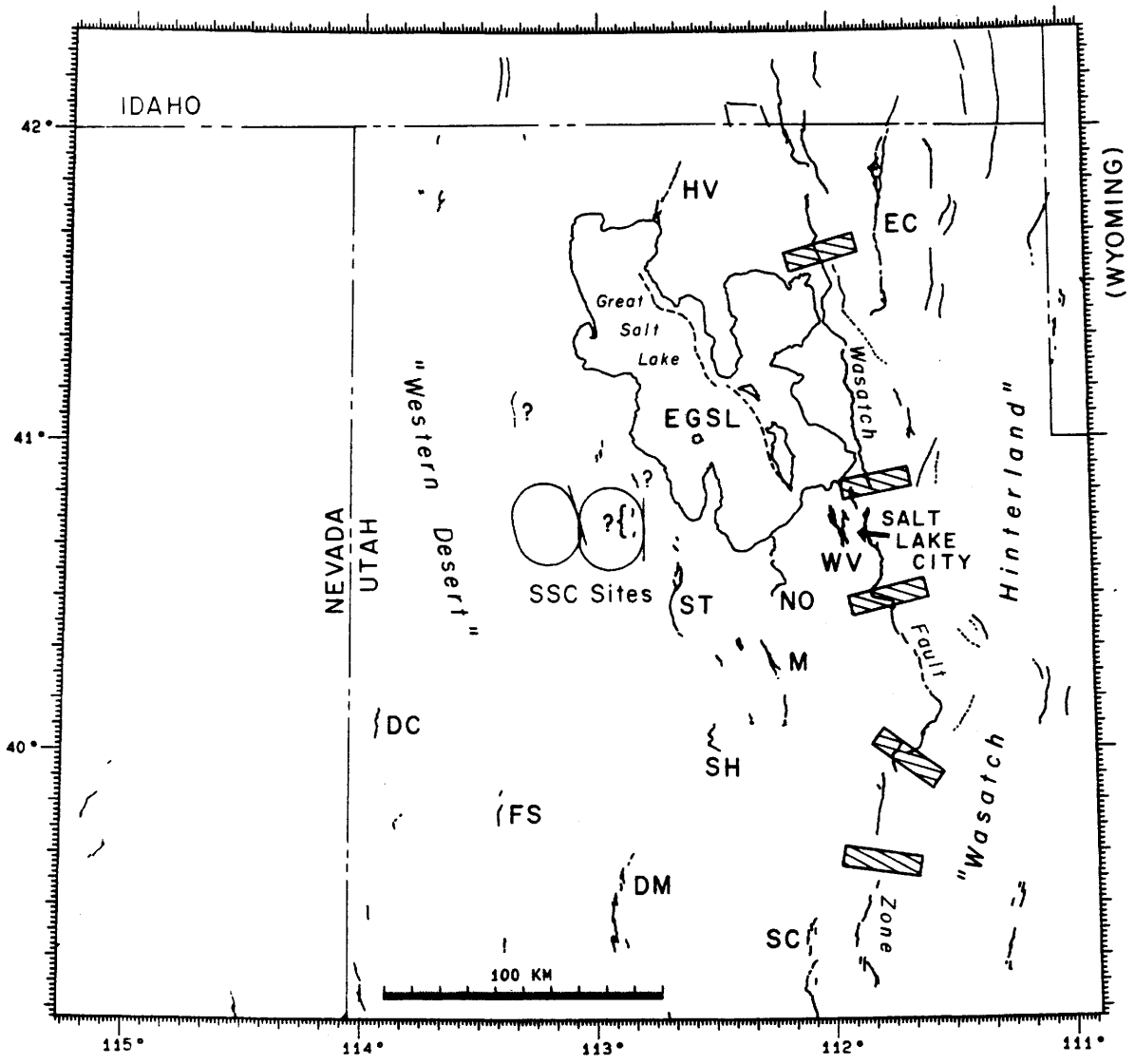

Figure 2.5 Map of late Quaternary faulting within the regional area surrounding the SSC candidate sites. Queries indicate suspected faulting. Hachured boxes delimit major segments of the Wasatch fault zone interpreted by Schwartz and Coppersmith (1984). Specific faults within 100 km of the SSC sites are identified and described in Figure 4.2 and Table 4.1. For general orientation, the following faults are labeled: DC, Deep Creek Mts.; DM, Drum Mts.; EC, East Cache; EGSL, East Great Salt Lake; FS, Fish Springs; HV, Hansel Valley; M, Mercur; NO, Northern Oquirrh; SC, Scipio; SH, Sheeprock Mts.; ST, Stansbury Mts.; WV, West Valley.

500,000 yrs B.P.) age. We proceed to describe the map compilation in general terms and then provide more detailed information in section 4.2.2 on specific faults located within 100 km of the perimeter of the candidate SSC sites.

The following sources were used to compile the digitized base map of Figure 2.5: The trace of the Wasatch fault is based chiefly on detailed mapping done by Cluff et al. (1970, 1973, 1974) and was taken, in part, from subsequent compilations by Davis (1983a,b; 1985). Depiction of the West Valley fault zone near Salt Lake City is from unpublished mapping by S.J. Olig and J. Keaton of Dames and Moore (personal communication, 1987). Faulting to the east of the Wasatch fault throughout the "Wasatch Hinterland" in Utah is from detailed maps of Sullivan et al. (1986) and Foley et al. (1986); that in Wyoming, from Gibbons and Dickey (1983). The trace of the East Great Salt Lake fault, lying within the bounds of the Great Salt Lake, was taken from Cook et al. (1980) and Viveiros (1986). Between 112°W and 114°W, we relied heavily on maps of fault scarps in unconsolidated sediments published by Bucknam (1977) and Bucknam and Anderson (1979b). West of 114°W, the small-scale map of Howard et al. (1978) supports Wallace's (1981) generalization of the absence of late Quaternary faulting in easternmost Nevada (Figure 2.4b). However, a few fault traces shown in Nevada west of 114°W in the southwestern corner of the map are estimated to be of late Pleistocene, post-Bonneville (less than 15,000 yrs B.P.) age (B.A. Schell, 1982, personal communication to R.B. Smith). Faulting identified by Anderson and Miller (1979) and not mapped by others in the "Western Desert" region of Utah was added for completeness. Finally, faulting to the north of 42°N in Idaho, other than the northern extension of the Wasatch fault, was taken from Witkind (1975).

There is some inhomogeneity in Figure 2.5 in that some of the fault traces to the west of the Wasatch fault within the Basin and Range province reflect only the extent of mapped fault scarps in unconsolidated deposits and not necessarily the entire length of a seismogenic range-front fault. The primary sources from which the map compilation was made warn of possible incompleteness in recognizing late Quaternary faulting in the "Western Desert" region of Figure 2.5. Fluctuation of ancient Lake Bonneville, especially between about 25,000 yrs and 13,000 yrs ago (Currey et al., 1984), could have obliterated evidence of late Quaternary surface faulting in many places.

2.3.2 Wasatch and East Great Salt Lake Fault Zones

Two first-order faults that form part of the seismotectonic framework of the region surrounding the SSC sites (Figure 2.5) are the Wasatch fault zone and the East Great Salt Lake fault. Here we briefly summarize their characteristics.

The Wasatch fault is by far the best-studied fault depicted in Figure 2.5. Data from 5 trenches across the fault summarized by Schwartz and Coppersmith (1984) and Schwartz et al. (1984) indicate late Quaternary slip rates of about 1 mm/yr and vertical displacements during prehistoric earthquakes of 1.6-2.7 meters, with an average displacement per event of about 2 m. Average recurrence intervals determined at four trenching sites along the central part of the fault between about 39°25'N and 41°00'N range from 1,700 to 3,000 years.

Although the total length of the Wasatch fault is 370 km, only a fraction of its total fault length is expected to break during a single earthquake, judging from the rupture lengths of historical normal faulting earthquakes in the western United States summarized below in sections 2.3.3 and 2.3.4. Schwartz and Coppersmith (1984) proposed that the Wasatch fault is divided up into 6 major segments (Figure 2.5) which break in separate earthquakes, and which range in length from 35 km (the Salt Lake City and Nephi segments) to 70 km (the Ogden segment). On the basis of this segmentation model, they calculated a preferred recurrence interval for the entire fault zone of 444 years. In other words, they estimate that a large earthquake would be expected to occur somewhere along the fault on the average of once every 444 years. More recently, Machette et al. (1986) have suggested that some of the segments of Schwartz and Coppersmth (1984) are subdivided into smaller segments, to give a total of ten fault segments ranging in length from 14 to 57 km. If there are, in fact, ten segments, then it is not possible to accurately determine recurrence intervals for the entire fault zone without information from additional trenching. Youngs et al. (1987) estimate a return period for magnitude 7.0 or greater events of 330±90 years, depending on the number of segments and other uncertainties.

A second major fault zone shown in Figure 2.5 is one beneath the Great Salt Lake. This fault zone, named the East Great Salt Lake fault zone by Cook et al. (1980), can be clearly seen in seismic reflection profiles across the lake (Mikulich and Smith, 1974; Smith and Bruhn, 1984; Viveiros, 1986). Considering the block-faulted nature of the Basin and Range province and the fact that the Promontory Mountains, Fremont Island, and Antelope Island form a NNW-trending linear topographic high, the presence of a fault zone along the western side of this topographic high is not particularly surprising. Reflection data and well data indicate that the sedimentary basin underlying the lake deepens towards the east where it is bounded by the East Great Salt Lake fault. The deepest part of the basin contains more than 10,000 feet (3,048 m) of post-Miocene sedimentary rocks (Mikulich and Smith, 1974; Viveiros, 1986), indicating major subsidence during the past 25 million years.

The East Great Salt Lake fault cuts sediments identified as Quaternary on the basis of well data (Mikulich and Smith, 1974; Viveiros, 1986) and must be considered active. Seismic reflection data (Mikulich and Smith, 1974; Viveiros 1986) indicate that the East Great Salt Lake fault appears to offset sediments to within at least 0.015-0.025 sec two-way travel time beneath the lake bottom, corresponding to an approximate depth of less than 14-23 m , which implies that slip has occurred in the recent geologic past.

Viveiros (1986, p. 72) estimated fault slip rates on the East Great Salt Lake fault of 0.96 mm/yr during the Pliocene and 1.48 mm/yr during the Quaternary from the thicknesses of sedimentary deposits—dependent upon an interpreted geometry of faulting. Pechmann (1987) interpreted fault slip rates of about 0.4 mm/yr during the Pliocene and 0.5 mm/yr during the Quaternary from a true-scale cross section constructed by Viveiros (1986). These slip rates are about half the recent slip rates along the Wasatch fault.

2.3.3 The 1959 Hebgen Lake and 1983 Borah Peak Earthquakes

As noted in section 2.2.1, the only historical earthquake in the Utah region known to have produced surface faulting occurred on March 12, 1934, in Hansel Valley just north of the Great Salt Lake (Figure 2.3). This earthquake was assigned a magnitude of 6.6 by Gutenberg and Richter (1954), and is the largest earthquake to have occurred in the Utah region since 1850 (Arabasz et al., 1979). Because earthquakes with surface displacements much larger than the Hansel Valley event (0.5 m) are expected to occur in Utah in the future based on geologic evidence, we must rely upon information from large surface faulting earthquakes elsewhere in the Intermountain seismic belt and in the Basin and Range province to predict their magnitudes and other characteristics.

In the Intermountain seismic belt, there have been two large, historic normal faulting earthquakes over magnitude 7.0, both of which produced surface rupture: the October 28, 1983, M_S7.3 (NEIS determination) Borah Peak earthquake in central Idaho, and the August 18, 1959, (GMT), M_S7.5 Hebgen Lake earthquake in southern Montana (Figure 2.2). These two earthquakes are generally considered to be good models for future large earthquakes on the Wasatch fault and other major faults in Utah (Smith and Richins, 1984; Doser, 1985a). The surface wave magnitude (M_S) of 7.5 for the Hebgen Lake event is from Abe (1981), and is probably more accurate than the magnitude of 7.1 given in Figure 2.2, which is attributed by Murphy and Brazee (1964) to Pasadena. The Hebgen Lake earthquake was accompanied by 35 km of surface faulting along the Red Canyon and Hebgen faults with vertical displacements of up to 5.5±0.3 m (Bonilla et al., 1984; Witkind, 1964) and an average displacement of 2.1 m (Hall and Sablock, 1985). The Borah Peak earthquake produced 36 km of surface faulting along the Lost River and Arentson Gulch faults with vertical displacements of up to 2.7 m and an average displacement of 0.8 m (Crone and Machette, 1984; Crone et al., 1987). Both earthquakes nucleated at depths of about 15-16 km and ruptured upward along faults dipping at 45°-60° (Doser, 1985a, b; Doser and Smith, 1985).

The most reliable and physically meaningful measurement of earthquake size is the seismic moment, M_0, (Aki, 1966) given by

$$M_0 = \mu S d$$

where μ is the shear modulus, S is the area of the rupture surface, and d is the average displacement along the rupture surface. From the seismic moment, a moment magnitude, M_W (Kanamori, 1977; Hanks and Kanamori, 1979) can be calculated from the definition

$$M_W = (2/3)\log M_0 - 10.7$$

M_W should be comparable to M_S for earthquakes of $5.0 \leq M_W \leq 7.5$ (Hanks and Kanamori, 1979). The Hebgen Lake earthquake had a seismic moment of 1.0×10^{27} dyne-cm (Doser, 1985b), which converts to a moment magnitude of 7.3. The Borah Peak earthquake had a moment of 2.1×10^{26} (Doser and Smith, 1985) to 3.1×10^{26} (Ekstrom and Dziewonski, 1985), which gives a moment magnitude of 6.8 to 7.0.

2.3.4 Maximum Earthquake Size

The M_S7.5 Hebgen Lake earthquake is considered by some to represent the maximum earthquake for the Intermountain seismic belt (e.g. Doser, 1985a). However, it is worth noting that earthquakes larger than this have occurred in the western Basin and Range Province. Slemmons (1980) lists 13 historic surface faulting earthquakes in the western Great Basin. These include two events of magnitude greater than 7.5: the March 26, 1872 Owens Valley, California earthquake of estimated magnitude 8.0, and the October 3, 1915 Pleasant Valley, Nevada earthquake of magnitude 7.75. Slemmons (1980) lists a rupture length of 110 km for the Owens Valley event with a maximum displacement of 6.44 m, and a rupture length of 62 km with a maximum displacement of 5.6 m for the Pleasant Valley event. Thus, both of these earthquakes have a maximum displacement comparable to that of the Hebgen Lake event, but significantly longer rupture lengths. The magnitude of 7.75 for the Pleasant Valley event is from Gutenberg and Richter (1954), and is nearly identical to the surface wave magnitude of 7.7 calculated by Abe (1981). The magnitude of the Owens Valley event is more controversial, owing to the lack of seismographic instruments at the time. Magnitude estimates for this earthquake based on felt reports range from 8.3 (Oakeshott et al., 1972) to 7.2 (Evernden, 1975). From the surface faulting, Beanland and Clark (1987) estimate a moment magnitude of 7.5 to 7.7.

The slip that occurred during the 1872 Owens Valley earthquake had a large strike-slip component to it (Richter, 1958; Oakeshott et al., 1972) and may even have been dominantly strike-slip (Beanland and Clark, 1987). Faults in the Wasatch Front region show predominantly normal slip, although there is abundant evidence of strike-slip faulting in south-central Utah (Anderson and Barnhard, 1984). Thus, the Pleasant Valley and Hebgen Lake earthquakes may be better models for the maximum credible Wasatch Front earthquake than the Owens Valley earthquake. The characteristics of the Pleasant Valley and Hebgen Lake earthquakes suggest that future Wasatch Front earthquakes could have surface wave magnitudes of up to 7.5-7.7, rupture lengths of up to 35-65 km, and maximum vertical displacements of up to about 6 m. In this report we follow consensus judgment (e.g., Youngs et al., 1987) in adopting M_S7.5 as a maximum probable size, although a maximum credible size might be a few tenths of a unit larger.

2.3.5 Threshold of Surface Faulting

Various authors (e.g. Arabasz, 1984; Arabasz and Julander, 1986; Doser, 1985a) have suggested that the threshold magnitude for surface faulting in Utah is approximately 6.0-6.5. This conclusion appears to be well founded based on the historical record of earthquakes in the Intermountain seismic belt and in the Basin and Range Province. Bucknam et al. (1980) note that all 7 historic earthquakes of M_L 6.3 or greater in the Great Basin have produced surface faulting, including the 1934 M_L 6.6 Hansel Valley, Utah event. In their tabulation of 11 earthquakes with historic surface faulting in the Basin and Range Province, all 5 events with $M_L \leq$ 6.8 had maximum displacements of less than 1 meter. In the Intermountain seismic belt, Doser (1985a) points out that neither the 1975 M_L 6.0 Pocatello Valley earthquake or the 1975 M_L 6.1

Yellowstone Park earthquake (Figure 2.2) had identifiable surface faulting, although both earthquakes were accompanied by an apparently coseismic subsidence of up to 12-13 cm (Bucknam, 1976; Pitt et al., 1979). The implication of the M_L 6.0-6.5 threshold for surface faulting is that one can argue that earthquakes up to this size could occur anywhere in the Wasatch Front region within the main seismic belt, even where there is no geologic evidence for surface faulting. We elaborate in the following subsection.

2.4 Problematic Correlation of Seismicity with Geologic Structure

There are fundamental problems in correlating diffuse seismicity with mapped Cenozoic faulting and subsurface geologic structure in the Utah region (e.g., Arabasz 1984; Arabasz and Julander, 1986). Problems include: (1) uncertain subsurface structure, which typically is more complex along the main seismic belt than apparent from the surface geology; (2) observations of discordance between surface fault patterns and seismic fault slip at depth (Arabasz et al., 1981; Zoback, 1983); (3) a paucity of historic surface faulting; and (4) inadequate focal-depth resolution from regional seismic monitoring.

Crustal structure along the eastern Great Basin is known to involve vertically stacked plates separated by low-angle detachments resulting from relict pre-Neogene thrustbelt structure and/or Neogene extension (Allmendinger et al., 1983; Smith and Bruhn, 1984;). Smith and Bruhn (1984) present a summary of seismic-reflection data that indicate the widespread presence of low-angle and downward-flattening faults in the subsurface and an intimate relationship between pre-Neogene thrustbelt structure and young normal faults along the eastern Basin and Range margin. Seismological evidence to date indicates that, at least for small to moderate earthquakes, seismic slip in this region predominates on fault segments with moderate (≥30°) to high-angle dip (Zoback, 1983; Arabasz and Julander, 1986).

Given the relatively high threshold of surface faulting and observations of discordance between surface fault patterns and seismic slip at depth, one can argue that—with the sole exception of the 1934 Hansel Valley earthquake—no other of Utah's 15 historical earthquakes of M_L 5.5 or greater (Table 1.1) can be confidently associated with a mapped surface fault. Within the domain of Utah's main seismic belt, future seismicity below the threshold of surface faulting (M_L approx. 6 to 6½) thus cannot be confidently precluded by knowledge of the surface geology alone. Where subsurface structure is complex, moderate size earthquakes may occur on "blind" subsurface structures that have no direct surface expression.

On the basis of special earthquake studies in the southern Wasatch Front area, neighboring parts of central Utah, and southeastern Idaho, the following working hypothesis was offered by Arabasz (1984; see also Arabasz and Julander, 1986) to explain observations of diffuse background seismicity. Background seismicity, it was suggested, is fundamentally controlled by variable mechanical behavior and internal structure of individual horizontal plates within the seismogenic upper crust. Diffuse epicentral patterns may then result from the superposition of seismicity occurring within individual plates, and also perhaps from favorable conditions for block-interior rather than block-boundary microseismic slip. Figure 2.6 schematically shows some aspects of the working hypothesis relating diffuse seismicity to vertically stacked plates in the upper crust.

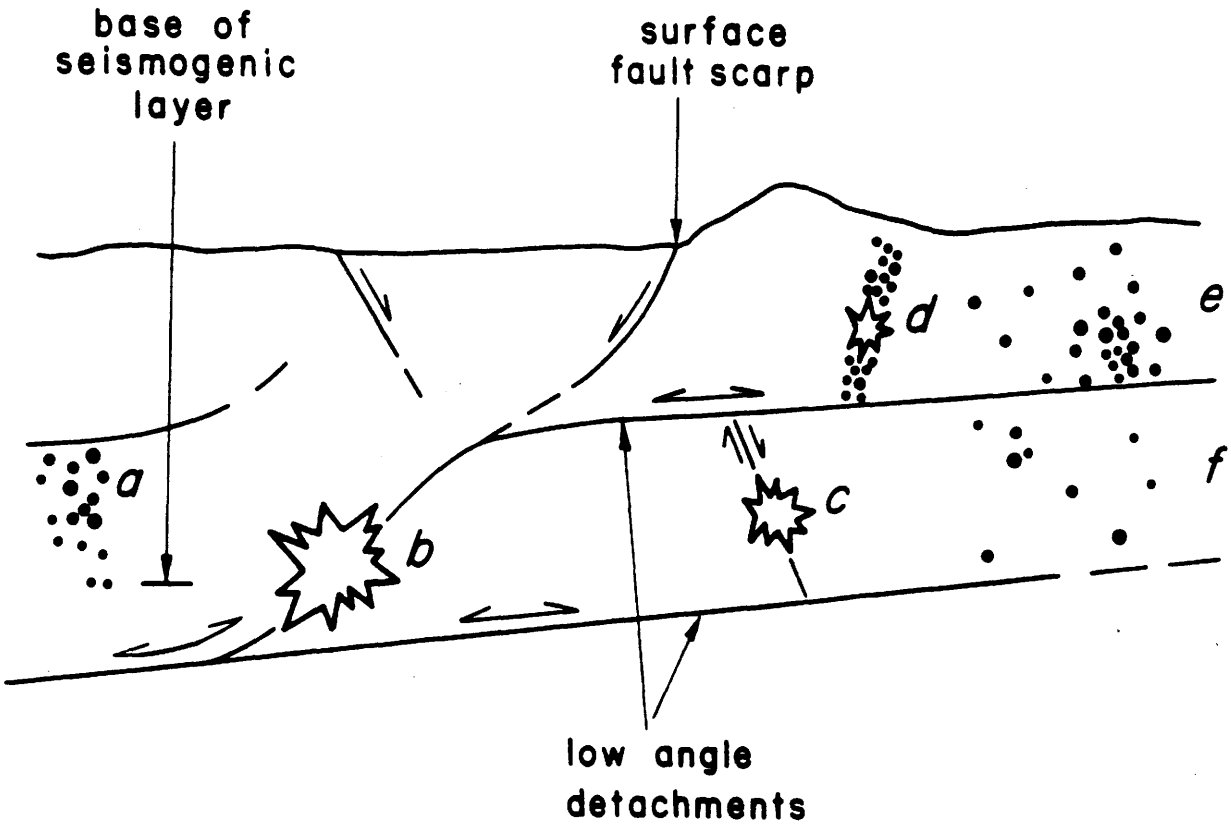

Figure 2.6 (a) Schematic geologic cross-section of the upper crust illustrating complex association of seismicity with geological structure in the Intermountain seismic belt. Starbursts indicate foci of moderate-to-large earthquakes; small circles, microseismicity; lines in subsurface, faults. Arrows indicate sense of slip on faults; two-directional arrows, extensional backsliding on pre-existing low-angle faults possibly formed as thrust faults. Base of seismogenic layer is approximately at 10-15 km depth. Letters identify aspects (not exhaustive) of observations and a working hypothesis (Arabasz, 1984; Arabasz and Julander, 1986) relating seismicity to structure: (a) local predominance of seismicity within a lower plate; (b) nucleation of a large normal-faulting earthquake near the base of the seismogenic layer, hypothetically on an old thrust ramp, and with linkage or an established rupture pathway to a major surface fault; (c) occurrence of a moderate-size earthquake within a lower plate, without linkage to a shallow structure; (d) occurrence of a moderate-size earthquake and aftershocks on a secondary fault where an underlying detachment restricts deformation to the upper plate; (e) diffuse block-interior microseismicity predominating within an upper plate--perhaps responding to extension enhanced by gravitational backsliding on an underlying detachment; and (f) diffuse block-interior microseismicity within a lower plate where frequency of occurrence is markedly lower than in the overlying plate.

3. HISTORICAL AND INSTRUMENTAL EARTHQUAKE RECORD

3.1 Earthquake Recording in Utah

The most prominent sources of earthquake data for the Utah region are (1) compilations made by the University of Utah (Arabasz et al., 1979; Richins et al., 1981, 1984; Brown et al., 1986; also, unpublished data) and (2) data files of the National Geophysical Data Center, National Oceanic and Atmospheric Administration (NOAA). In this paper, we rely heavily upon the University of Utah's data base, which represents the primary source of instrumental earthquake data since mid-1962 for the region and which includes a comprehensive listing of historical seismicity. A recent compilation published by the U.S. Geological Survey (Stover et al., 1986) essentially duplicates the NOAA data file. It should be noted that the published compilation of Stover et al. (1986) omits at least four shocks of magnitude 5 or greater since 1959—presumably due to editorial error.

The catalog of documented earthquakes in the Utah region, as elsewhere in the western United States, is a mixed one variously relying upon early reports and newspaper accounts, and later upon seismographic recordings during several stages of evolving instrumental coverage (Figure 3.1; see Arabasz et al., 1979, for complete details).). The historical earthquake record effectively dates from 1850 with the publication of the first newspaper in the region, shortly after settlement by Mormon pioneers beginning in 1847. Instrumental earthquake locations in the region, based on regional seismographic recordings in the western United States, date chiefly from about 1950. The 1955 time frame shown in Figure 3.1 includes a seismograph station at Salt Lake City and another to the north at Logan. Although seismographs were first installed on the University of Utah campus in 1907, contributions to the instrumental location of regional earthquakes postdate 1939 when photographic records from modern seismographs began to be routinely forwarded from Salt Lake City to the U.S. Coast and Geodetic Survey.

Systematic computerized locations based on local seismographic coverage in the Utah region by the University of Utah date from mid-1962. From that time to late 1974, a skeletal statewide network of several widely-spaced stations was in operation (see 1965 time frame, Figure 3.1). Since late 1974, the University of Utah has operated a modern telemetered network of high-gain short-period seismographic stations in the Intermountain region. Fifty-six stations of an 85-station network currently lie within the Utah region (see 1985 time frame, Figure 3.1) and provide regional seismographic monitoring of the area of the proposed SSC sites. The seismographic data are centrally recorded at the University of Utah in Salt Lake City. From 1974 through 1980 the recording was in analog form, and since January 1, 1981, in digital form.

The proposed SSC sites lie along the western margin of Utah's Wasatch Front region, for which Arabasz et al. (1980) estimated the historical earthquake catalog to be complete for: I_o (Modified Mercalli epicentral intensity) ≥ VIII (or M_L ≥~6.3) since 1850; I_o ≥VII (or M_L

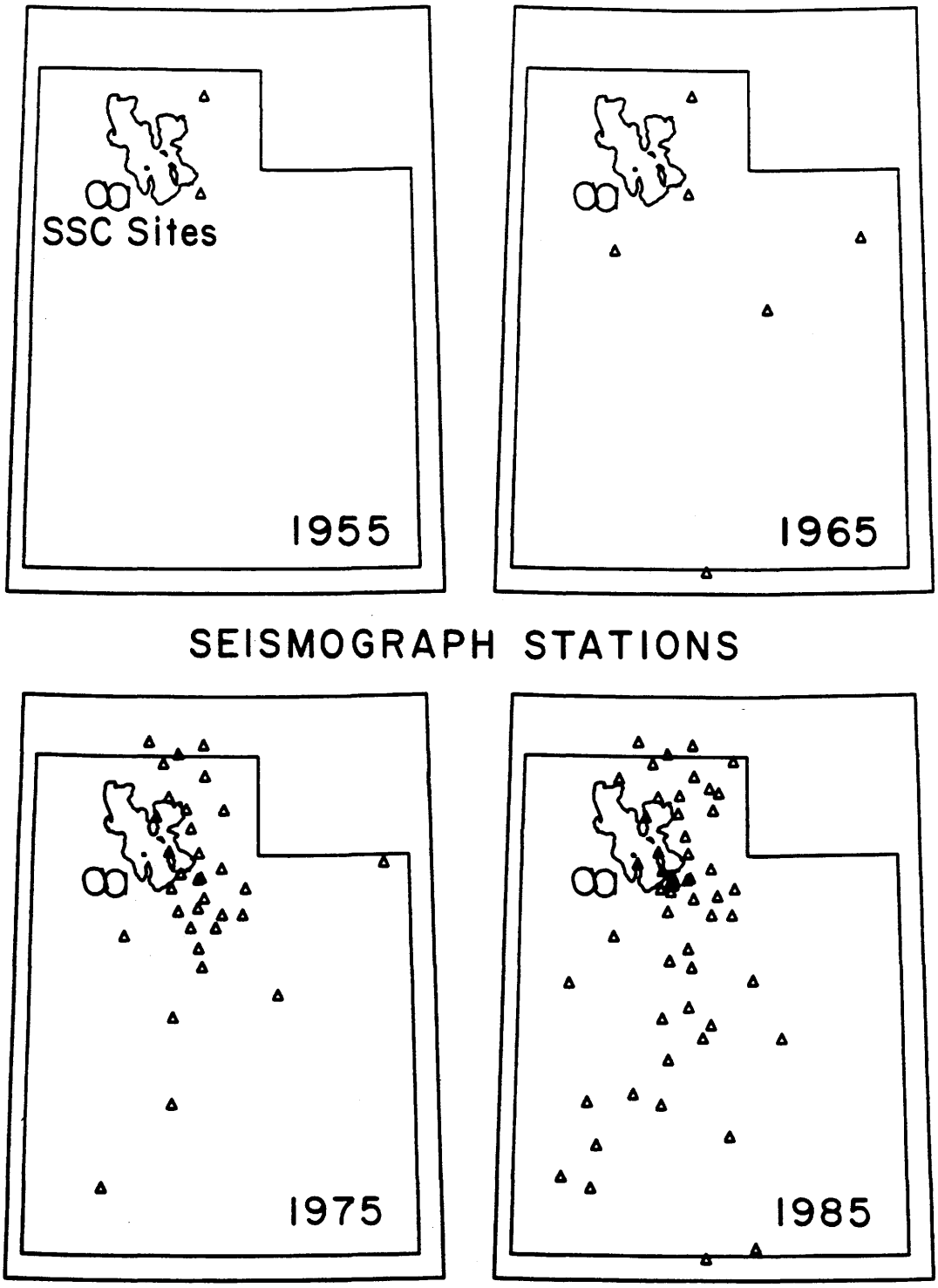

Figure 3.1 Map of the Utah region showing distribution of seismograph stations (triangles) for four different times, 1955-1985. Proposed SSC sites shown for reference.

≥~5.7) since about 1880; and $I_o \geq$ VI (or $M_L \geq$~5.0) since about 1940. Completeness for $I_o \geq$V (or $M_L \geq$~4.3) was assumed since 1950. The threshold of completeness for instrumental monitoring of this area since mid-1962 is estimated as M_L 2.3 (Arabasz et al., 1980). We discuss below the thresholds of completeness for areas surrounding the SSC sites.

3.2 Earthquake Data Base

The study area for this report extends outward 160 km (100 miles) from the edges of the proposed SSC sites (Figure 3.2). This area lies primarily within Utah, but also encompasses parts of northeastern Nevada, southern Idaho, and southwestern Wyoming. For task (b) of this study (see section 1.2), we undertook a compilation of historical and instrumental seismicity data within this study area. The solid box in Figure 3.2 labeled "Near-Site Region" extends outward about 60 km from the centers of the two proposed SSC sites. Within the near-site region, we analyzed all of the available data and performed a special blast discrimination study (task (c), section 1.2). Elsewhere in the study area, the emphasis in this report is on earthquakes of $M_L \geq$3.0.

In order to construct the most complete earthquake catalog possible for the study area, we merged data from the University of Utah earthquake catalog with data from the Nevada earthquake catalog of the University of Nevada at Reno and the worldwide earthquake catalog of the National Oceanic and Atmospheric Administration (NOAA). Together, these three catalogs include all of the available epicentral data for this region. The study area west of 114°15'W falls outside of the reporting area for the published University of Utah catalogs. However, locatable earthquakes outside this reporting area are still included in the University of Utah computer files. The Nevada earthquake catalog consists primarily of earthquakes located using a telemetered network of seismograph stations operated by the University of Nevada since 1969 in western and southern Nevada (see, for example, Vetter and Corbett, 1987). The catalog also contains some older earthquakes from the catalog of Slemmons et al. (1965), whose locations and magnitudes were determined on the basis of felt reports and sparse instrumental data. The NOAA catalog was compiled from a wide variety of sources, and includes both instrumental and non-instrumental epicentral locations and magnitudes (see Rinehart et al., 1985). The more recent locations in the NOAA catalog (post-1962) are from a widely-spaced worldwide network of seismograph stations.

The best earthquake data available for the study area are from the University of Utah seismic network, discussed in the previous section. Although the western half of the study area lies beyond the boundaries of this network, (Figure 3.1), the University of Nevada stations are located even farther from the study area. Consequently, we used the University of Utah catalog as the primary data source for this study. The University of Nevada and NOAA catalogs were then searched for earthquakes within the study area that are not included within the University of Utah catalog. There are 14 earthquakes listed in the Nevada catalog which are not in the Utah catalog, and these were added to the compilation. The largest of these 14 earthquakes is a magnitude 5.2 earthquake on September 5, 1928, in the northwest corner of the study area. The location of this earthquake was determined from S-P intervals measured

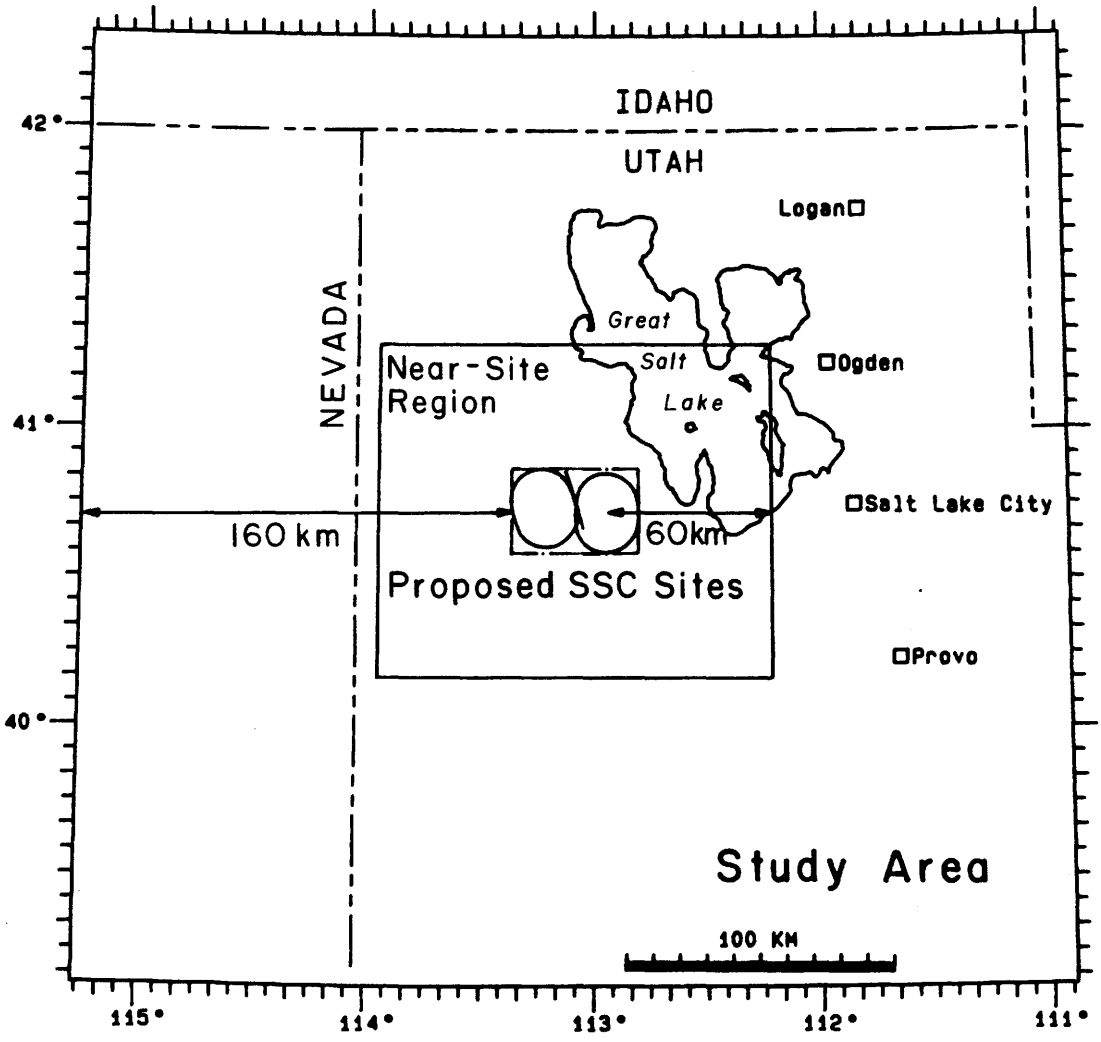

Figure 3.2 Study area for this report. Includes the region 160 km from the edges of the proposed SSC sites. Central box (solid line) delineates area for which special blast removal was done (see Figures 3.5 and 3.7).

on seismograms recorded at Reno, Nevada, and Mount Hamilton, California (Slemmons et al., 1965). The rest of the additions from the Nevada catalog are all modern instrumental locations of post-1970 earthquakes in eastern Nevada.

The NOAA catalog included 28 earthquakes in the study region that were apparently not listed in either the Utah or the Nevada catalogs. Since most of these entries were based on felt reports, the origin times and locations are somewhat uncertain. We therefore carefully checked these entries against other sources such as Williams and Tapper (1953), Arabasz and McKee (1979), Coffman et al. (1982), and the United States Earthquakes Series, formerly published by the U.S. Coast and Geodetic Survey and now published by the U.S. Geological Survey. From these sources, we identified 10 of these 28 earthquakes as duplicates of earthquakes already in the University of Utah catalog. The remaining 18 events were added to the compilation.

Instrumental magnitudes were not available for the 13 pre-1963 events added from the NOAA catalog. We calculated magnitudes for these events from the maximum Modified Mercalli Intensity, I_o, with the Gutenberg and Richter (1956) relationship used by Arabasz and McKee (1979) in assembling the Utah earthquake catalog for 1850 through June 1962:

$$M_L = 1 + (2/3)I_o$$

A U.S. Geological Survey local magnitude (M_L) was available for the most recent addition from the NOAA catalog, a M_L 3.0 event on June 9, 1977 in eastern Nevada. Only body wave magnitudes (m_b) were available for the 4 NOAA events between 1963 and 1970, which had m_b's of 3.4-3.7. This presented a problem since, according to Dewey (1987), m_b values in the NOAA catalog for small ($m_b \leq 4.0$), shallow earthquakes before the mid-1970's probably overestimate event size by nearly one magnitude unit. Figure 3.3 is a plot of M_L from the University of Utah versus m_b from NOAA for events listed in Stover et al. (1986). It is clear from this plot that the NOAA m_b values are systematically higher that the University of Utah M_L values. A linear least squares regression of M_L versus m_b yields the relationship

$$M_L = 1.022m_b - 0.892$$

We used this relationship to convert the 4 NOAA m_b values in question to equivalent local magnitudes.

Figure 3.4 is a plot of M_L from the University of Utah versus M_L from the University of Nevada for 10 eastern Nevada earthquakes recorded by both networks. Although the data are sparse, it appears that the Nevada magnitudes are systematically higher than the Utah magnitudes. A linear least squares regression yields the relationship

$$M_L(UU) = 1.14\ M_L(UN) - 0.984$$

In the interests of keeping the size measurements in the merged catalog consistent, we used this equation to adjust the magnitudes of the 13 post-1974 earthquakes added from the University of Nevada catalog. The largest of these events had a magnitude of 4.3 in the Nevada catalog, which was revised downward to 3.9.

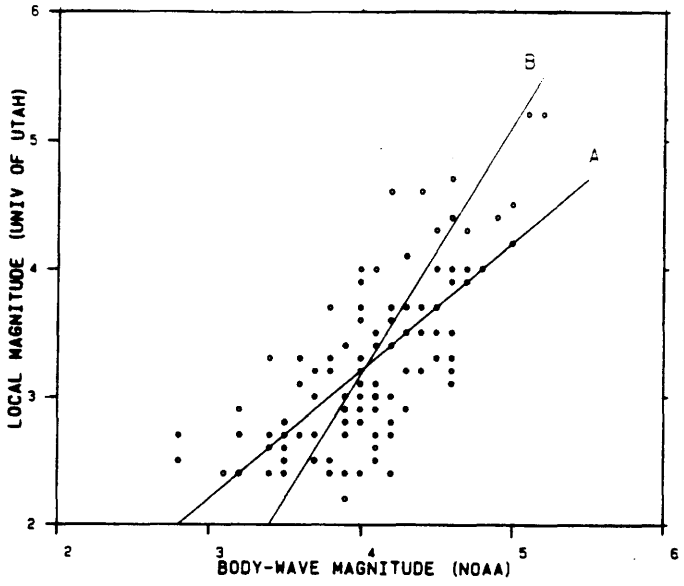

Figure 3.3 Comparison between m_b values (from NOAA) and M_L values (from UUSS). Data are magnitude values from 108 events listed in Stover et al. (1986). Lines "A" and "B" are the least-squares linear regressions for M_L as a function of m_b and m_b as a function of M_L, respectively (see text for relation).

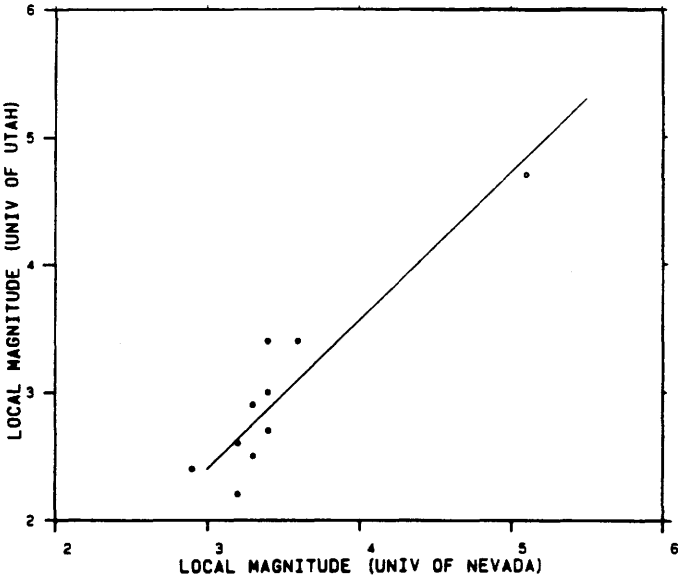

Figure 3.4 Comparison between M_L (University of Utah) and M_L (University of Nevada). Data are magnitude values from 10 post-1970 events recorded by both the Utah and Nevada networks. Line shown is the least-squares linear regression for M_L (UU) as a function of M_L (UN) (see text for relation).

Appendix A lists all of the earthquakes in our compilation of magnitude 2.7 and greater. The footnotes identify the events from the Nevada and NOAA catalogs.

3.3 Blast Discrimination

Blasting for mining, military ammunition disposal, construction, and seismic exploration is common in the Utah region. Although efforts are made to remove these blasts from the University of Utah earthquake bulletins before publication, the catalog does still include some blasts. For this reason, we undertook a special investigation of seismic events included in our compilation and located within the near-site region (solid box, Figure 3.2) in order to remove any remaining blasts. Figure 3.5 shows all of these events (circles), together with the approximate locations of known blasting sites in the region (stars). The sites labeled Promontory Point, USAF Disposal, and USAF South Range were found during the course of this study. We routinely identify and remove blasts from the other 6 sites when compiling our published earthquake bulletins (see Brown et al., 1986). However, judging from the clusters of epicenters centered on these sites, it appears that this has not always been done consistently in the past.

The procedure that we used to identify the blasts is similar to our routine blast discrimination procedure. We prepared listings of all seismic events within a 10 km radius, or, in some cases, a 20 km radius of the centers of known blasting sites (circles, Figure 3.5). Events within these areas that occurred during daytime hours are considered possible blasts. The sizes of the search areas are designed to take into account both the area extent of the region over which blasting takes place and the accuracy of the epicentral determinations. Since most of the blasts are small ($M_L \leq 2.0$) and most of the blasting sites in Figure 3.5 are located on the fringes of the network (Figure 3.1), the location accuracy is probably no better than about ±5 km for most events and may be worse for poorly recorded events.

As part of our current procedure for compiling the quarterly Utah preliminary epicenter listings, we contact individual blasting operations and attempt to confirm the times and sources of suspected blasts. Unfortunately, most blasters do not keep good records of their blasting times and, at best, are only able to verify blasts that occurred within the past several months. Since most of the suspected blasts in Figure 3.5 are old (89% occurred before 1983), it was not possible to confirm individual seismic events as blasts in this manner. Nearly all of the suspected blasts from 1983 through 1987 occurred at either the Southern Pacific Promontory Point quarry or the U.S. Air Force Ordinance Disposal area. For both localities, we were able to verify that blasting was going on during the general time period when the suspected blasts were observed.

On the basis of both their origin times and locations, we consider all but three of the seismic events within the circles in Figure 3.5 to be probable blasts and have removed them from the catalog for the study area. Occasional blasting is also done within the Dugway Proving Grounds in the southernmost part of Figure 3.5 (not shown). However, we did not feel sufficiently confident in the non-seismic origin of the 4 events located on or near the Dugway Proving Grounds to remove them from the catalog. Appendix B lists all of the probable blasts

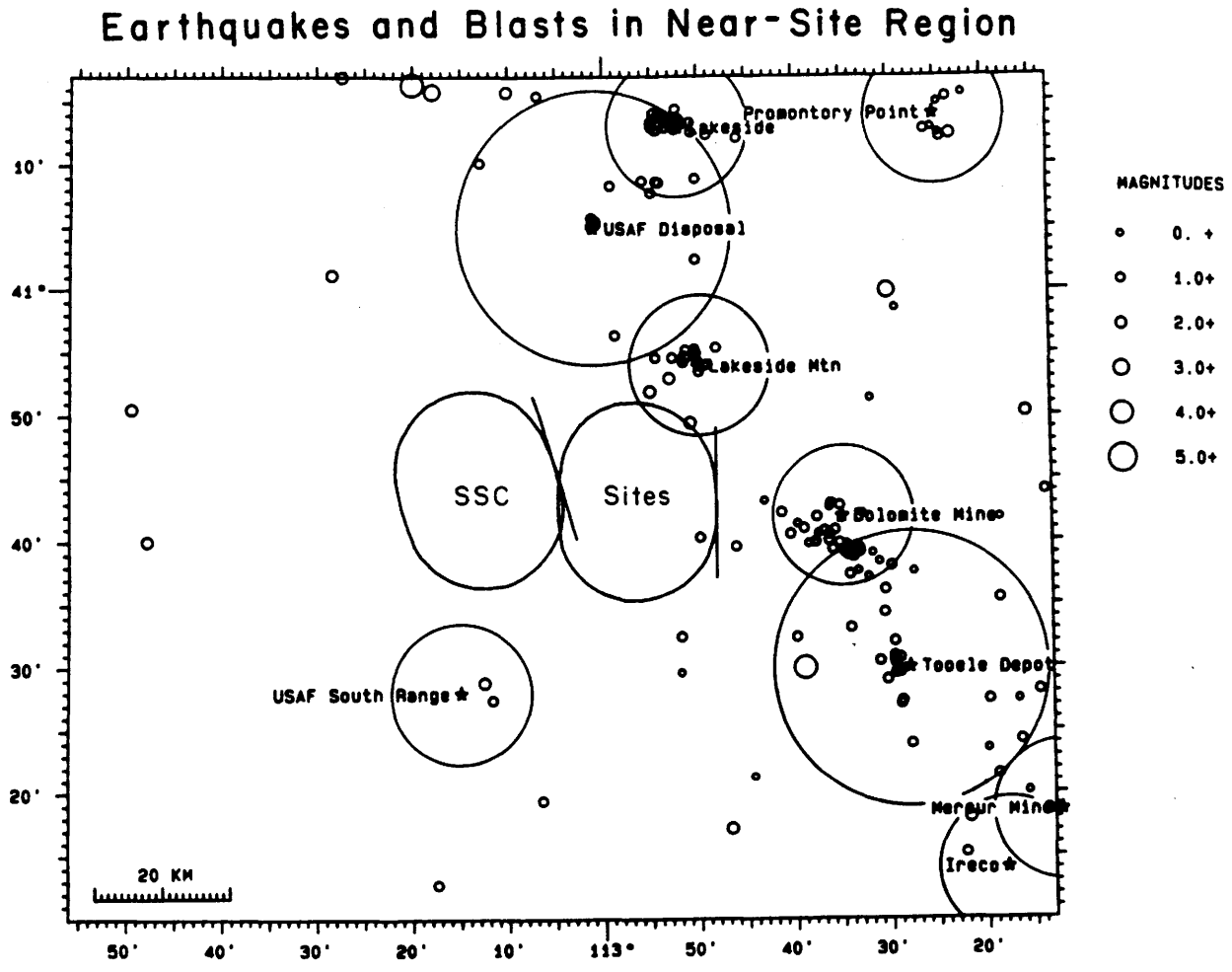

Figure 3.5 All seismic events in our catalog within the near-site region. These data include both earthquakes and blasts. Local areas of blasting are shown as stars. Circles surrounding blast areas show the extent of blasting for each area, allowing for location errors. All events within the blasting areas were checked to eliminate man-made events (Appendix B).

around each blasting site that we removed from the catalog. Since some of the circles in Figure 3.5 overlap, some of the events are listed under more than one site. To convert the UTC origin times given in Appendix B to local time, subtract 7 hours to obtain a Mountain Standard Time and 6 hours to obtain Mountain Daylight Time. Note the relatively small variations in the origin times of the events given in each listing in Appendix B.

Appendix C lists the 28 seismic events within the area of Figure 3.5 that were left after the probable blasts were removed. We believe that most of these events are earthquakes, but we cannot rule out the possibility that some may still be blasts. Of the 28 events, 17 occur between the hours of 8:00AM and 6:00PM, local time. This number is somewhat greater than the 12 that would be expected given a random distribution of origin times, which should be the case for a catalog that contains only naturally occurring seismic events.

3.4 Regional Seismicity

The epicenter map in Figure 3.6 shows earthquakes of $M_L \geq 2.7$ that occurred within the study area between 1850 and March 31, 1987. Circles indicate earthquakes that occurred after the establishment of the University of Utah network in July 1962, and squares indicate earlier earthquakes. Table 3.1 is a tabulation of these earthquakes by magnitude. We estimate that the current uniform detection threshold is about magnitude 3.0 in the westernmost part of the study area where station coverage is poorest. (see section 4.3 below). The magnitude cutoff of 2.7 was chosen to insure that all earthquakes of magnitude 3.0 and greater were included, allowing for a magnitude uncertainty of ±0.3. The blast discrimination study discussed above did not encompass the entire study area, but the magnitude cutoff of 2.7 should serve to remove virtually all of the unrecognized blasts. Note that none of the probable blasts that we removed from the catalog (Appendix B) are larger than magnitude 2.3. The epicenters in Figure 3.6 are superimposed upon a map of late Quaternary fault scarps (<500,000 years, approximately), discussed below in section 4.

The western boundary of the ISB as depicted by Arabasz and Smith (1981) (Figure 2.2) trends north-south through the center of Figure 3.6. This diffuse boundary is evidenced by decreased seismic activity in the western half of Figure 3.6 relative to the eastern half of Figure 3.6, rather than a complete absence of activity west of the ISB boundary. The decreased rate of seismic activity in the western part of the study area extends to the larger magnitudes, and is therefore not an artifact of the poor detection threshold in this region. Since the University of Utah seismic network was established in 1962, there have been only 2 independent mainshocks of M_L 4.0-4.9 in the study area west of 113°05', and none of $M_L \geq 5.0$. This compares to 10 independent mainshocks of M_L 4.0-4.9, 2 of M_L 5.0-5.9, and 1 of M_L 6.0 in the study area east of 113°05'. For the time period from 1850 through June 1962, the study area west of 113°05' had 2 independent mainshocks of M4.0-4.9 and 2 of M5.0-5.9, while east of 113°05' there were 30 mainshocks of M4.0-4.9, 11 of M5.0-5.9, and 3 of M6.0-6.9. Since much of the pre-1962 catalog is based on felt reports, the distribution of earthquakes for this period of time is probably biased by the concentration of population centers along the Wasatch front. The more recent instrumental data, on the other hand, are very unlikely to be biased at

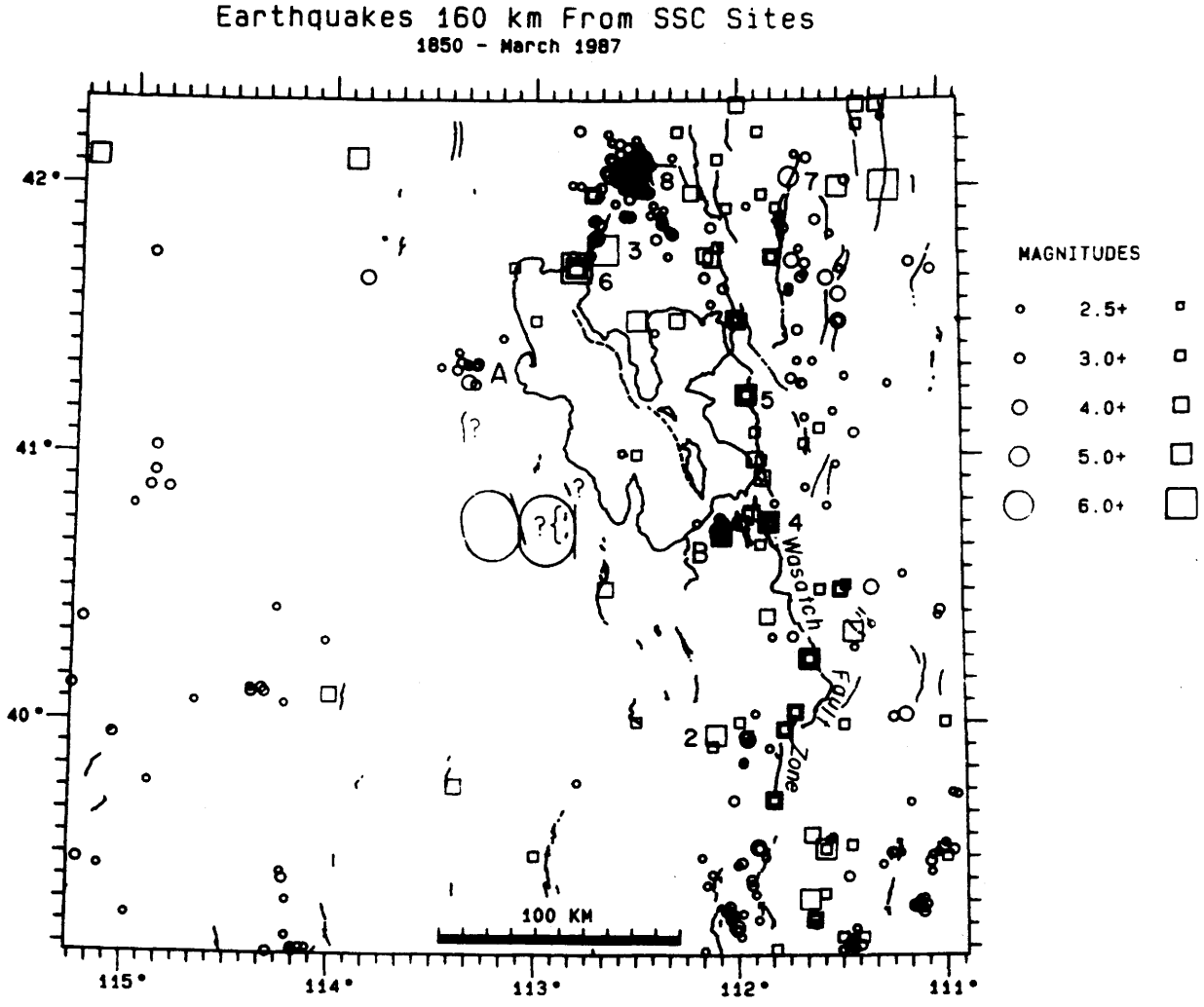

Figure 3.6 All earthquakes of $M_L \geq 2.7$ from 1850 to March 31, 1987 and late Quaternary fault scarps (<500,000 years). Squares are events which occurred before the establishment of the University of Utah network in July 1962. Mainshocks of $M_L > 5.5$ are numbered chronologically (see Table 2.1). "A" and "B" mark clusters of seismicity discussed in the text.

TABLE 3.1

NUMBER OF EARTHQUAKES IN STUDY AREA*

M_L	1850-June1962	July 1962-March 1987	Total
2.7-3.9	82*	314*	396*
4.0-4.9	38 (32)	18 (12)	56 (44)
5.0-5.9	16 (13)	2 (2)	18 (15)
6.0-6.9	4 (3)	1 (1)	5 (4)

*Counts in parentheses are for independent main shocks; these were not determined for smaller events.

the $M_L \geq 4.0$ level.

Figure 3.6 shows a conspicuous lack of epicenters within about 50 km of the proposed SSC sites. The nearest concentration of seismic activity is located approximately 50 km north of the western ring, between the Newfoundland and Hogup Mountains at location A in Figure 3.6. There has been sporadic earthquake activity of $M_L \leq 4.0$ since at least 1965 at this locality, including a swarm of 10 events ($1.1 \leq M_L \leq 3.2$) in March and April of 1979 and another swarm of 9 events ($1.3 \leq M_L \leq 3.1$) in April of 1980. 60 km east of the eastern ring is a cluster of earthquakes in the western Salt Lake Valley (location B, Figure 3.6). This cluster includes the September 1962 M_L 5.2 Magna earthquake, and another earthquake of comparable size in February 1943 (MM VI).

Independent mainshocks in the study area of magnitude 5.5 or greater (or MM VII or greater) are numbered chronologically on Figure 3.6. The eight events, which are included in Table 1.1 and also shown on Figure 2.3, are: (1) a magnitude 6.3 earthquake in Bear Lake Valley in November, 1884, (2) a magnitude 5.7 earthquake near Eureka in August 1900, (3) a magnitude 6.3 earthquake in Hansel Valley in October 1909, (4) a magnitude 5.7 earthquake close to Salt Lake City in May 1910, (5) a magnitude 5.7 earthquake close to Ogden in May 1914, (6) a magnitude 6.6 earthquake in Hansel Valley in March 1934, (7) a magnitude 5.7 earthquake in Cache Valley in August 1962, and (8) a magnitude 6.0 earthquake in Pocatello Valley in March 1975.

The apparent clustering of pre-1962 epicenters along the Wasatch fault (squares, Figure 3.6) largely reflects the concentration of cities and towns along the Wasatch front, since noninstrumental earthquake locations are assigned to the location where the felt effects are the strongest (Arabasz et al., 1980). Thus, this clustering is not necessarily indicative of earthquake activity on the Wasatch fault itself. Of the eight $M_L \geq 5.5$ earthquakes, the Salt Lake City and Ogden events are the only ones that might have been associated with the Wasatch fault, and even these two could have been on some other nearby fault.

3.5 Near-Site Seismicity

Figure 3.7 is a map showing all known earthquakes that occurred in the near-site region (Figure 3.2) from 1850 through March 1987. The area shown extends outward about 60 km from the centers of the two proposed SSC sites. Blasts have been removed from the catalog for this region, as described in section 3.3 above.

Figure 3.7 confirms that the seismicity in the near vicinity of the proposed sites is indeed very low. There are only 28 earthquakes on the plot in Figure 3.7, all from the University of Utah catalog (Appendix C). The four events of $M_L \geq 3.0$ are labeled with their year of occurrence and magnitude. At the northern edge of the area shown, the M_L 4.0 and 3.6 events in February and July of 1967, respectively, are part of the cluster of activity at location A in Figure 3.6. The location of the January 1958 event in the Great Salt Lake is from instrumental data, but the magnitude of 3.0 was arbitrarily assumed by Arabasz and McKee (1979) in the absence of any size information. The location of the August 1915 M4.3 event was assumed on the basis of felt reports, and may therefore be in error by up to 25-50 km (Arabasz and

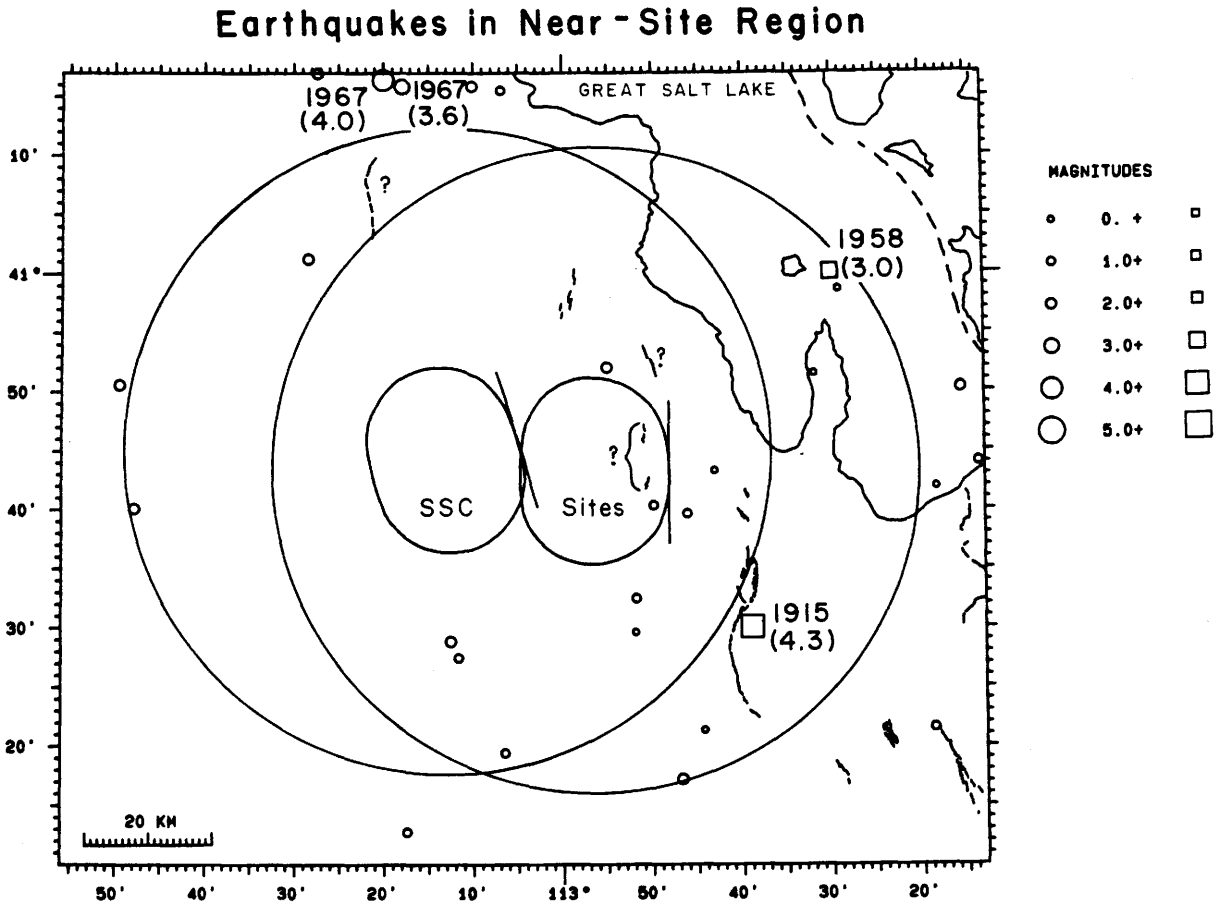

Figure 3.7 All earthquakes within the near-site region, blasts removed (see Figure 3.5). The four events of $M_L \geq 3.0$ are labeled by year and magnitude. The two circles centered on the sites have radii of 50 km and represent the area around each site for which recurrence modelling was done (see Section 4.3). Squares and circles indicate earthquakes before and after July 1962, respectively.

McKee, 1979).

The paucity of even small magnitude events within the area of Figure 3.7 may be at least partially an artifact of the poor station coverage in this region (Figure 3.1). Nevertheless, large numbers of small magnitude blasts ($M_L \leq 2$) have been detected and located in the eastern part of this area since the major expansion of the University of Utah network in 1974 (see, for example, Appendix B). Thus, a uniform detection threshold since 1974 of M_L 2.0-2.5 seems reasonable for this area. During this time period (12.5 years), there have been 4 events of $M_L \geq 2.0$ and none of $M_L \geq 2.5$.

The August 11, 1915 earthquake is the largest known historical earthquake in the near-site region, and therefore bears some discussion. This earthquake was felt at Iosepa, Utah, which is located at the western foot of the Stansbury Range at 40°32'N, 112°44'W. A report filed from an early observing station of the U.S. Weather Bureau at Iosepa indicated "rumbling" of approximately 6 sec duration accompanying a single shock at 10:20 GMT (03:20 a.m. local time) and an estimated Rossi-Forel intensity of VII (?) (or Modified Mercalli intensity VI (?)) (S.D. Oaks, University of Colorado /USGS, personal communication, 1987). Stover et al. (1986) have recently assigned a Modified Mercalli (MM) intensity of VI to the shock, ascribing the intensity assignment to W.J. Humphreys in the Monthly Weather Review of August 1915. The size estimate for this earthquake also appears as MM V (Coffman and von Hake, 1973; see also Coffman et al., 1982), and MM VIII (?) (Williams and Tapper, 1953).

The size estimate for the August 11, 1915 earthquake listed in the University of Utah catalog (Arabasz and McKee 1979) follows Coffman and von Hake (1973). An MM intensity of V is approximately equivalent to M_L 4.3. The assumed location listed in the University of Utah catalog for the shock (40°30'N, 112°39'W) is close to the location of the original felt report at Iosepa. The value of MM intensity VI listed by Stover et al. (1986) would be approximately equivalent to M_L 5.0. The possibility of an estimated magnitude higher than the value of 4.3 in the University of Utah catalog must be admitted. However, if the earthquake originated close to Iosepa—say, along the range-front fault on the west side of the Stansbury Mountains— our modern experience would make us doubt a magnitude as high as 5.0. We base this judgment on the apparent absence of felt aftershocks and the absence of felt reports in the populated parts of the Salt Lake Valley 50 to 70 km to the east, together with observations of the attenuation of intensity in Utah (McGuire, 1983). These arguments would not necessarily apply if the earthquake originated, say, to the west of Iosepa in a distal direction from the Salt Lake Valley.

4. EVALUATION AND INTERPRETATION OF HISTORICAL/INSTRUMENTAL SEISMICITY

4.1 General Remarks

The purpose of this section is to provide an interpretation and evaluation of the observed seismicity surrounding the SSC candidate sites with the goal of assessing the potential effects on the proposed SSC alignments from future earthquake activity. A standard characterization of seismicity involves (1) a compilation and description of the historical and modern earthquake record (which we have presented in section 3); (2) the identification and depiction of seismic source zones within which earthquakes are likely to originate within the future; and (3) the specification of seismicity parameters for respective source zones, including rates of activity and the expected distribution of earthquakes as a function of size up to some maximum size.

Our current understanding of the regional seismotectonic framework for the proposed SSC sites leads to the position that seismic hazard arises from two fundamental sources: first, the occurrence of infrequent large (magnitude 6.5 to 7.5±0.2) surface-faulting earthquakes on identifiable faults having evidence of late Quaternary displacement; and, second, small to moderate-size (up to magnitude 6.5) earthquakes that are not constrained in location to mapped faults and which may occur randomly in space throughout broadly defined regions. This position is consistent with the experience and judgment of seismologists and geologists working in the Intermountain region. It is an outgrowth of the problematic correlation of seismicity and geological structure that we have discussed in section 2.5 and of detailed studies of active faulting in the region (e.g., Swan et al. 1980; Schwartz et al., 1984). An elaborate seismic hazard study of the Wasatch Front region by Youngs et al. (1987) and another of the "Wasatch Hinterland" by Sullivan et al. (1986) include identical premises; both studies are based on detailed analyses of seismicity and seismic geology.

4.1.1 Mathematical Background for Rate Estimation

The most commonly used mathematical model for the occurrence of independent earthquake main shocks is their representation by the well-known Poisson process, that is, a random memoryless arrival process in which events occur with a stationary average rate λ and with interevent times that have an exponential distribution. In considering the estimation of rate of earthquake occurrence—both from the historical and instrumental earthquake record and from geological observations of surface-faulting—it will be convenient to use properties of the Poisson process. Accordingly, we present mathematical background in this section for later reference.

The fundamental equation that describes the probability mass function for a Poisson distribution (e.g., Benjamin and Cornell, 1970) can be written in the form:

$$p(n|\lambda,t) = (\lambda t)^n \frac{e^{-\lambda t}}{n!}$$

where λ is the mean process rate and the random variable n represents the number of events occurring within a time interval t. The equation reads that the probability of n events, given λ and t, is computed from the right-hand side of the equation.

The problem we wish to consider is one where λ is not known *a priori*. Consider a basic case in which a Poisson process is operative and n events are observed in t years. We want to estimate the rate λ given these observations. Appropriately, we can use a maximum-likelihood approach in which a likelihood function, $L(\lambda)$, describes the relative likelihood that the parameter λ has a certain value, given the observations (e.g., Benjamin and Cornell, 1970). The likelihood function of λ, given *n* events in *t* years is given by (D. Veneziano, personal communication, 1987):

$$L(\lambda | \text{n events in t years}) = (\lambda t)^n e^{-\lambda t}$$

The maximum-likelihood estimator of λ is in fact n/t and gives the "most likely" value of λ. A plot of the likelihood function, for example Figure 4.1, gives the relative likelihood of other values of λ. If the likelihood function is normalized so that the area under its curve equals 1.0, then the normalized likelihood function is in effect a probability density function of λ, and confidence intervals can be identified in the usual way be relating the area under the density curve to cutoff values. Figure 4.1 illustrates a normalized likelihood function for λ given an observation of 1 event in 15,000 years. The most likely value of λ is 1 divided by 15,000 or 6.67×10^{-5} events/yr. There is a probability of 0.95 that the true value of λ is less than or equal to $\lambda_{.95}$ or 3.13×10^{-4} events/yr. Hence, $\lambda_{.95}$ provides an upper-bound estimate of λ that can be made with 95 percent confidence.

4.2 Seismic Source Zones

4.2.1 Source Zones Based on Seismicity

The summary plot of regional seismicity surrounding the proposed SSC sites (Figure 3.6), described in section 3.4, is dominated by small to moderate-size earthquakes, the largest of which is the M_S6.6 Hansel Valley earthquake of 1934. Seismicity compilations with magnitude thresholds below the 2.7 value of Figure 3.6 emphasize the diffuse scatter of seismicity (Arabasz et al., 1980; Arabasz, 1984), and results of detailed portable-array studies confirm the pattern and verify that the spatial scatter is not simply due to inadequate epicentral precision (e.g., Arabasz and Julander, 1986). Accordingly, we define a background source zone that extends throughout the study area of Figure 3.6 and which has a maximum magnitude of 6.5—based on the magnitude 6.0 to 6.5 threshold of surface faulting (section 2.3.5). A similar approach was adopted by Youngs et al. (1987). In their use of a logic-tree approach for parameter selection, they adopted a maximum magnitude (with assigned weight) of 6 (0.2), 6¼ (0.5), and 6½ (0.3) for a background source zone.

Because we believe that earthquakes larger than magnitude 6.5 will occur on identifiable faults, there remains no practical need to depict isolated source zones based on seismicity

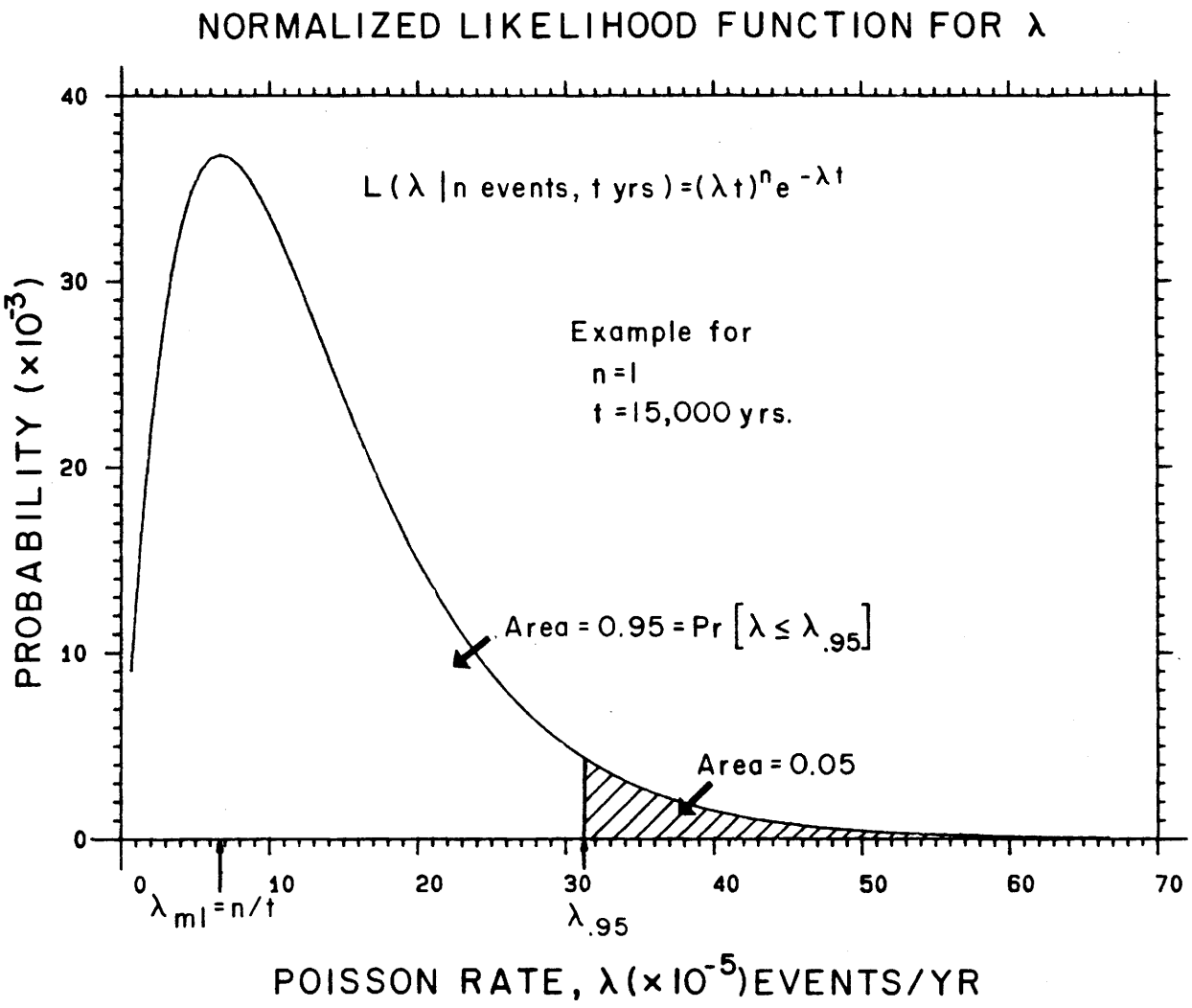

Figure 4.1 An example of a normalized likelihood function for estimating λ, the rate parameter of a Poisson process, when the true value of λ is unknown. The likelihood function arises from the observed occurrence of n events during a total time period of t years. λ_{ml} is the "most likely" value of λ; λ_{95} is an upper limit of λ estimated with 95 percent confidence. (See text for further explanation.)

alone. This is particularly true for seismicity within the site vicinity (Figure 3.7), whose spatial randomness is apparent. Inspection of the density pattern of epicenters in Figure 3.6 suggests distinct inhomogeneity in activity rate for a background source extending throughout the regional study area. This problem is addressed specifically in section 4.3.

4.2.2 Fault-Specific Sources—Identification and Recency of Movement

Following the compilation of a map of late Pleistocene and Holocene faulting for the regional study area (Figure 2.5), fault-specific seismic sources were identified within 100 km of the perimeter of the candidate SSC sites. Twenty-one fault sources within that distance have been labeled in Figure 4.2., and basic information compiled for these sources is summarized in Table 4.1. A goal of the tabulation was the estimation of a maximum earthquake and the probability of such an event occurring within each identified fault source.

The rationale for special identification of fault-specific sources out to a distance of 100 km was the following. Campbell (1987) presents a range of median estimates of peak horizontal acceleration appropriate for the Wasatch Front region incorporating variability in fault type, site amplification, and anelastic attenuation. Taking the upper envelope of these median estimates for a magnitude 7.5 earthquake, only earthquakes closer than 90 km contribute a peak horizontal acceleration of 0.1 g or greater, which was judged to be an appropriate threshold of interest.

With three exceptions, all of the fault sources labeled in Figure 4.2 are known to be active. The exceptions are sources 1, 2, and 4, which have been included for the sake of argument. Source 1 is based on ongoing mapping of fault scarps within the Tooele 1° x 2° map sheet by T.P. Barnhard of the U.S. Geological Survey (personal communication, 1987), as a follow-up to earlier mapping by Bucknam (1977). Source 1 is identified as suspected Pleistocene faulting on the east flank of the Cedar Mountains based on photolineaments which Barnhard had not yet checked in the field. Source 2 represents suspected Quaternary faulting on the west flank of the Lakeside Mountains described by Anderson and Miller (1979) from earlier work. Such faulting does not appear on the map of Bucknam (1977), and T.P. Barnhard (personal communication, 1987) recognizes a lineament at that location which closely follows one contour interval, making it doubtful in his opinion that it is of fault origin. Source 4 represents suspected Quaternary faulting on the east flank of the Newfoundland Mountains, which Anderson and Miller (1979) ascribe to earlier mapping; at the same time they note a personal communication from R.C. Bucknam expressing doubt in the existence of such faulting at that location.

As typical for any compilation of fault parameters, complete information was not available for Table 4.1, and generalizations were necessary, especially regarding the recurrence of faulting on an individual source. Beginning with the age of last movement, there is one fault (source 3) within the 50-km-radius zone that may have ruptured in Holocene time. From fault-scarp geomorphometry, T.B. Barnhard (personal communication, 1987) recognizes two separate faulting events on source 3 located in northwestern Puddle Valley: (1) an event predating the Bonneville shoreline, which is dated as 15,000 yrs old; and (2) a younger post-

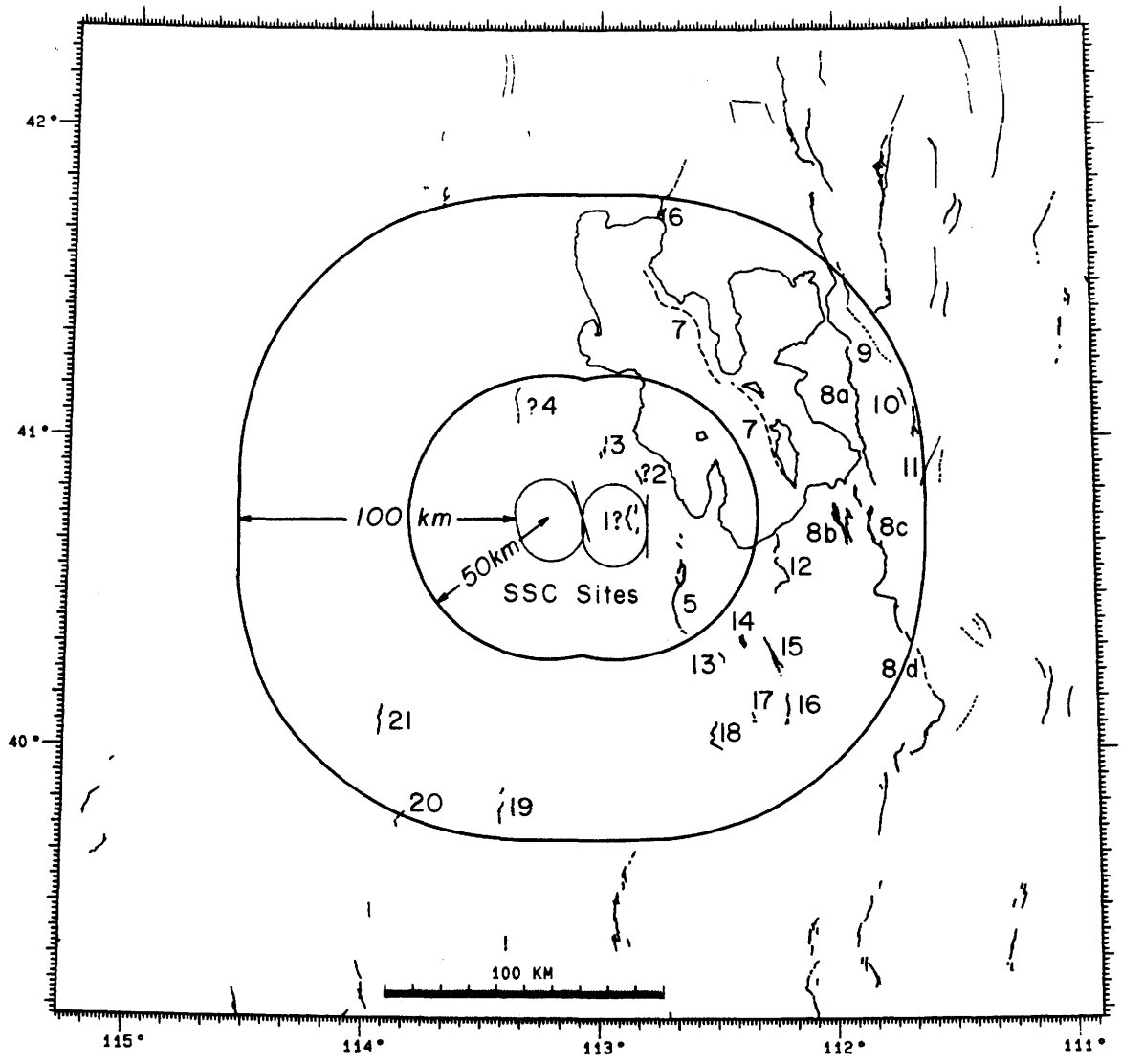

Figure 4.2 Map of late Quaternary faulting within the regional area surrounding the SSC candidate sites (as in Figure 2.5). Queries indicate suspected faulting. Fault-specific seismic source zones within 100 km of the perimeter of the SSC alignments are numbered and described in Table 4.1.

TABLE 4.1 INFORMATION FOR FAULT-SPECIFIC SOURCES†
(KEYED TO FIGURE 4.2)

	Fault Source	Age of Last Movement	Approx. Length	Maximum Magnitude. M_s	Minimum Distance To Site	Annual Probability of Max. Earthquake
1.	E. flank of Cedar Mts., suspected Pleistocene faulting (T. Barnhard, USGS, pers. comm., 1987)	(>15K yr)	10 km	(6.6)	<5 km	($\leq 1.0 \times 10^{-4}$)
2.	W. flank of Lakeside Mts., suspected Quaternary fault (Anderson and Miller, 1979)	(>>15K yr)	5-7 km	(6.5)	<5 km	($\leq 1.0 \times 10^{-4}$)
3.	NW Puddle Valley (Bucknam, 1977; T. Barnhard, USGS, pers. comm., 1987)	9-15K yr	≥7-10 km	(6.6)	10 km	($\leq 1.0 \times 10^{-4}$)
4.	E. flank of Newfoundland Mts., suspected Quaternary fault (Anderson and Miller, 1979)	(>>15K yr)	15 km	(6.8)	20 km	($\leq 1.0 \times 10^{-4}$)
5.	W. flank of Stansbury Mts. (Bucknam, 1977; T. Barnhard, USGS, pers. comm., 1987)	20-24K yr	30-40 km	(7.3)	10 km	($\leq 1.0 \times 10^{-4}$)
6.	Hansel Valley fault (Youngs et al., 1987)	53 yr	25 km	7.0	95 km	$\leq 1.7 \times 10^{-4}$
7.	East Great Salt Lake fault (Pechmann, 1987)	<10K yr?	53 km	(7.4)	45 km	$[2.5\text{-}7.5] \times 10^{-4}$
8a.	Wasatch fault, Ogden segment (Youngs et al., 1987; Schwartz and Coppersmith, 1984)	≤500 yr	78 km	7.5	75 km	$\leq 1.0 \times 10^{-3}$
8b.	West Valley fault zone (Youngs et al., 1987; S.J. Olig, written comm., 1986)	<10K yr	18 km	6.75	65 km	$\leq 3.7 \times 10^{-4}$
8c.	Wasatch fault, Salt Lake City segment (Youngs et al., 1987; Schwartz and Coppersmith, 1984)	<2K yr	45 km	7.5	75 km	$\leq 7.2 \times 10^{-4}$
8d.	Wasatch fault, Provo segment (Youngs et al., 1987; Schwartz and Coppersmith, 1984)	1-3K yr	70 km	7.5	90 km	$\leq 7.2 \times 10^{-4}$
9.	Ogden Valley fault zone (Sullivan et al., 1986)	>10K yr	≥18 km	(6.9)	90 km	$\leq 4.0 \times 10^{-5}$
10.	Morgan fault (Sullivan et al., 1986)	<10K yr	18 km	(6.9)	95 km	$\leq 4.0 \times 10^{-5}$

TABLE 4.1 (CONTINUED)

	Fault Source	Age of Last Movement	Approx. Length	Maximum Magnitude. M_s	Minimum Distance To Site	Annual Probability of Max. Earthquake
11.	East Canyon fault (Sullivan et al., 1986)	>10K yr	≥12 km	(6.7)	100 km	$\leq 4.0 \times 10^{-5}$
12.	N. Oquirrh Mts. fault fault zone (Youngs et al., 1987; T. Barnhard, USGS, pers. comm., 1987)	8-13.5K yr	35 km	(7.3)	45 km	$(\leq 1.0 \times 10^{-4})$
13.	Clover--NE flank of Onaqui Mts. (Bucknam, 1977; T. Barnhard, USGS, pers. comm., 1987) Everitt and Kaliser, 1980)	>15K yr	4-7 km	(6.5)*	45 km	$(\leq 1.0 \times 10^{-4})$
14.	Saint John Station--central Rush Valley (Bucknam, 1977; T. Barnhard, USGS, pers. comm., 1987; Everitt and Kaliser, 1980)	>15K yr?	6 km	(6.5)*	45 km	$(\leq 1.0 \times 10^{-4})$
15.	Mercur--SW flank of Oquirrh Mts. (Bucknam, 1977; T. Barnhard, USGS, pers. comm., 1987; Everitt and Kaliser, 1980)	>15K yr?	15 km	(6.8)	55 km	$(\leq 1.0 \times 10^{-4})$
16.	Topliff Hill--W flank of Northern E. Tintic Mts. (Bucknam, 1977; T. Barnhard, USGS, pers. comm., 1987; Everitt and Kaliser, 1980)	>15K yr?	11 km	(6.7)	70 km	$(\leq 1.0 \times 10^{-4})$
17.	Vernon Hills (Bucknam, 1977; T. Barnhard, USGS, pers. comm., 1987; Everitt and Kaliser, 1980)	>15K yr	4-7 km	(6.5)	70 km	$(\leq 1.0 \times 10^{-4})$
18.	E. flank of Sheeprock Mts. (Bucknam, 1977; T. Barnhard, USGS, pers. comm., 1987; Bucknam and Anderson, 1979b; Everitt and Kaliser, 1980)	>15K yr?	11-14 km	(6.8)	65 km	$(\leq 1.0 \times 10^{-4})$
19.	E. flank of Fish Spring Mts. (Bucknam and Anderson, 1979a,b)	~2K yr	13 km	(6.8)	80 km	$(\leq 1.0 \times 10^{-4})$
20.	SE flank of Deep Creek Mts. (Bucknam and Anderson, 1979a,b)	>15K yr	6 km	(6.5)*	100 km	$(\leq 1.0 \times 10^{-4})$
21.	NW flank of Deep Creek Mts. (Bucknam, 1977; T. Barnhard, USGS, pers. comm., 1987)	>15K yr	12 km	(6.7)	75 km	$(\leq 1.0 \times 10^{-4})$

†Values in parentheses calculated or estimated in this report (see text).
*Computed value slightly less than 6.5; threshold value of 6.5 assumed.

Bonneville event that occurred 9,000 years ago at the latest—making the faulting latest Pleistocene or early Holocene (?). Hence, the generalization implied in Figure 2.4a that the SSC sites lie within a domain of Holocene faulting is plausible but not certain.

Within the 50-to-100-km distance range, Holocene faulting is well established on the Wasatch fault zone (sources 8a, 8c, 8d), the West Valley fault zone (source 8b), the Morgan fault (source 10), and along the eastern flank of the Fish Springs Mountains (source 19). Holocene faulting seems highly probable on the East Great Salt Lake fault (source 7; see section 2.3.2). On the other sources, the age of last movement is either unquestionable pre-Holocene or the possibility of rupture in earliest Holocene time must be considered.

In the southeast quadrant from the SSC sites there are eight sources (5, 12, 13, 14, 15, 16, 17, 18) that lie within a domain characterized by Bucknam et al. (1980) as having late Quaternary faulting but no Holocene faulting (compare Figures 2.4a and 4.2). Young faulting on each of these sources has been studied by T.P. Barnhard (personal communication, 1987) using fault-scarp geomorphometry, and he confirms that result. A possible exception is the Northern Oquirrh Mountains fault zone (source 12), on which Barnhard recognizes a faulting event younger than 15,000 years in age that may be "earliest Holocene at best." Youngs et al. (1987) describe information suggesting a bracketing of the most recent faulting event on source 12 as between 8,000 and 13,500 years ago.

It should be noted that Everitt and Kaliser (1980) conflict in their interpretation with those of Bucknam et al. (1980) and T.P. Barnhard in that the former interpret post-Bonneville faulting on sources 5, 14, 15, 16, and 18—with the possibility of Holocene faulting on sources 5 and 18. Results of fault-scarp geomorphometry applied by Barnhard (personal communication, 1987) rely on studies by Pierce and Coleman (1986) for careful calibration, and, we suggest, may be more reliable than those of Everitt and Kaliser (1980). Throughout the entire area of the Tooele 1° x 2° map sheet (40°N-41°N, 112°W-114°W), Barnhard (personal communication, 1987) has identified only two faults with evidence of faulting younger than 15,000 years—the faulting already described in Puddle Valley (source 3) and on the Northern Oquirrh Mountains fault zone (source 12); regarding the most recent faulting on the west flank of the Stansbury Mountains (source 5), Barnhard determines an estimated age of 20,000 to 24,000 years. In Table 4.1 we have queried the age of last movement on sources 14, 15, 16, and 18 to call attention to the conflicting interpretations of Everitt and Kaliser (1980).

4.2.3 Fault-Specific Sources—Recurrence and Maximum Magnitude

The information just presented on recency of faulting is important for estimates of recurrence (and hence the annual probability of occurrence) for the maximum earthquake on the fault-specific seismic sources. The best estimates of recurrence tabulated in Table 4.1 are for sources 6, 8a, 8b, 8c, and 8d, for which Youngs et al. (1987) were able to use available paleoseismicity data. Sullivan et al. (1986) similarly provide reasonable estimates for sources 9, 10, and 11, and an estimate by Pechmann (1987; see also section 2.3.2) for source 7 is reasonably based. For the remainder of the faults in Table 4.1, all of which lie within the Basin and Range province and within the "Western Desert" region, a generic approach was adopted

for estimating the annual probability of occurrence of the maximum earthquake. These values appear in parentheses. We proceed to explain our logic.

The faults we are considering total 15 in number (sources 1-5, 12-21) and lie 35-120 km west of the Wasatch fault. Although slip-rate data are not readily available for these faults, slip rates are likely to be of the order of 0.1-0.2 mm/yr or less (e.g., Schwartz, 1987), which is the case for faulting away from the Wasatch fault in the Wasatch Hinterland (Sullivan et al., 1986; Nelson and Van Arsdale, 1986) and for the East Cache and Hansel Valley faults (Youngs et al., 1987). For one of the faults, the Northern Oquirrh fault zone (source 12), Youngs et al., (1987) evaluate the slip rate as being 0.2 mm/yr or less with a subjective probability of 0.94. An average earthquake recurrence interval can be estimated by dividing the slip rate into the displacement per event (Wallace, 1970). Assuming displacements of 1.0-4.0 m (justified below), with a typical displacement on these faults of 2 m (T.P. Barnhard, personal communication, 1987), a slip rate of 0.1 mm/yr would imply an average recurrence of 10,000 to 40,000 yrs; similarly a slip rate of 0.2 mm/yr would imply an average recurrence of 5,000 to 20,000 yrs.

There are inadequate data in the Wasatch Front region to model the interevent times of surface-faulting events on the same fault or fault segment, but such intervals in intraplate environments such as the Great Basin are highly variable and can differ by a factor of four or five (Schwartz, 1987). Wallace (1987) argues for considerable nonuniformity of fault recurrence in the Great Basin. Thus while fault recurrence on major faults in California might be more time-predictable because of high strain rates and relatively constant stress accumulation (Schwartz, 1987), a Poisson model of random occurrence is reasonable to consider for surface-faulting on the Basin-Range faults we are evaluating.

If we consider the occurrence of only one surface-faulting event during a period of 15,000 yrs, which was the described case for the Puddle Valley and Northern Oquirrh faults (sources 3 and 12), then we can use the mathematical arguments developed in section 4.1.1 if we assume a Poisson arrival process. The observation of 1 event in 15,000 yrs leads to an upper-bound estimate of λ at the 95-percent confidence level of 3.13×10^{-4} events/yr, or a *minimum* average recurrence interval of 3200 yrs.

The observed pattern of late Pleistocene-Holocene surface faulting on the faults we are considering provides an important perspective. We have pointed out that only 3 (sources 3, 12, and 19) of the 15 faults have produced surface-faulting during the past 15,000 years, and only as single events. Allowing for argument the uncertainty introduced by the interpretations of Everitt and Kaliser (1980), the number would increase to 7. Figure 4.3 shows a plot of probabilities of observing no event, exactly one event, one event or less, and two events or less during a period of 15,000 years—assuming different average recurrence intervals for a Poisson process. The important observation is that the likelihood of observing the paucity of surface faulting that in fact we see during the past 15,000 yrs is more consistent with an average recurrence interval exceeding 10,000 yrs than the *minimum* interval of 3200 yrs that we first calculated.

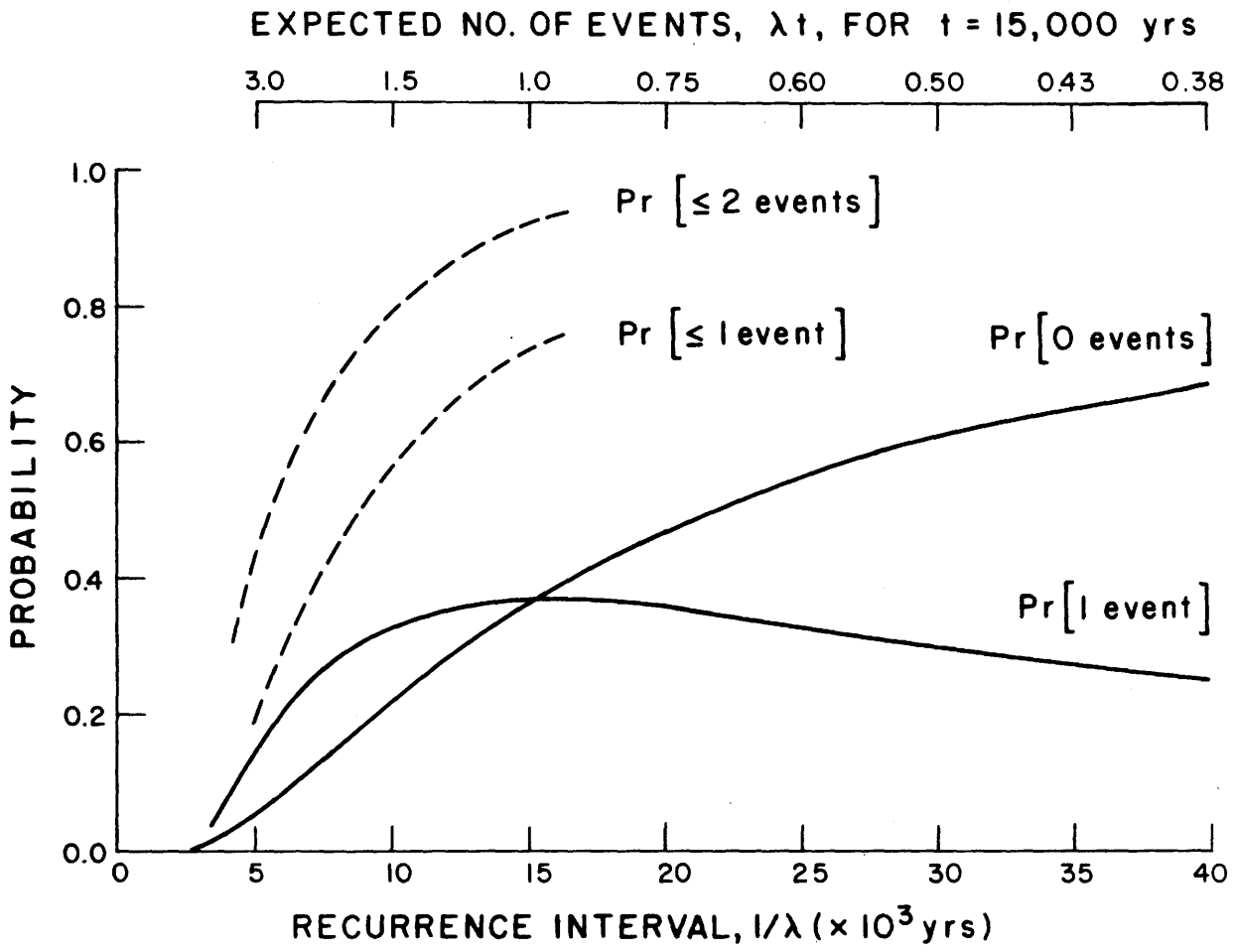

Figure 4.3 Probabilities of occurrence of a specified number of surface-faulting events, on an individual fault, during a period of 15,000 yrs as a function of average recurrence interval, assuming a Poisson arrival process (see section 4.1.1 for background).

Another way to view the observed pattern of late Pleistocene-Holocene surface faulting is the following. From our observation of 3 to 7 surface-faulting events on 15 faults during a time period of 15,000 yrs we can compute $\lambda_{.95}$ using our likelihood-function approach again. Assuming 3 events, $\lambda_{.95}$ = 0.51 events per 15,000 yers per fault—or 29,400 yrs average recurrence per fault. Assuming 7 events, the average recurrence interval becomes 17,400 yrs. Doubling the number of potentially active faults reduces the average recurrence interval per fault to 8,700-14,700 yrs.

On the basis of inferred slip rates, the observation of 3 to 7 single-event fault scarps on 15 faults during the past 15,000 yrs, and the probabilities of observing such a paucity of faulting as a function of recurrence interval, we judge that the average recurrence interval characterizing the group of faults we are evaluating exceeds 10,000 yrs. We adopt 10,000 yrs as a conservative estimate and find no reason to assign a smaller value to any individual fault within the group. Accordingly, the annual probability estimated for each fault source of this generic group is $\leq 1.0 \times 10^{-4}$.

Our final consideration for the fault-specific seismic sources is that of assessing maximum magnitude. Youngs et al. (1987) outline three general approaches to estimating maximum magnitude for fault sources in the Wasatch Front region variously using three widely accepted techniques based respectively on empirical estimates of magnitude from rupture length, rupture area, and seismic moment. Estimates of maximum magnitude in Table 4.1 from Youngs et al. (1987) for sources 6, 8a, 8b, 8c, and 8d are judged to be well-founded. The value tabulated is the maximum value cited for those sources, even though it may not have had the greatest weight in the logic-tree formulation by Youngs et al. (1987).

For consistency with the probabilistic hazard analysis of the Wasatch Front region carried out by Youngs et al. (1987), we have judged it appropriate to follow their approach to maximum magnitude—with some suitable modifications. Figure 4.4 outlines the basic approach. Where information on maximum fault displacement was available, procedure (A) was used; otherwise, procedure (B) was more generally followed. The weighting scheme follows the conditional subjective probabilities used by Youngs et al. (1987).

The specific empirical relations used in conjunction with the logic tree of Figure 4.4 were the following. For estimation of magnitude from rupture length, the relation selected from Slemmons (1982) was that for normal-slip earthquakes given by:

$$M_S = 0.809 + 1.341 \text{ (log length, meters)}$$

A similar relation selected from Bonilla et al. (1984) was their relation based on data for all faults and given by:

$$M_S = 6.04 + 0.708 \text{ (log length, kilometers)}$$

For estimating magnitude from fault area, we have preferred to adopt a relation from Singh et al. (1980) instead of one from Wyss (1979) that was used by Youngs et al. (1987). The relation given by Singh et al. (1980) was derived from data for intraplate earthquakes and is given by:

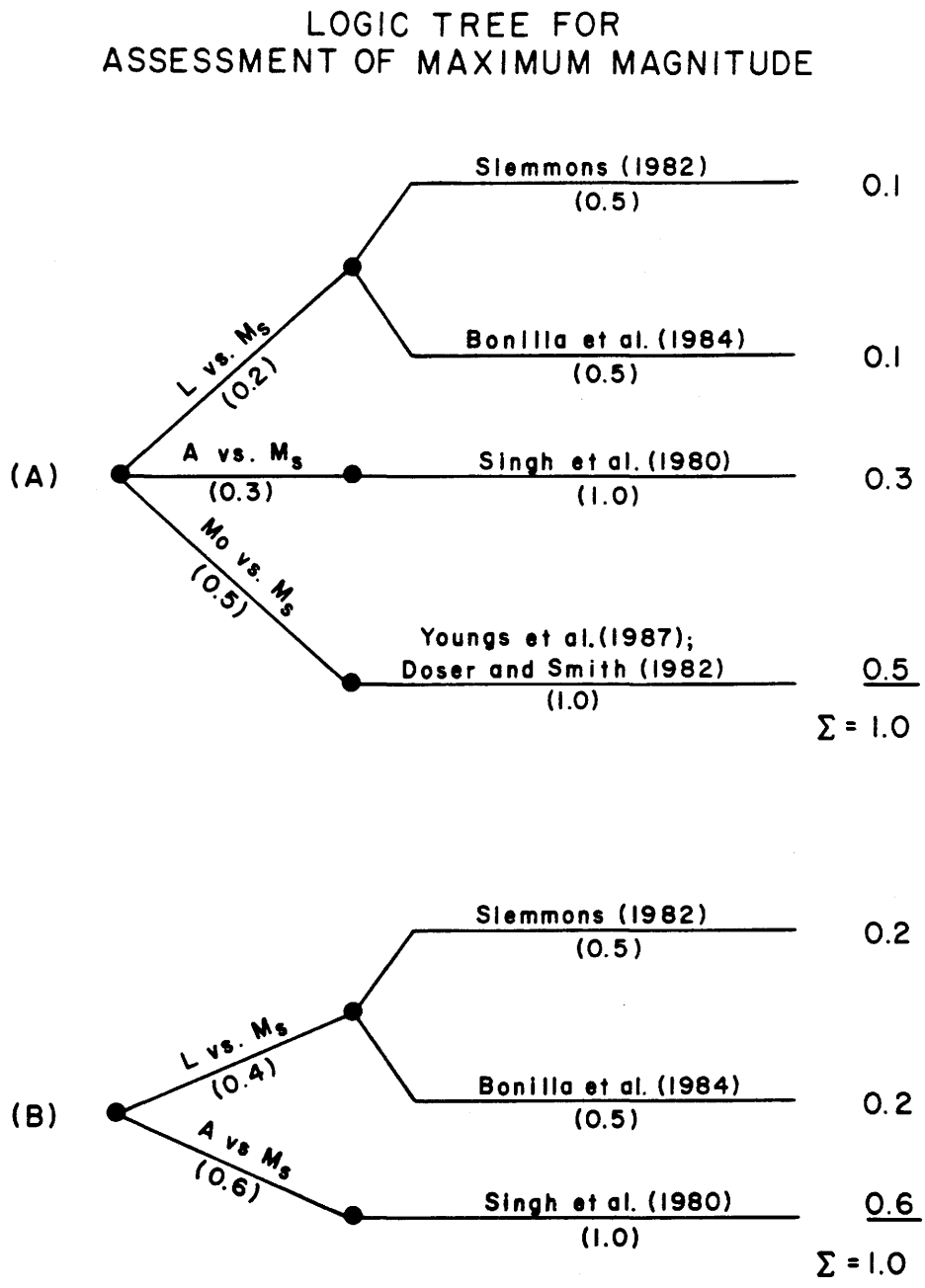

Figure 4.4 Logic-tree outline of methods and corresponding weights used to assess a maximum magnitude for fault-specific sources (see text). L represents rupture length; A, rupture area; M_S, surface-wave magnitude; M_O, seismic moment.

$$M_S = \log (\text{area, km}^2) + 4.53$$

Rupture area was estimated by assuming rupture on a fault dipping 60° extending to the bottom of a seismogenic layer 15 km thick. The relation of Singh et al. (1980) was chosen because of its agreeable predictions for the 1934 Hansel Valley, Utah, earthquake (M_S = 6.8 versus 6.6 observed), the 1959 Hebgen Lake, Montana, earthquake (M_S = 7.3 versus 7.5 observed), and the 1983 Borah Peak, Idaho, earthquake (M_S = 7.3 versus 7.3 observed).

We were able to use a moment magnitude approach for five fault sources for which T.P. Barnhard (personal communication, 1987) was able to provide maximum displacements from single-event scarps that had been carefully profiled—and for which the values were judged to be representative of the maximum earthquake for those sources. These were: 4.08 m for the Northern Oquirrh Mountains fault zone (source 12), 3.86 m for the Stansbury Mountains fault zone (source 5), 1.93 m for the Mercur fault (source 15), 2.34 m for the Puddle Valley fault (source 3), and 0.65 m for the Clover fault (source 13). The *average* surface displacement d was assumed to be 0.5 times the maximum displacement (see Youngs et al., 1987), from which seismic moment M_0 was estimated from the relation (section 2.3.3):

$$M_0 = \mu S d$$

where μ is the shear modulus (3.3×10^{11} dyne/cm^2) and S is the fault rupture area. Magnitude was then estimated from a regression relationship derived by Youngs et al. (1987) by inverting moment-versus-magnitude data for the Utah region from Doser and Smith (1982):

$$M_S = -16.22 + 0.885 \log_{10} (M_0, \text{ dyne-cm})$$

In the case of the East Great Salt Lake fault, it should be noted that the tabulated length (and corresponding maximum magnitude) assumes that the fault is divided into two segments. For this fault, and all the others for which a maximum magnitude was estimated by the procedure outlined in Figure 4.4, the estimated values are systematically in good agreement with our seismological judgment and experience in the Intermountain seismic belt.

4.3 Seismicity Parameters

The standard way to characterize seismicity in any seismically active region is with the Gutenberg-Richter exponential frequency-magnitude relationship given by

$$\log N = a - bM$$

where N is the average number of independent events per year of magnitude M or greater and a and b are constants appropriate for the particular region. If we define A as the average number of events per year of $M \geq 3.0$, then the above equation can be rewritten as

$$N = A\ 10^{-b(M-3.0)}$$

For the purposes of this study, we are interested in modeling the frequency of occurrence of earthquakes in the near-site vicinity of $M_L \leq 6.5$, the approximate threshold of surface faulting. We chose to define the near-site vicinity as a circle extending 50 km outward

from the center of either of the proposed SSC sites (circles, Figure 3.7). These regions extend 35-38 km beyond the edges of the SSC rings. The area chosen was motivated both by seismicity patterns and by ground motion considerations. From Figures 3.6 and 3.7, the seismicity within a 50 km radius of the centers of the rings appears to be spatially homogeneous, and therefore we can assume that earthquakes have a uniform probability of occurrence anywhere within these two circles. Regarding ground motions, the attenuation relationship of Campbell (1987) predicts that a M_L 6.5 earthquake at the edge of one of these circles would cause a peak horizontal ground acceleration of 0.07-0.15 g on soil at the SSC site 35 km away. Ground motion having a peak horizontal ground acceleration of 0.1 g is generally taken to be the threshold of damage for weak construction.

Because of the very low rate of seismicity within the circular areas marked on Figure 3.7, it is not possible to obtain estimates of the seismicity parameters A and b directly from the observed seismicity in these regions. Within these regions, we believe that the earthquake catalog is complete above M_L 3.0 since July 1962 and above M_L 2.0-2.5 since October 1974. However, no earthquakes of $M_L \geq 3.0$ have been observed since July 1962 and only 4 earthquakes of $M_L \geq 2.0$ and none of $M_L \geq 2.5$ have been observed since October 1974. Because of the lack of earthquake activity above the uniform detection thresholds, we decided to incorporate information from a larger region in order to obtain estimates of earthquake recurrence.

In order to obtain meaningful estimates of earthquake recurrence from seismicity data, it is first necessary to remove from the data set dependent events such as aftershocks, foreshocks, and swarms. Shimizu (1987) identified dependent and independent events in the University of Utah catalog for the period July 1962 through December 1985 by applying the local clustering method of Veneziano and Van Dyck (1986). Shimizu's listing of independent events of $M_L \geq 2.0$ in the catalog for this time period was supplied to us on computer tape by D. Veneziano. The listing contained 468 events within the study area. To this listing, we added 8 independent events of $M_L \geq 2.0$ from the University of Nevada and NOAA catalogs. We used the resulting catalog of 476 mainshocks to determine detection thresholds and seismicity parameters for our study area.

One way to identify the uniform detection threshold for an area is to use a recurrence plot (log N versus M) to find the magnitude below which the observed frequency of events drops below the frequency expected from a linear extrapolation of the curve for larger events. Figure 4.5 is a cumulative recurrence plot for independent mainshocks in the western and eastern halves of the study area (solid curves) and in the study area as a whole (dots) from July 1962 through December 1985. The curve for the eastern half of the study area shows no signs of leveling off at smaller magnitudes. If anything, it appears to have a steeper slope for $M_L \leq 3.0$. The curve for the western half of the study area does not have a very well-defined slope above magnitude 3 due to the small number of events. Nevertheless, the observed frequency of earthquakes smaller than about magnitude 3 appears to fall below the expected frequency extrapolated from the larger events. Based on Figure 4.5 and similar plots for the time periods July 1962 through September 1974 and October 1974 through December 1985, we estimate that the uniform detection threshold since July 1962 is M_L 3.0 in the western half of

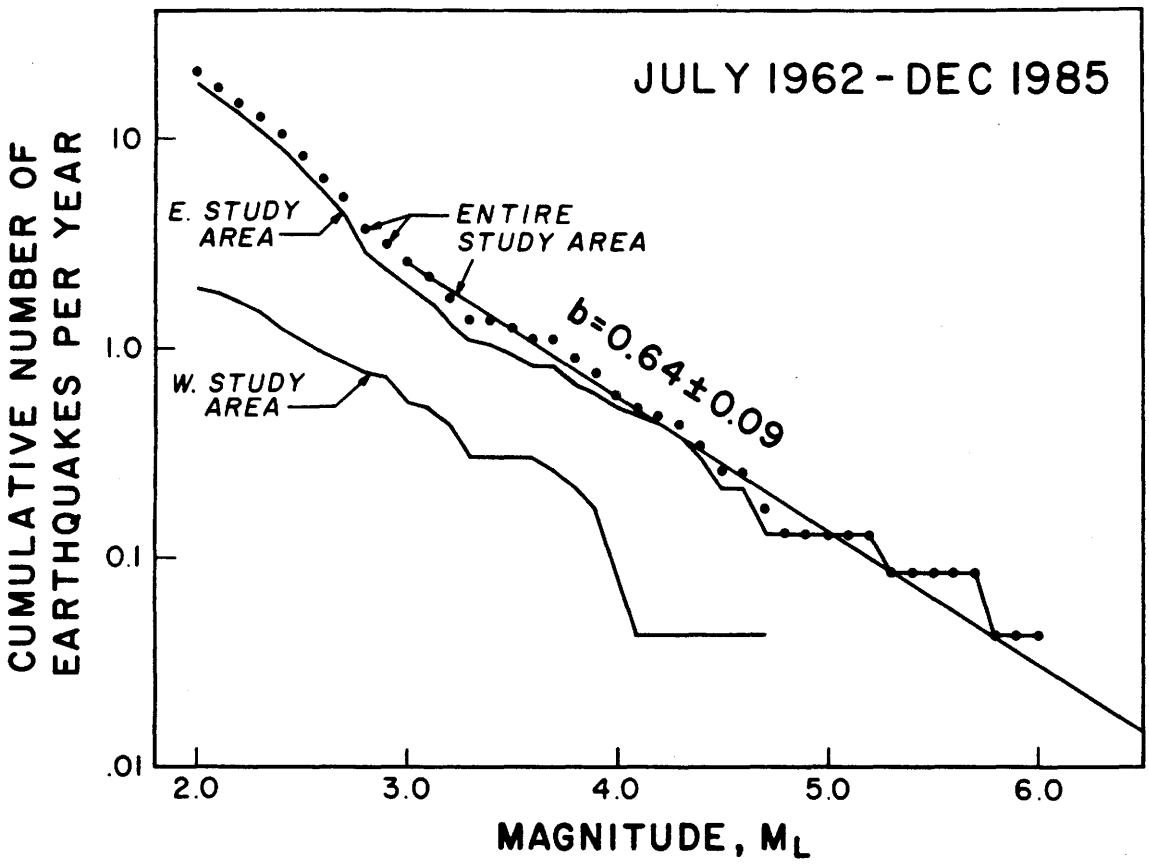

Figure 4.5 Recurrence data for independent mainshocks in the study area from July 1962 through December 1985. The plot shows the cumulative number of earthquakes per year greater than or equal to the local magnitude, M_L, given on the horizontal axis. The solid curves show the data for the western and eastern halves of the study area, with the dividing line at 113°05'W (Figure 3.6). The dots show the data for the entire study area. The straight line through the dots for $M_L \geq 3.0$ has a slope, b, of 0.64±0.09, calculated using the maximum likelihood method of Weichert (1980).

the study area and M_L 2.0 or less in the eastern half of the study area.

To determine an overall b-value for the study area, we fit a straight line to the recurrence data for independent mainshocks (dots, Figure 4.5) above M_L 3.0 using the maximum likelihood technique of Weichert (1980). The resulting line, which is shown on Figure 4.5, has a slope of b = 0.64±0.09. Since b values do not tend to vary greatly from one region to another, it is reasonable to assume that this b-value also applies to the near-site region (Figure 3.7).

Unfortunately, estimating an A-value for the region within 50 km of the SSC sites is not as straightforward as estimating a b-value. On a regional scale (Figure 3.6), the proposed SSC sites lie within a transition zone between the very active Wasatch front area to the east and the less active Great Salt Lake Desert to the west (see section 3.4 above). Thus, there is considerable uncertainty regarding the appropriate geographic area from which to calculate the A-value. The lack of seismicity near the sites suggests that the rate of activity there is probably more similar to that of the western half of the study area (Figure 3.6) than to the eastern half of the study area. We therefore decided to calculate estimates for A based on the observed seismicity in the following three areas: (1) a circle of 100 km radius around the center of the Cedar Mountains Site (eastern site, Figure 3.6); (2) the study area west of 113°05'; and (3) the study area as a whole. In our judgment, these values should constitute respectively a best estimate, lower bound, and upper bound for A.

During the 23.5 year period from July 1962 through December 1985, there were 9 independent mainshocks of $M_L \geq 3.0$ within the 100 km circle around the Cedar Mountains site. During this same period of time there were 13 such events in the western half of the study area and 60 such events in the entire study area. Normalizing these rates of occurrence to a circular region of radius 50 km yields average rates of 0.096, 0.068, and 0.157 $M_L \geq 3.0$ events per year, respectively. The latter rate of 0.157 derived from the earthquake count for the entire study area represents an average between the normalized rates for the eastern and western halves of the study area. Since we wish to use the rate for the entire study area as an upper bound on the A value, it is perhaps more appropriate to use the upper bound estimate for this rate at the 95% confidence level, 0.187, rather than the maximum likelihood estimate of 0.157 (see section 4.1.1). Thus, our upper bound estimate for the A-value is 0.187, our best estimate is 0.096, and our lower bound is 0.068. We used these A values, together with b-values of 0.64±0.09, to calculate best estimates and lower and upper bounds on the recurrence rates of earthquakes in the vicinity of the SSC sites.

Table 4.2 lists average return periods for earthquakes within 50 km of the proposed SSC sites. The preferred estimates shown for each magnitude cutoff were calculated using A = 0.096 and b = 0.64. The values in parentheses are lower and upper limits calculated using limiting values for the recurrence parameters estimated above: A = 0.187, b = 0.55, and A = 0.068, b = 0.73. The preferred estimates for the return periods given in Table 4.2 seem reasonable in light of the observed near-site seismicity (section 3.5). Within 50 km of the sites (circles, Figure 3.7), available records indicate a M_L 4-5 event in 1915, a M_L 3.0 (assumed) event in 1958, a M_L 2.5 event in 1965, and four M_L 2.0-2.3 events from October 1974 through March 1987. This observed activity is well within the expected levels given the estimated

TABLE 4.2

ESTIMATED AVERAGE RETURN PERIODS FOR EARTHQUAKES WITHIN 50 KM OF THE CENTER OF ALTERNATIVE SSC SITES

M_L	Return Period* (years)
≥2.0	2 (1-3)
≥3.0	10 (5-15)
≥4.0	45 (20-80)
≥5.0	200 (70-420)
≥6.0	870 (240-2300)

*The first number given is our preferred estimate. The numbers in parentheses give the lower and upper limits.

return periods listed in Table 4.2.

A more rigorous way to compare the observed and predicted seismicity rates is to apply the Poisson model to the earthquake activity in this region (see section 4.1.1). As mentioned previously, we believe that the earthquake catalog for the area shown in Figure 3.7 is complete at the $M_L \geq 3.0$ level since July 1962. No $M_L \geq 3.0$ events have occurred within a 50 km radius of either site since then. For a Poisson process, the probability P of having no occurrences within a time period t is given by

$$P = e^{-\gamma t}$$

Setting t = 25 years and γ = A, we obtain P = 18% for A = 0.068, P = 9% for A = 0.096, and P = 1% for A = .187. The first two probabilities are low but within the realm of possibility. The last probability is very small. Thus, this calculation suggests that an A value of 0.068-0.096 is much more likely than 0.187, which can be regarded as a very conservative upper limit.

4.4 Estimation of Site-Specific Ground Motion

Probabilistic estimates of maximum ground acceleration in Utah have been published by Bucknam et al. (1980), Algermissen et al, (1982), and Youngs et al. (1987). Of these studies, only that of Algermissen et al. (1982) encompasses the proposed SSC sites. On their map showing horizontal acceleration values in rock with a 90% probability of not being exceeded in 50 years, the sites fall between the 0.1 g and 0.2 g contours but closer to the 0.1 g contour (Figure 4.6). We therefore infer a value for the proposed SSC sites of about 0.15 g. For a 250 year exposure period, the sites lie close to the 0.4 g contour, indicating a 90% nonexceedance acceleration level of 0.4 g.

The study by Youngs et al. (1987) presents detailed probabilistic estimates of ground motion for the Wasatch front region, but unfortunately their study area only extends westward to about 112°20'. Along the western boundary of their study area at the latitude of the SSC sites, peak horizontal ground accelerations on rock with a 90% probability of not being exceeded are approximately 0.2 g and 0.5 g, for exposure times of 50 and 250 years, respectively. Since their peak acceleration contours decrease westward going away from the Wasatch fault, the acceleration values at the SSC sites should be less than these. Thus, the results of Youngs et al. (1987) are compatible with those of Algermissen et al. (1982) for the proposed SSC locations.

Bucknam et al. (1980) calculated maximum ground accelerations on rock with a 90% probability of nonexceedance in 50 years along a profile extending westward from the Wasatch fault near Salt Lake City. Although their calculation incorporated only earthquakes originating along the Wasatch fault zone, the Wasatch fault zone is a major contributor to seismic hazard in the region near the fault. This is especially true if one considers the Wasatch fault zone to be an important source of moderate as well as large earthquakes, as did Bucknam et al. At a distance of 75 km from the fault, the distance of the closest proposed SSC ring, their results indicate probable accelerations of 0.1 or less (Figure 4.7). These numbers are somewhat

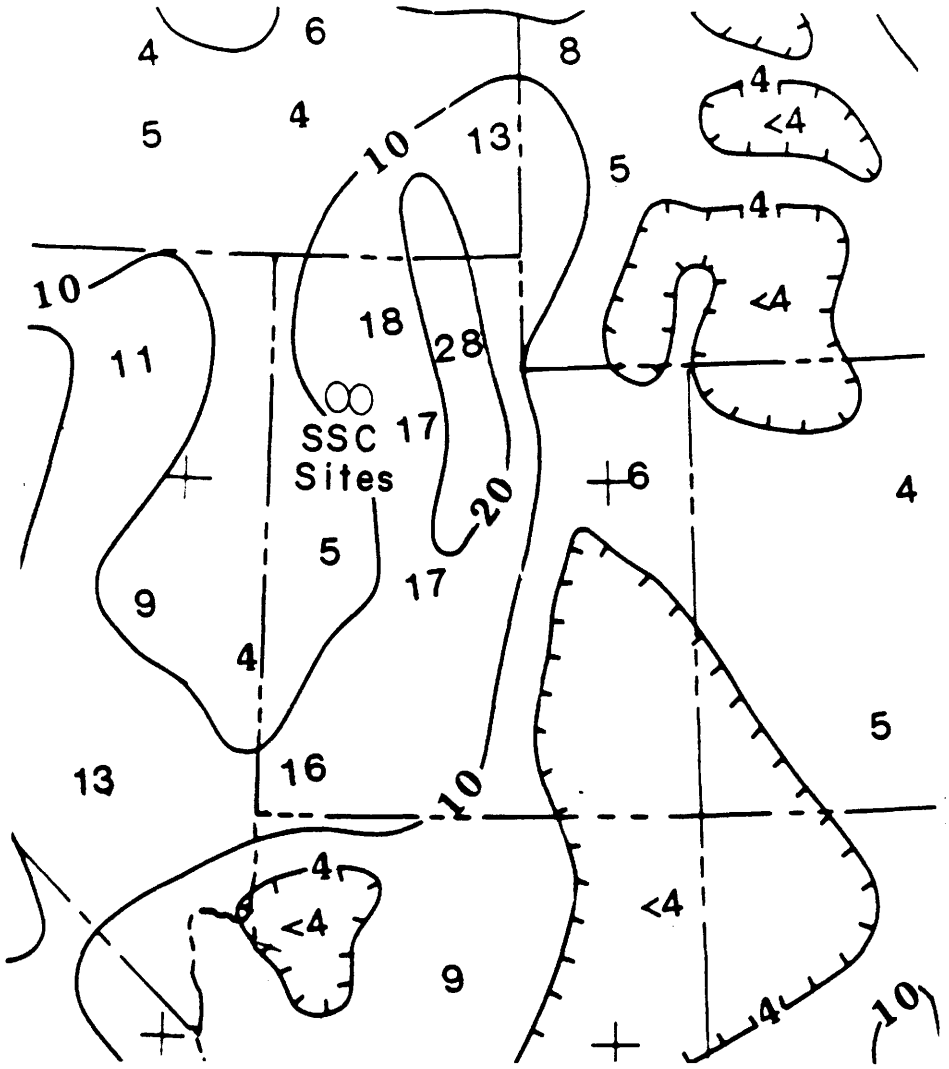

Figure 4.6 Location of the proposed SSC sites in Utah with respect to probabilistic ground motion map of Algermissen et al. (1982).

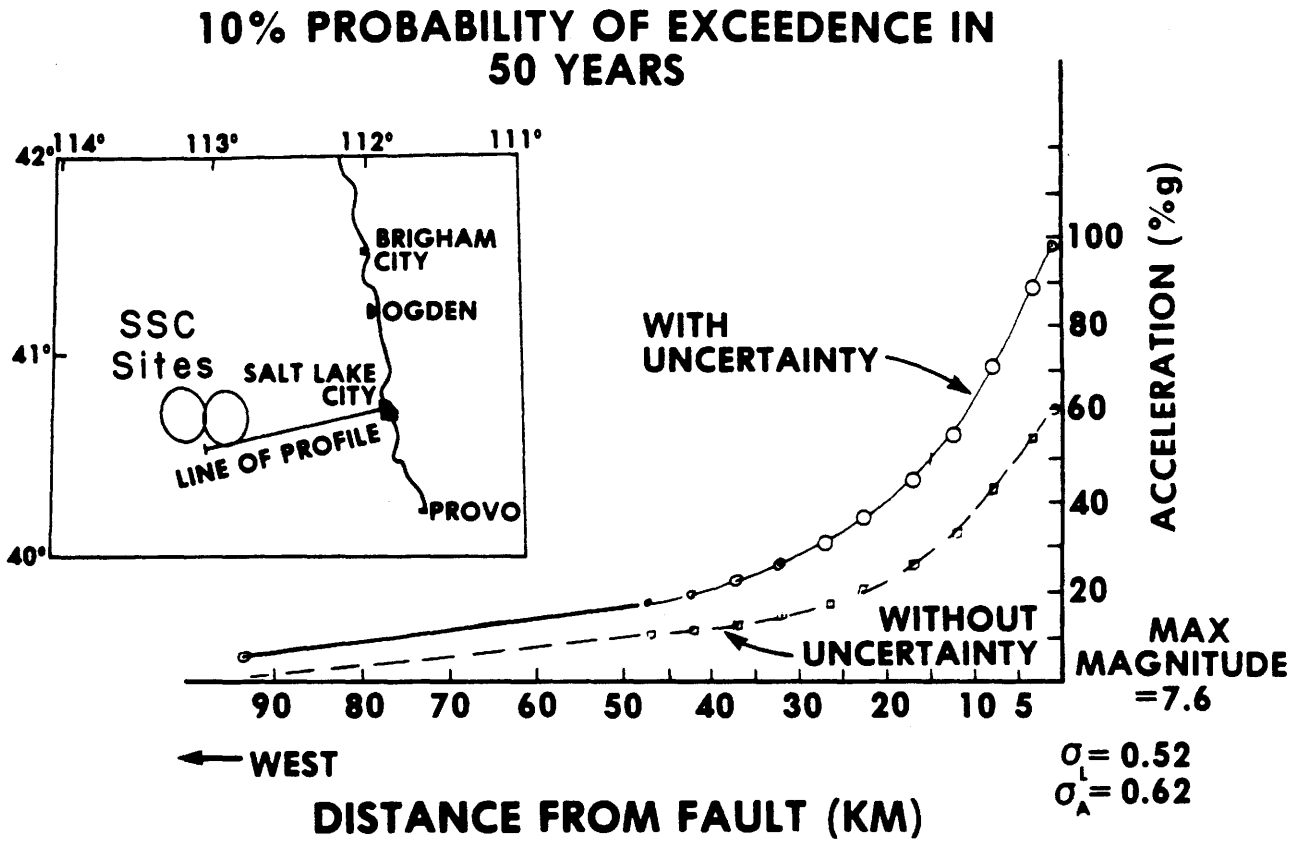

Figure 4.7 Probabilistic estimates of peak horizontal acceleration in rock on a profile perpendicular to the Wasatch fault with a 10 percent probability of exceedance in 50 years (from Bucknam et al., 1980). This computation is for earthquakes on the Wasatch fault only. The locations of the proposed SSC sites are shown for reference.

smaller than the value of 0.15 g estimated from the map of Algermissen et al. (1982), but this is expected since the latter study includes more seismic sources.

As a check on these published studies, we performed some simplified site-specific probabilistic calculations of ground shaking hazard using the method of Cornell (1968). Our calculation incorporated the two fundamental types of earthquake sources discussed above: (1) moderate ($M_L \leq 6.5$) earthquakes within a circular source area of radius 50 km centered on the site, and (2) the fault-specific sources in Table 4.1, which have maximum magnitudes of 6.5-7.5. Earthquakes within the circular source area are assumed to be independent in size and location, have a spatially uniform probability of occurrence, and have an exponential magnitude distribution. We used the seismicity parameters estimated in the previous section to characterize this source area. For the fault-specific sources, only the contribution of the maximum earthquake to the hazard was included in the computation. For these maximum earthquakes, the contribution to the annual probability of exceedance of a given peak acceleration value is the product of two factors: (1) the annual probability of occurrence of the earthquake, and (2) the probability that the given peak acceleration level will be exceeded if an earthquake with the specified magnitude and distance occurs. For sources 1, 2, and 4, the contribution to the hazard was multiplied by an additional factor of 0.5 to reflect the uncertainty regarding whether or not these faults are active.

Peak horizontal acceleration as a function of magnitude and distance was calculated using the constrained relationship of Campbell (1987). In this relationship, we used Campbell's value of anelastic attenuation for California (0.0059) and constants appropriate for strike-slip earthquakes (as opposed to reverse-slip earthquakes, the only other choice available) and deep soil ($\geq$ 10 m) or rock conditions. The natural log of the peak acceleration was assumed to be normally distributed about the predicted median value with a standard deviation of 0.3, the standard error given by Campbell. Some assumption about the depths of the earthquakes was necessary since Campbell defines source-to-site distance as the shortest distance between the site and the zone of seismogenic rupture. We assumed that the zone of seismogenic rupture penetrates to within 5 km of the surface for all earthquakes included in the computation. However, the assumed depth is important only for the small to moderate earthquakes (M_L 3.0 to 6.5) very near the site.

Most probabilistic ground motion studies, including the three published for Utah cited above, calculate the annual probability that various peak ground motion values will be exceeded at a specific point or series of points on the map. Because of the large size of the planned SSC facility, such an approach may underestimate the hazard to the facility as a whole. Accordingly, we decided to calculate the annual probability that ground acceleration values would be exceeded somewhere on a circle of radius 13 km, the average radius of the proposed SSC rings. For the small to moderate "background" earthquakes, events both inside and outside the circle were included in the computation. For the fault-specific sources, the source-to-site distance used was the minimum distance from the fault to either of the two proposed SSC rings, as listed in Table 4.1. Since most of the active faults in Table 4.1 lie to the east of the proposed sites (Figure 4.2), this set of distances is more applicable to the Cedar

Mountains (eastern) ring than to the Ripple Valley ring, but is conservative for either of the two rings considered separately.

Figure 4.8 presents preliminary graphs of the probability of exceedance per year versus peak horizontal ground acceleration for the proposed SSC rings. The three different curves were calculated using the three sets of seismicity parameters determined in section 4.3. Assuming that earthquake occurrence is a Poisson process, peak acceleration values having a 90% probability of nonexceedance in 50 years have an annual probability of 0.0021 or a return period of 475 years (horizontal line, Figure 4.8). For the middle curve (our best estimate) this acceleration value is 0.14 g. For the other two curves, the values are 0.11 and 0.20. Peak acceleration values having a 90% probability of nonexceedance in 250 years have a mean annual probability of 0.00042 or a return period of 2373 years. Our best estimate for this value is 0.27 g with lower and upper bounds of 0.23 g and 0.33 g, respectively.

Campbell (1987) presents another set of median attenuation curves for peak horizontal acceleration that he believes represent an upper bound for Utah given the current state of knowledge. These upper bound curves were calculated using a lower value for the anelastic attenuation constant (0.0044), plus a multiplicative factor of 1.4 derived for reverse and thrust earthquakes and an additional multiplicative factor of 1.5 for amplification on shallow soils ($\leq$10 m deep). The upper bound curves predict peak horizontal accelerations about a factor of two higher than his other set of curves. The multiplicative factor of 1.4 for reverse faults was found by regression analysis. The rationale for applying this factor in a normal-faulting regime such as Utah is that both normal faults and reverse faults typically have non-vertical dips. It is possible that the higher ground motions observed for reverse faults are due primarily to the fault dip rather than to the sense of slip. The amplification factor for shallow soils may apply to some parts of the Cedar Mountains site near the range front. Additionally, Campbell (1987) speculates that this factor may be appropriate for thick unconsolidated deposits, such as those in the Salt Lake Valley where U.S. Geological Survey seismologists have observed large amplifications of spectral velocities in certain frequency bands (Hays and King, 1982, 1984a, 1984b; Rogers et al., 1984; King et al., 1987).

The dashed curves in Figure 4.9 show the results of the hazard computation using Campbell's upper bound peak acceleration relationship. The annual probabilities of exceedance for all acceleration levels are significantly higher than those indicated by the solid curves. Acceleration values with a 90% probability of nonexceedance in 50 years are 0.24 g, 0.30 g, or 0.44 g, depending on the seismicity parameters assumed. For a 250 year exposure time, the values are 0.49 g, 0.57 g, and 0.70 g.

It is important to keep in mind that the calculations of probabilistic peak acceleration presented in Figures 4.8 and 4.9 are not directly comparable to the published calculations summarized in Figures 4.6 and 4.7. Our calculations are for a ring of radius 13 km rather than for point localities, and should therefore show a higher level of hazard. In order to assess the effect of the size and geometry of the proposed facility on our calculations, we determined another set of hazard curves for a point located at the center of the Cedar Mountains site (Figure 4.10). To compute these curves, we set the radius of the ring equal to zero in our program

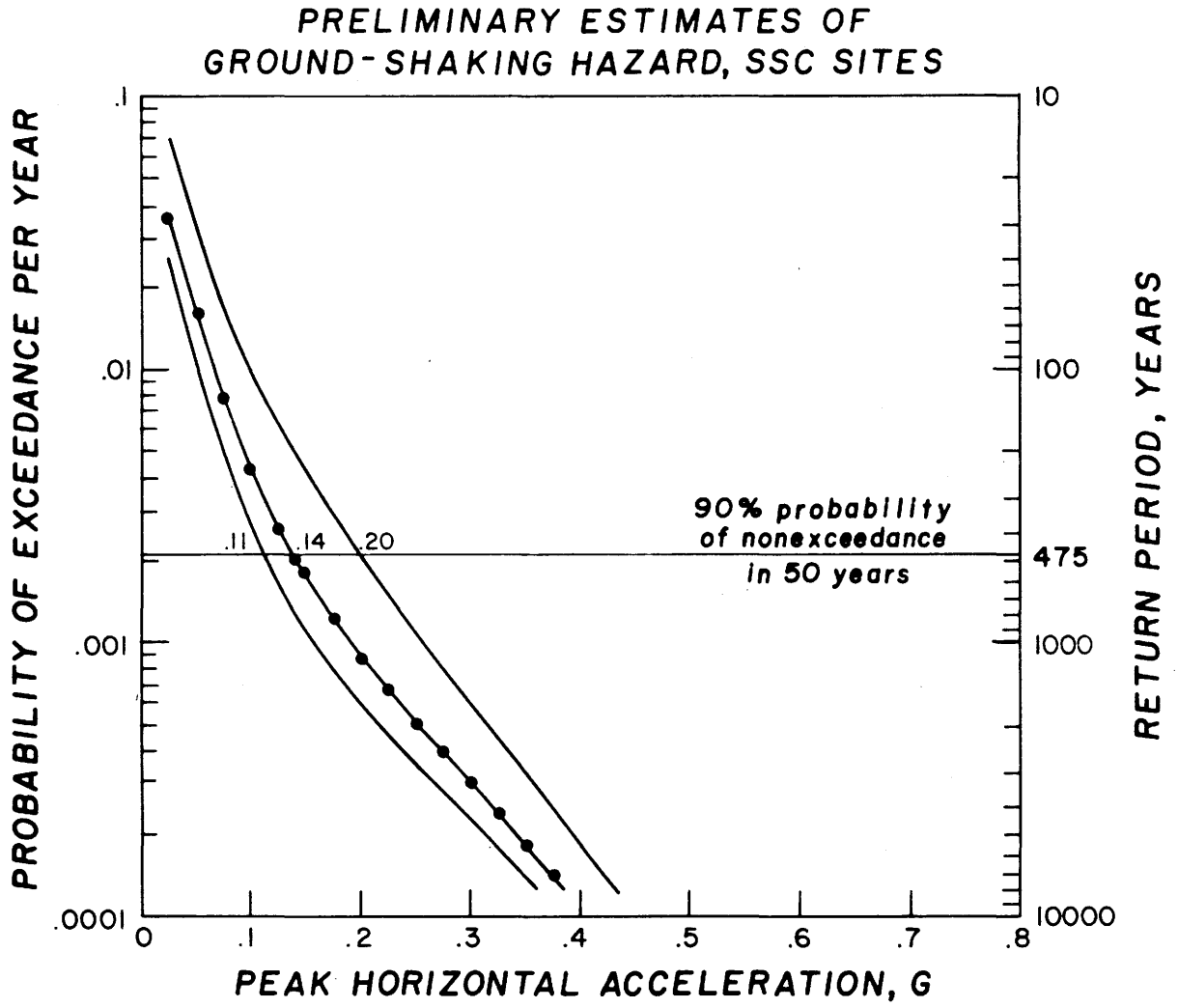

Figure 4.8 Preliminary graphs showing the probability of exceedance per year for peak horizontal ground accelerations on soil at the proposed SSC sites. The middle curve with dots showing the computed probability values was calculated using our best estimate for the seismicity parameters. The other two curves were calculated with the seismicity parameters used to determine the upper and lower limits on the return periods listed in Table 4.2. The vertical axis at the right shows the average return period in years (the inverse of the annual probability). The horizontal line marks the 475 year return period. The peak acceleration values with this return period (labeled) have a 90% probability of not being exceeded in 50 years.

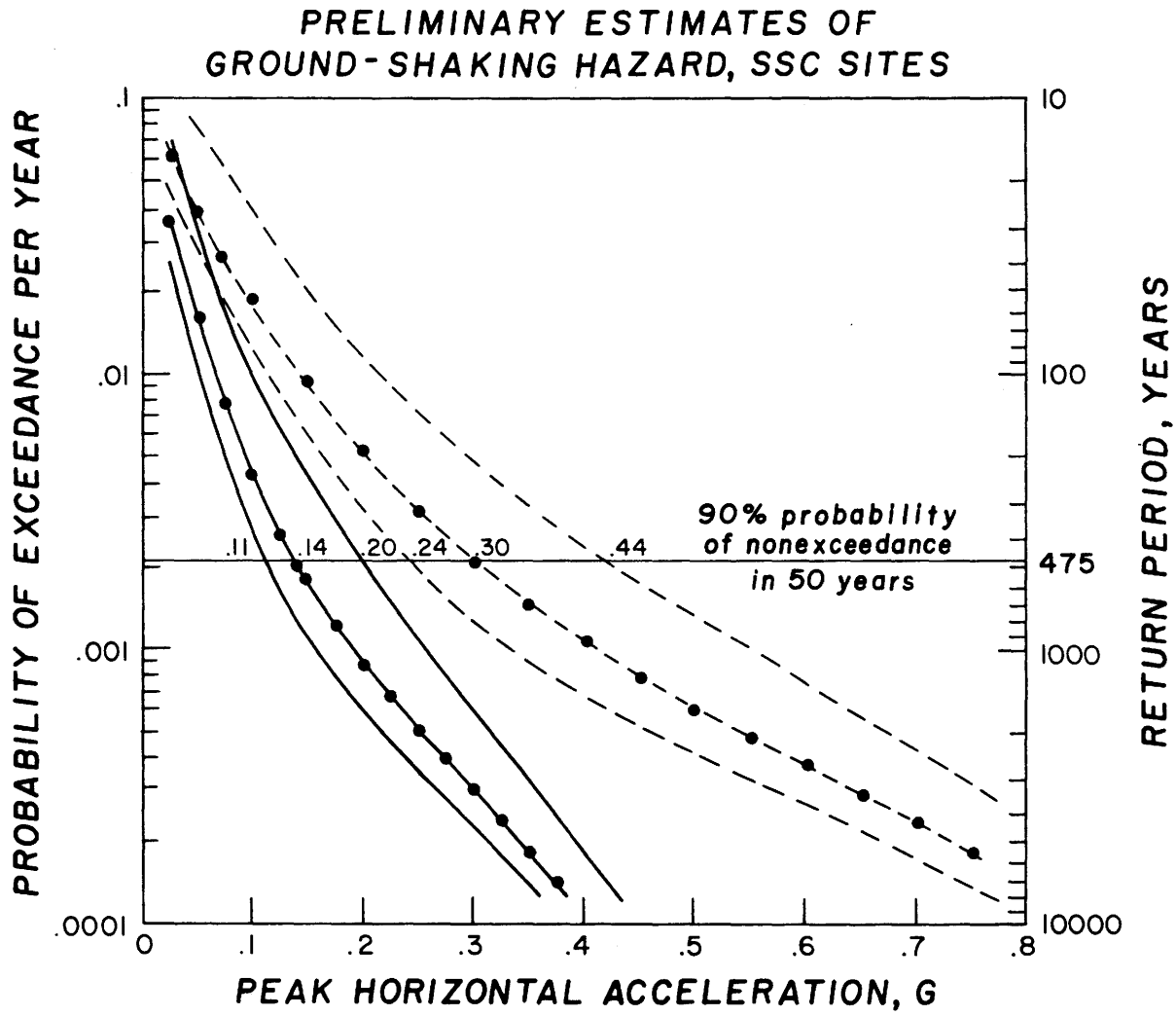

Figure 4.9 Alternative estimates of the ground shaking hazard at the SSC sites. The solid curves are the same as in Figure 4.8. The dashed curves were calculated with the same three sets of seismicity parameters but using the upper bound peak acceleration estimates of Campbell (1987) (see text).

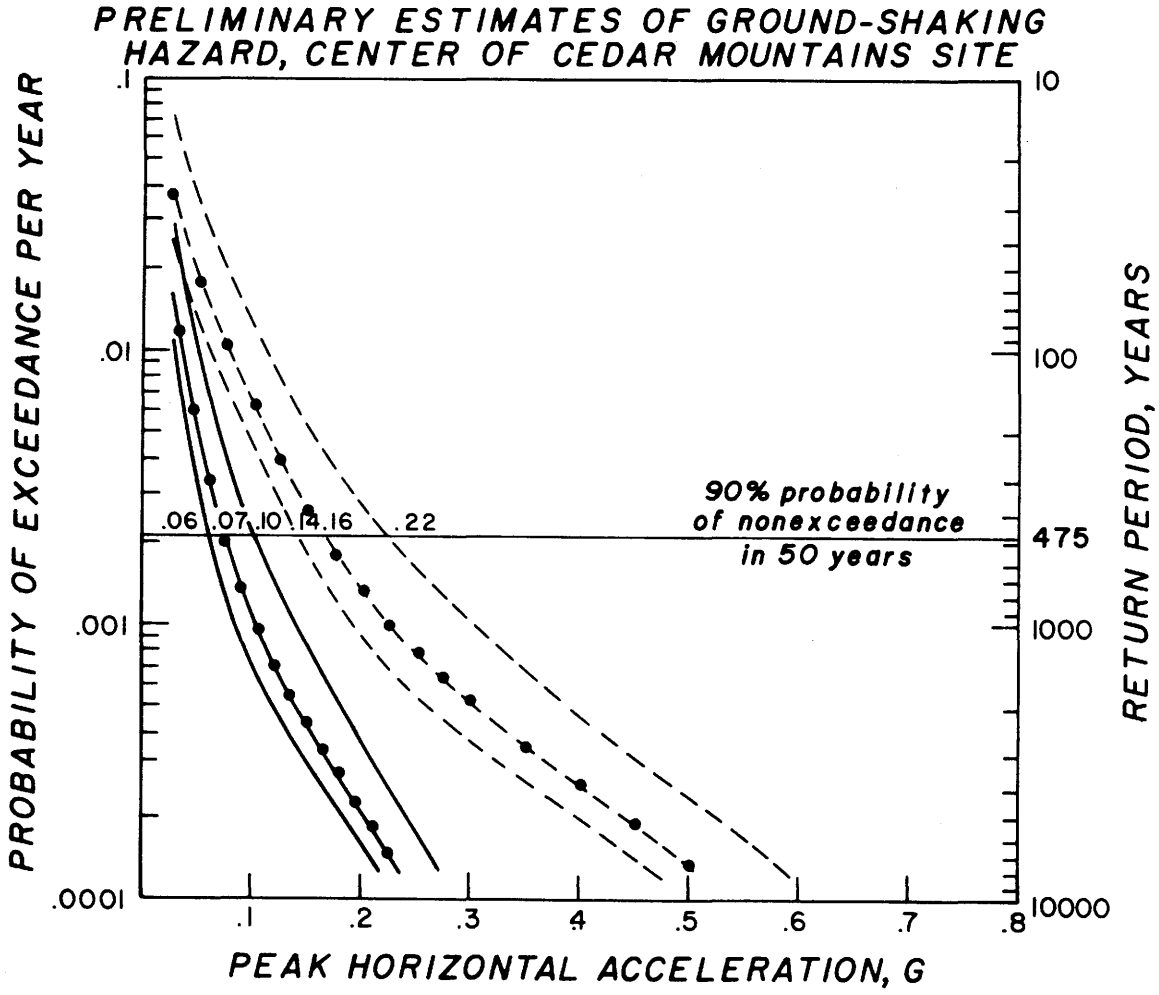

Figure 4.10 Preliminary graphs showing the probability of exceedance per year for peak horizontal ground accelerations on soil at the center of the proposed Cedar Mountains SSC site. The solid curves were calculated using a peak acceleration relationship determined by Campbell (1987). The dashed curves were calculated using an alternative upper-bound peak acceleration relationship proposed by Campbell (1987). The three different curves in each set correspond to the three different sets of seismicity parameters determined in section 4.3. The 6 curves are similar to those in Figures 4.8 and 4.9, except that the probabilities of exceedance are for a single point location and not for the entire SSC ring.

and replaced the distances of the fault-specific sources listed in Table 4.1 with the minimum distances between the faults and the center of the Cedar Mountains ring. All of the other parameters used in the calculation were kept the same.

Figure 4.10 shows the hazard curves for the center of the Cedar Mountains site. Comparison of these six curves with the six curves shown in Figure 4.9 indicates that the annual probability of exceeding a given peak acceleration value at the center of the Cedar Mountains ring is a factor of 2 to 6 lower than the annual probability of exceeding the same acceleration value somewhere along the ring. This decrease in the rate of exceedance is due to a decreased contribution from both the fault-specific sources and the random $M_L \leq 6.5$ earthquakes, but especially the latter. Hazard curves for other locations within and on the proposed SSC rings should be similar to those in Figure 4.10, at least for the return periods of primary interests for this study (500 years or less). Thus, the probability of exceeding a given acceleration value at any particular point on the proposed SSC rings appears to be significantly lower than the probability of exceedance for the ring as a whole.

From Figure 4.10, estimates of the peak horizontal acceleration having a 90% probability of nonexceedance in 50 years at the center of the Cedar Mountains site range from 0.06 to 0.22 g, depending on the seismicity parameters assumed and the relationship used to predict peak acceleration as a function of magnitude and distance. These accelerations are a factor of two smaller than the corresponding probabilistic accelerations for the ring indicated on Figure 4.9. The value of 0.15 g inferred from the map of Algermissen et al. (1982) (Figure 4.6) falls near the middle of the 0.06 to 0.22 g range, but is larger than the value of 0.07 g obtained using our preferred input parameters (solid curve with dots, Figure 4.10). The difference between our preferred estimate of 0.07 g and the estimate of 0.15 g from the Algermissen et al. map appears to be attributable primarily to differences in the seismicity parameters used in the calculations. In the Algermissen et al. study, the SSC sites lie within a seismic source zone that includes a large part of the Intermountain seismic belt in Utah. The data presented in this study, however, show that the rate of earthquake activity near the sites is markedly lower than it is to the east in the main part of the Intermountain seismic belt in Utah. Algermissen et al. (1982) used the attenuation relationship of Schnabel and Seed (1973) for their calculations. This relationship in general predicts peak accelerations that are closer to Campbell's lower bound values than his upper bound values.

An interesting result of our probabilistic hazard calculation for the proposed SSC facility (Figures 4.8 and 4.9) is that for return periods of 475 years, the dominant contribution to the hazard is from moderate earthquakes of up to magnitude 6.5. These contribute 74% to 86% of the hazard, depending on the assumptions used. If the hazard at a particular location such as the center of the Cedar Mountains site is considered (Figure 4.10), the moderate earthquakes contribute 54% to 85% of the hazard at return periods of 475 years. Doubling the radius of the circular source area and quadrupling the A value has a negligible effect on the hazard curves. This demonstrates that our chosen source radius of 50 km is sufficiently large for this calculation, at least when earthquakes of $M_L \leq 6.5$ are the only ones considered. The fault-specific sources of magnitude 6.5 and larger become the dominant source of hazard for return

periods longer than 1500 years or more, depending on the parameters used for the calculation and whether it is done for a ring or for a point.

The range in the hazard curves shown in Figures 4.9 and 4.10 is unfortunately rather large, but is not unusual for studies of this type (see, for example, Youngs et al.(1987)). The problem of uncertainty in hazard calculations is usually handled by either selecting a preferred estimate or else by generating a large number of curves using different assumptions weighted as to their likelihood and then calculating a mean or median curve. The latter approach is clearly beyond the scope of this study. A design acceleration value of 0.1 - 0.2 g appears to be reasonable for a time period of 50 years and a 90% probability of nonexceedance, based on published studies and the solid curves in Figures 4.8 and 4.9. However, it should be kept in mind that differing assumptions about ground motions can result in acceleration values that are a factor of two higher than this.

5. CONSIDERATIONS OF EARTHQUAKE HAZARDS AT THE PROPOSED SSC SITES IN TOOELE COUNTY

In this final section, we present a brief discussion of earthquake-related hazards that might represent adverse risk factors for the proposed SSC facilities. Our intent is not to repeat the discussion of previous sections, nor to provide an exhaustive analysis of site-specific hazards. Rather, the outline is intended to serve a "Devil's Advocate," brainstorming purpose.

5.1 Ground Motion

5.1.1 General Remarks

Over time periods comparable to the anticipated lifetime of the SSC facility (less than 50 years), the dominant contribution to the ground-shaking hazard comes from possible moderate earthquakes of $M_L \leq 6.5$ that could occur in the near vicinity (within 50 km) of the proposed SSC sites. This is true despite the relatively low historical seismicity in this area, because all of the nearby major faults capable of generating larger earthquakes have recurrence intervals that are long relative to the return periods of interest.

Quantification of the ground-shaking hazard is subject to uncertainty because of problems in defining the seismicity rate and the lack of data on strong ground motion from earthquakes in Utah. The probabilistic ground motion map for the United States published by Algermissen et al. (1982) indicates that a peak horizontal ground acceleration of about 0.15 g has a 90% probability of not being exceeded in 50 years at a point in the general area of the proposed sites. We obtained a value of 0.14 g for the proposed facility from some preliminary site-specific calculations that we performed using the attenuation relationship of Campbell (1987) and our best estimate of the seismicity parameters. Our calculations fall far short of a complete probabilistic evaluation of ground shaking hazard for the site, but they do incorporate up-to-date information and properly take into account the large size of the proposed SSC ring.

A noteworthy conclusion of our preliminary hazard calculations is that the large size of the proposed SSC facility is an important factor that needs to be taken into account in any probabilistic evaluation of the ground shaking hazard. Most critical facilities are small enough that they can be treated adequately as a point location for these types of studies, but this is not true for the Supercollider. At the location of the proposed SSC sites in Utah, we found that the annual probability of exceeding a given peak acceleration somewhere along a ring of radius 13 km is significantly higher than the probability of exceeding this acceleration at any specific point such as the center of the ring. We expect that this will be true for any site located within a seismically active region because: (1) the average distance between a ring of radius 13 km and a group of potential earthquake sources will always be less than the average distance between any specific point on the ring and the same group of sources, (2) ground motion from earthquakes attenuates significantly over a distance of 26 km, the average diameter of the

proposed SSC ring.

For purposes of design, the probability of exceeding a critical level of ground motion anywhere along the ring would appear to be more pertinent than the probability of exceeding this acceleration at a particular location. Thus, we consider the set of curves in Figures 4.8 and 4.9 to be a more relevant characterization of the ground-shaking hazard to the facility than the curves in Figure 4.10. However, for purposes of comparison with published regional studies and with site-specific studies for other candidate SSC sites that do not take into account the size of the rings, the set of curves in Figure 4.10 should be used.

In both Figures 4.9 and 4.10, the middle solid curve with the dots represents our best preliminary estimate of the ground-shaking hazard. However, use of Campbell's alternative upper bound curves for peak horizontal acceleration in our calculations leads to significantly different results, as indicated by the dashed curves with dots. The acceleration with a 90% probability of nonexceedance in 50 years along the SSC ring increases by a factor of two to 0.30 g, given our best-estimate seismicity parameters (Figure 4.9). Although this higher value cannot be ruled out given the present state of knowledge, it is important to note that most published attenuation relationships in current use would lead to values more consistent with our preferred estimate of 0.14 g.

Campbell's attenuation relationships have been developed as part of a U.S. Geological Survey earthquake hazards program focused on the Wasatch Front, and will be considered by many to represent the state-of-the-art for application in Utah. Nevertheless, Campbell's attenuation relationships may not be universally agreed upon by other practitioners. Future studies should help to reduce the uncertainty in ground motion estimates for normal-faulting earthquakes in Utah.

5.1.2 Site Effects

The seismic velocities and other mechanical properties of the surficial materials underlying a site are well known to have a major effect on the shape and amplitude of the spectrum of ground motion. Essentially, deep and/or soft unconsolidated material has a tendency to amplify ground motions at certain periods, particularly periods longer than about 0.5 sec (e.g. Seed and Idriss, 1982, pp. 43-47). Such effects have been well documented in alluvial valleys along the Wasatch Front by U.S. Geological Survey seismologists (Hays and King, 1982, 1984a, 1984b; Rogers et al., 1984; King et al., 1987). Since both of the proposed SSC sites would lie partially on unconsolidated alluvial and lake deposits, the possible amplification of earthquake ground motion by this material should be taken into account in any detailed seismic design study.

In general, the material underlying a site appears to have a much smaller effect on maximum ground accelerations than it does on ground velocities. According to Seed and Idriss (1982, p. 34-37), values of peak acceleration in soils are not appreciably different from those on rock, and may even be substantially less on some materials such as soft to medium stiff clay and sand. The peak acceleration relationship of Campbell (1987), however, contains an empirically-derived amplification factor of 1.5 for soils less than 10 m deep. The physical

cause of this amplification is probably resonance within the low velocity soils (Campbell, 1987). Campbell argues that this amplification factor may also be applicable to deeper unconsolidated deposits in Utah, where large amplification of spectral velocities relative to rock sites has been measured (see references cited above). This factor was included in the calculation of the dashed hazard curves in Figure 4.9, but not the solid curves. Regardless of whether or not Campbell's amplification factor is applicable to peak ground accelerations at the proposed SSC sites, it is reasonable to expect some amplification of ground velocity in certain frequency bands at those parts of the sites underlain by unconsolidated deposits. These possible site effects should be carefully evaluated and incorporated into the seismic design criteria.

5.2 Surface Faulting Earthquakes

5.2.1 General Remarks

Seismic hazards at the SSC sites associated with possible surface-faulting earthquakes include strong ground shaking, the potential for surface rupture at the sites, and possible static deformation from nearby surface faulting. We have developed a perspective in this report that there is a likelihood of very long recurrence intervals for surface faulting on any individual fault or fault segment. Nevertheless, fault scarps perhaps as young as 9,000 years lie only 10 km to the north of the Cedar Mountains site in Puddle Valley, and the Cedar Mountains alignment straddles the Cedar Mountains where there must be some finite (albeit low) probability of range-front faulting. First, we will briefly summarize some key points made in earlier sections and then consider some additional factors.

We can begin by affirming the premise that the historical and instrumental earthquake record provides an inadequate guide to assessing seismic potential at the SSC sites and that information from late Quaternary faulting is essential to consider (section 2.3.1). Seismicity is clearly very low in the immediate vicinity of the proposed sites (Figure 3.7), and the sites are marginal to, and arguably outside of Utah's main seismic belt (e.g. Figures 2.3, 3.6). Background seismicity, however, does not simply correlate with mapped Cenozoic faulting in the Intermountain seismic belt (section 2.4), such that the potential for surface faulting effectively must be considered independently of observed seismicity. The occurrence of the 1983 M_S 7.3 Borah Peak, Idaho, surface-faulting earthquake in an area of low historic seismicity (Richins et al., 1987; Dewey, 1987)—but in an area of clearly recognizable late Quaternary faulting— is a case in point.

The SSC sites lie within a part of the Basin and Range province where there is clear evidence of late Pleistocene and some Holocene faulting (section 4.2.2). Slip rates on these faults are inferred to be of the order of 0.1 to 0.2 mm/yr or less (section 4.2.3), 5 to 10 times lower than on the Wasatch fault (e.g., Schwartz and Coppersmith, 1984; Machette et al., 1986; Youngs et al., 1987). Various lines of probabilistic reasoning suggest that active faults in the general vicinity of the SSC sites have average recurrence intervals for surface faulting on an individual fault or fault segment of the order of 10,000 years or perhaps significantly more (section 4.2.3).

We have noted that the record of late Quaternary faulting in the "Western Desert" region surrounding the SSC sites is incomplete because of fluctuations of ancient Lake Bonneville, although the Holocene record of any significant surface faulting should be complete (section 2.3.1). Because of the presence of many single-event fault scarps in this region, the incomplete late Quaternary record, and the low slip rates (long recurrence), the possibility of future surface rupture cannot be confidently restricted to those fault sources identified in Table 4.1 and Figure 4.2.

If recurrence intervals of surface faulting on an individual fault are of the order of 10,000 years, and if many of the faults have not ruptured in Holocene time, can it be argued that such lengthy elapse times now imply an increased probability of faulting? Limits of applicability of the memoryless Poisson process for probabilistic hazard analysis have recently been investigated for similar problems in the central and eastern United States (EPRI, 1986). The result is that probabilistic hazard estimates for 50-year exposure periods based on a Poisson model are generally adequate if (1) the average recurrence interval exceeds the elapsed time since the last significant event, and (2) if there is reason to believe that a fault displays strongly regular, "characteristic time" behavior.

It is conceivable that for some (many?) of the faults in the "Western Desert" region the elapsed time since the last earthquake exceeds the average recurrence interval, but there is no evidence of strongly regular, "characteristic time" behavior on these faults. Thus, there simply is no way to resolve this issue. Conventional wisdom argues that, lacking evidence to the contrary, the Poisson model is not unreasonable physically, and the sum of non-Poissonian processes may be approximately Poisson (EPRI, 1986).

A final consideration for surface-faulting is the thesis developed by Wallace (1987) that "slip accompanied by surface faulting events, and displacement of range blocks in the Great Basin province..., have not been uniform." Wallace (1987) argues for the spatial and temporal grouping of large surface faulting events such that periods of active faulting might be separated by dormant periods that may last tens of thousands of years."

Machette et al. (1986) have suggested a causal relationship between an apparent increase in slip rate on the Wasatch fault about 15,000 years ago and isostatic rebound caused by the catastrophic draining of Lake Bonneville. Speculative arguments might be made that many of the fault scarps in the "Western Desert" region could reflect temporal clustering of surface faulting events in latest Pleistocene-early Holocene time due to effects of Lake Bonneville. If so, then the average recurrence intervals that we calculated for these faults may in fact be longer than we have estimated.

5.2.2 Static Deformation from Nearby Surface Faulting

Large normal-faulting earthquakes can cause permanent tilting of the ground surface at distances of up to 20 km or more from the surface fault trace. To illustrate the nature and magnitude of this effect, Figure 5.1 shows profiles of elevation changes caused by the Hebgen Lake, Borah Peak, and Dixie Valley (Nevada, 1954) earthquakes. All three of these earthquakes were accompanied by substantial surface faulting (see section 2.3.3). In the case of the

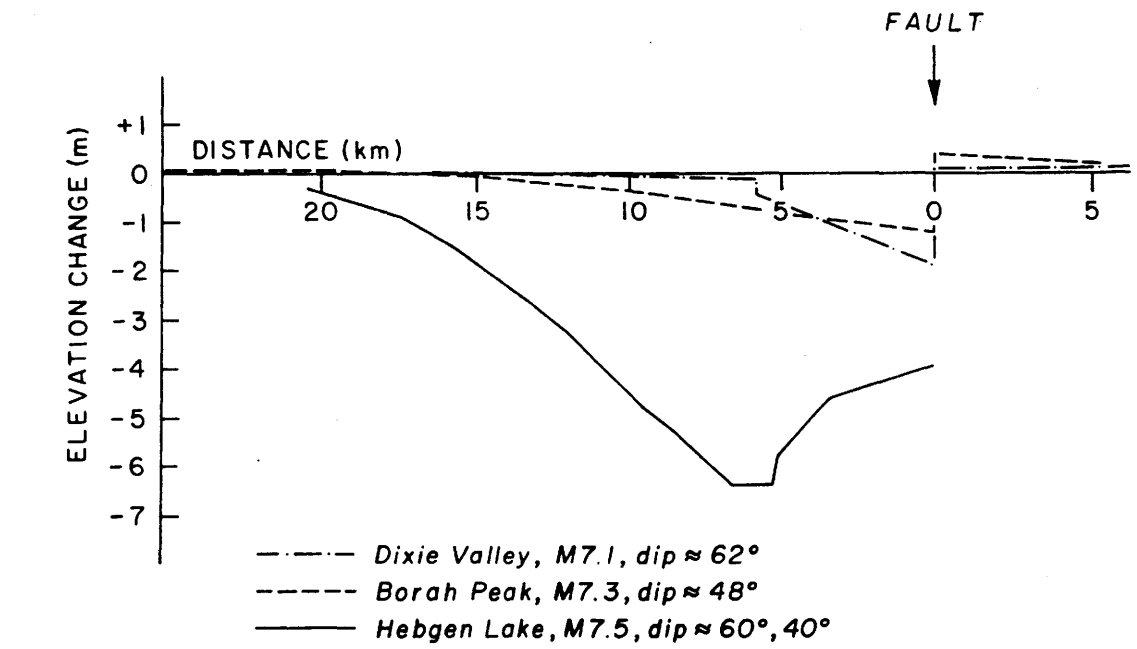

Figure 5.1 Vertical surface deformation caused by three M7+ earthquakes in the Intermountain Seismic Belt and the Basin and Range Province: 1954 M_S 7.1 Dixie Valley, Nevada; 1983 M_S 7.3 Borah Peak, Idaho (Stein and Barrientos, 1985); and 1959 M_S 7.5 Hebgen Lake, Montana (Savage and Hastie, 1966). Figure from Smith and Richins (1984).

Hebgen Lake earthquake, surface faulting occurred on two separate fault traces separated by about 5 km along the measured profile. With this in mind, it is clear from Figure 5.1 that the vertical displacements and tilting are greatest near the surface break and gradually diminish at larger distances.

Earthquakes that do not cause surface faulting may cause warping of the ground surface above the subsurface fault. As we mentioned in section 2.3.5, both the 1975 M_L 6.0 Pocatello Valley earthquake and the 1975 M_L 6.1 Yellowstone Park earthquake produced apparently coseismic subsidence of up to 12-13 cm, but no identifiable surface faulting. For any earthquake, the amount of deformation at the ground surface will depend on such factors as the amount of displacement on the fault and the size, geometry, and depth extent of the fault break.

In the vicinity of the proposed SSC sites, surface-faulting earthquakes on faults 1 through 5 (Figure 4.2) could cause measurable ground tilting at the rings. The other fault-specific sources in Figure 4.2 are too far away to cause tilting at the sites. There is some question about whether or not faults 1, 2 and 4 are active. If they are, then the annual probability of an earthquake on these faults and on faults 3 and 5 also is judged to be less than 1.0×10^{-4} (Table 4.1). Moderate earthquakes of $M_L \leq 6.5$, below the threshold of surface faulting, are more likely to occur near the sites. However, earthquakes of this size would have to occur within less than 10 km of the ring in order to cause tectonic deformation of more than about 1 cm. From Table 4.2, the estimated return period for earthquakes of $M_L \geq 5.0$ within 50 km of the center of either proposed site is 200 years. Since the maximum radius of the ring is about 15 km, the estimated return period for earthquakes within 10 km of the site perimeter would be about 4 times this or 800 years. Thus, the probability of earthquake-induced ground deformation at the proposed SSC sites is very small.

REFERENCES

Abe, K. (1981). Magnitudes of large shallow earthquakes from 1904 to 1980, *Phys. Earth Planet. Interiors, 27,* 72-92.

Aki, K. (1966). Generation and propagation of G waves from the Niigata earthquake of June 16, 1964, *Bull. Earthquake Res. Inst., Tokyo Univ., 44,* 23-88

Algermissen, S. T., D. M. Perkins, P. C. Thenhaus, S. L. Hanson and B. L. Bender (1982). Probabilistic estimates of maximum acceleration and velocity in rock in the contiguous United States, *U.S. Geol. Surv. Open-File Rept. 82-1033,* 107 p.

Allen, C.R. (1974). Geological criteria for evaluating seismicity, *Geol. Soc. Am. Bull., 86,* 1041-1057.

Allen, C.R. (1986). Seismological and paleoseismological techniques of research in active tectonics, in *Active Tectonics,* National Academy Press, Washington, D.C., 148-154.

Allmendinger, R. W., J. W. Sharp, D. Von Tish, L. Serpa, L. Brown, S. Kaufman, J. Oliver, and R. B. Smith (1983). Cenozoic and Mesozoic structure of the eastern Basin and Range province, Utah, from COCORP seismic reflection data, *Geology, 11,* 532-536.

Anderson, R. E., and T. P. Barnhard (1984). Extensional and compressional paleostresses and their relationship to paleoseismicity and seismicity, central Sevier Valley, Utah, *U.S. Geol. Surv. Open-File Rept. 84-763,* 515-546.

Anderson, R. E., and D. G. Miller (1979). Quaternary fault map of Utah, Technical Report, Fugro, Inc., 35 pp.

Arabasz, W. J., and M. E. McKee (1979). Utah Earthquake Catalog, 1850-June 1962, in *Earthquake Studies in Utah 1850-1978,* W. J. Arabasz, R. B. Smith, and W. D. Richins, Editors, Special Publication, University of Utah Seismograph Stations, 119-143.

Arabasz, W. J., R. B. Smith, and W. D. Richins, Editors (1979). *Earthquake Studies in Utah 1850 to 1978,* Special Publication, University of Utah Seismograph Stations, Salt Lake City, Utah, 552 pp.

Arabasz, W. J., R. B. Smith, and W. D. Richins (1980). Earthquake studies along the Wasatch front, Utah: Network monitoring, seismicity, and seismic hazards, *Bull. Seism. Soc. Am.,*

70, 1479-1499.

Arabasz, W. J., and R. B. Smith (1981). Earthquake prediction in the Intermountain seismic belt--An intraplate extensional regime, in *Earthquake Prediction--An International Review*, D. W. Simpson and P. G. Richards, Editors, Am. Geophys. Union, Maurice Ewing Series, v. 4, 248-258.

Arabasz, W.J., W.D. Richins, and C.J. Langer (1981). The Pocatello Valley (Idaho-Utah border) earthquake sequence of March to April 1975, *Bull. Seism. Soc. Am., 71*, 803-826.

Arabasz, W.J. (1984). Earthquake behavior in the Wasatch Front area: Association with geologic structure, space-time occurrence, and stress state, in Proceedings of Conference XXVI, A Workshop on "Evaluation of Regional and Urban Earthquake Hazards and Risk in Utah," W.W. Hays and P.L. Gori, Editors, *U.S. Geol. Surv. Open-File Rept. 84-763*, 310-339.

Arabasz, W.J. and D.R. Julander (1986). Geometry of seismically active faults and crustal deformation within the Basin and Range--Colorado Plateau transition in Utah, in *Extensional Tectonics of the Southwestern United States: A Perspective on Processes and Kinematics*, L. Mayer, Editor, *Geol. Soc. Am. Special Paper* 208, pp. 43-74.

Beanland, S., and M.M. Clark (1987). The Owens Valley fault zone, eastern California, and surface rupture associated with the 1872 earthquake, *Seism. Res. Lett., 58*, 32.

Benjamin, J.R., and C.A. Cornell (1970). *Probability, Statistics, and Decision for Civil Engineers*, McGraw-Hill Book Co., New York, 684 pp.

Bonilla, M.G., R.K. Mark, and J.J. Lienkaemper (1984). Statistical relations among earthquake magnitudes, surface rupture length, and surface fault displacement, *Bull. Seism. Soc. Am., 74*, 2379-2411.

Brown, E. D., W. J. Arabasz, J. C. Pechmann, E. McPherson, L. L. Hall, P. J. Oehmich, and G. M. Hathaway (1986). *Earthquake Data for the Utah Region: January 1, 1984 to December 31, 1985*, Special Publication, University of Utah Seismograph Stations, Salt Lake City, Utah, 83 pp.

Bucknam, R. C. (1976). Leveling data from the epicentral area of the March 27, 1975, earthquake in Pocatello, Idaho, *U.S. Geol. Surv. Open-File Rept. 76-52*, 6 pp.

Bucknam, R. C. (1977). Map of suspected fault scarps in unconsolidated deposits, Tooele, 1° x 2° sheet, Utah, *U.S. Geol. Surv. Open-File Rept. 77-495*.

Bucknam, R. C., and R. E. Anderson (1979a). Estimation of fault-scarp ages from a scarp-height slope-angle relationship, *Geology, 7,* 11-14.

Bucknam, R.C., and R.E. Anderson (1979b). Map of fault scarps on unconsolidated sediments, Delta 1° x 2° sheet, Utah, *U.S. Geol. Surv. Open-File Rept. 79-366,* 21 pp.

Bucknam, R. C., S. T. Algermissen and R. E. Anderson (1980). Patterns of late Quaternary faulting in western Utah and an application in earthquake hazard evaluation, in Proceedings of Conference X, Earthquake Hazards along the Wasatch Sierra-Nevada Frontal Fault Zones, *U.S. Geol. Surv. Open-File Rept. 80-801,* 299-314.

Campbell, K.W. (1987). Predicting strong ground motion in Utah, in Assessment of Regional Earthquake Hazards and Risk Along the Wasatch Front, Utah, *U.S. Geol. Surv. Prof. Paper,* in press.

Cluff, L.S., G.E. Brogan, and C.E. Glass (1970). Wasatch fault, northern portion: Earthquake fault investigation and evaluation, *Report to Utah Geol. and Min. Surv.,* Woodward-Clyde and Associates, 27 pp.

Cluff, L.S., G.E. Brogan, and C.E. Glass (1973). Wasatch fault, southern portion: Earthquake fault investigation and evaluation, *Report to Utah Geol. and Min. Surv.,* Woodward-Lundgren and Associates, 79 pp.

Cluff, L.S., G.E. Brogan, and C.E. Glass (1974). Investigation and evaluation of the Wasatch fault north of Brigham City and Cache Valley faults, Utah and Idaho: A guide to land-use planning with recommendations for seismic safety, *Report to U.S. Geol. Surv.,* Woodward-Lundgren and Associates, 147 pp.

Coffman, J.L., and C.A. von Hake, Editors (1973). *Earthquake History of the United States,* Publ. 41-1, U.S. Dept. Commerce, Washington D.C., 208 pp.

Coffman, J.L., C.A. von Hake, and C.W. Stover, Editors (1982). *Earthquake History of the United States,* U.S. Dept. Commerce, Washington, D.C., 258 pp.

Cook, K. L., E. F. Gray, R. M. Iverson, and M. T. Strohmeier (1980). Bottom gravity meter regional survey of the Great Salt Lake, Utah, in Great Salt Lake, A Scientific, Historical, and Economic Overview, J. W. Gwynn, Editor, *Utah Geol. and Min. Surv. Bull. 116,* 125-143.

Cornell, C.A. (1968). Engineering seismic risk analysis, *Bull. Seism. Soc. Am., 58,* 1583-1606.

Crone, A. J., and M. N. Machette (1984). Surface faulting accompanying the Borah Peak

earthquake, central Idaho, *Geology, 12,* 664-667.

Crone, A.J., M.N. Machette, M.G. Bonilla, J.J. Lienkaemper, K.L. Pierce, W.E. Scott, and R.C. Bucknam (1987). Surface faulting accompanying the Borah Peak earthquake and segmentation of the Lost River fault, central Idaho, *Bull. Seism. Soc. Am., 77,* 739-770.

Currey, D.R., G. Atwood, and D.R. Mabey (1984). Major levels of Great Salt Lake and Lake Bonneville, *Utah Geol. and Min. Surv. Map 73,* scale 1:750,000.

Davis, F.D. (1983a). Geologic map of the southern Wasatch Front, Utah, *Utah Geol. and Min. Surv. Map 55-A,* scale 1:100,000.

Davis, F.D. (1983b). Geologic map of the central Wasatch Front, Utah, *Utah Geol. and Min. Surv. Map 54-A,* scale 1:100,000.

Davis, F.D. (1985). Geologic map of the northern Wasatch Front, Utah, *Utah Geol. and Min. Surv. Map 53-A,* scale 1:100,000.

Dewey, J. W. (1987). Instrumental Seismicity of Central Idaho, *Bull. Seism. Soc. Am., 77,* 819-836.

Doser, D. I. (1985a). The 1983 Borah Peak, Idaho and 1959 Hebgen Lake, Montana Earthquakes: Models for normal fault earthquakes in the Intermountain seismic belt, in Proceedings of Workshop XXVIII on the Borah Peak, Idaho, Earthquake, R. S. Stein and R. C. Bucknam, Editors, *U.S. Geol. Surv. Open-File Rept. 85-290,* 368-384.

Doser, D. I. (1985b). Source parameters and faulting processes of the 1959 Hebgen Lake, Montana, earthquake sequence, *J. Geophys. Res., 90,* 4537-4555.

Doser, D. I., and R. B. Smith (1982). Seismic moment rates in the Utah region, *Bull. Seism. Soc. Am., 72,* 525-551.

Doser, D.I., and R.B. Smith (1985). Source parameters of the 28 October 1983 Borah Peak, Idaho earthquake from body wave analysis, *Bull. Seism. Soc. Am., 75,* 1041-1051.

Eddington, P.K., R.B. Smith, and C. Renggli (1987). Kinematics of Basin-Range intraplate extension, in *Continental Extensional Tectonics,* M.P. Coward, J.F. Dewey, and P.L. Hancock, Editors, Geological Society of London Special Publication, 371-392.

Ekstrom, G., and A. M. Dziewonski (1985). Centroid-moment tensor solutions for 35 earthquakes in western North America (1977-1983), *Bull. Seism. Soc. Am., 75,* 23-39.

EPRI (1986). Seismic hazard methodology for the central and eastern United States, *Technical Report EPRI NP-4726,* v. 1, Electric Power Research Institute, Palo Alto, California.

Everitt, B. L. and B. N. Kaliser (1980). Geology for Assessment of Seismic Risk in the Tooele and Rush Valleys, *Utah Geol. and Min. Surv. Special Studies 51,* 33 pp.

Evernden, J. F. (1975). Seismic intensities, "size" of earthquakes, and related matters, *Bull. Seism. Soc. Am., 65,* 1287-1313.

Foley, L.L., R.A. Martin, and J.T. Sullivan (1986). Seismotectonic study for Joes Valley, Scofield and Huntington, North Davis, Emery County and Scofield Project, Utah, *U.S. Bureau of Reclamation Report 83-288.*

Gibbons, A.B., and D.D. Dickey (1983). Quaternary faults in Lincoln and Uinta Counties, Wyoming, and Rich County, Utah, *U.S. Geol. Surv. Open-File Rept. 83-238.*

Gilbert, G. K. (1875). Report on the geology of portions of Nevada, Utah, California, and Arizona, examined in the years 1871 and 1872: U.S. Geog. and Geol. Surveys W. 100'th Mer. Rept., v. 3, p. 41.

Gilbert, G. K. (1928). Studies of Basin Range Structure, *U.S. Geol. Surv. Prof. Pap. 153,* 92 pp.

Gutenberg, B., and C. F. Richter (1954). *Seismicity of the Earth and Associated Phenomena,* Princeton University Press, Princeton, New Jersey, 2nd edn., 310 pp.

Gutenberg, B., and C.F. Richter (1956). Earthquake magnitude, intensity, energy, and acceleration, *Bull. Seism. Soc. Am., 46,* 105-145.

Hall, W. B., and P. E. Sablock (1985). Comparison of the geomorphic and surficial fracturing effects of the 1983 Borah Peak, Idaho earthquake with those of the 1959 Hebgen Lake, Montana earthquake, in Proceedings of Workshop XXVIII on the Borah Peak, Idaho, Earthquake, R. S. Stein and R. C. Bucknam, Editors, *U.S. Geol. Surv. Open-File Rept. 85-290,* 141-152.

Hanks, T. C., and H. Kanamori (1979). A moment magnitude scale, *J. Geophys. Res., 84,* 2348-2350.

Hays, W. W., and K. W. King (1982). Zoning of the earthquake ground shaking hazard along the Wasatch fault zone, Utah, *Third International Earthquake Microzonation Conference, Proceedings,* v. 111, p. 1307-1318.

Hays, W. W., and K. W. King (1984a). The ground-shaking hazard along the Wasatch fault zone, Utah, in Proceedings of Conference XXVI, A Workshop on "Evaluation of Regional and Urban Earthquake Hazards and Risk in Utah," W. W. Hays and P. L. Gori, Editors, *U.S. Geol. Surv. Open-File Rept. 84-763,* 133-147.

Hays, W. W., and K. W. King (1984b). The ground shaking hazard along the Wasatch fault zone, Utah, *Proc. Eighth World Conference on Earthquake Engineering,* v. I, 7-14.

Howard, K.A., J.M. Aaron, E.E. Brabb, M.R. Brock, H.D. Gower, S.J. Hunt, D.J. Milting, W.R. Muehlberger, J.K. Nakata, G. Plafker, D.C. Prowell, R.E. Wallace, and I.J. Witkind (1978). Preliminary map of young faults in the United States and a guide to possible fault activity, *U.S. Geological Survey Misc. Field Studies Map MF-916,* scale *1:7,500,000.*

Kanamori, H. (1977). The energy release in great earthquakes, J. Geophys. Res., 82, 2981-2987.

Keaton, J. (1984). Ground failure hazards and risks: Considerations and research needs applicable to Utah, in Proceedings of Conference XXVI, A Workshop on "Evaluation of Regional and Urban Earthquake Hazards and Risk in Utah," W. W. Hays and P. L. Gori, Editors, *U.S. Geol. Surv. Open-File Rept. 84-763,* 557-567.

King, K. W., R. A. Williams and D. L. Carver (1987). Relative ground response in Salt Lake City and areas of Springville-Spanish Fork, Utah, submitted to Assessment of Regional Earthquake Hazards and Risk Along the Wasatch Front, Utah, *U.S. Geol. Surv. Prof. Pap.*

Machette, M. N, S. F. Personius, and A. R. Nelson (1986). Late Quaternary segmentation and slip-rate history of the Wasatch fault zone, Utah, *EOS Trans. AGU, 67,* 1107.

McGuire, R.K. (1983). Estimation of seismic ground motion in northern Utah, *U.S. Geol. Surv. Technical Rept. 14-08-0001-19825,* 53 pp.

Mikulich, M., and R.B. Smith (1974). Seismic reflection and aeromagnetic surveys of the Great Salt Lake, Utah, *Geol. Soc. Am. Bull., 85,* 991-1002.

Murphy, L. M., and R. J. Brazee (1964). Seismological investigations of the Hebgen Lake earthquake, *U.S. Geol. Surv. Prof. Pap. 435-C,* 13-17.

Nelson, A.R. and R.B. Van Arsdale (1986). Recurrent late Quaternary movement on the Strawberry normal fault, Basin and Range--Colorado plateau transition zone, Utah, *Neotectonics, 1,* 7-37.

Oakeshott, G. B., R. W. Greensfelder and J. E. Kahle (1972). The Owens Valley earthquake

of 1872: One hundred years later, *Calif. Geol., 25,* 55-62.

Pechmann, J. C. (1987). Earthquake design considerations for the inter-island diking project, Great Salt Lake, Utah, Unpublished Technical Rept. submitted to Rollins, Brown, and Gunnell, Provo, Utah, 40 pp.

Pierce, K.L, and S.M. Coleman (1986). Effect of height and orientation (microclimate) on geomorphic degradation rates and processes, late-glacial terrace scarps in central Idaho, *Geol. Soc. Am. Bull., 97,* 869-885.

Pitt, A. M., C. S. Weaver, and W. Spence (1979). The Yellowstone Park earthquake of June 30, 1975, *Bull. Seism. Soc. Amer., 69,* 187-205.

Richins, W. D., W. J. Arabasz, G. M. Hathaway, P. J. Oehmich, L. L. Sells, and G. Zandt (1981). *Earthquake Data for the Utah Region: January 1, 1978 to December 31, 1980,* Special Publication, University of Utah Seismograph Stations, Salt Lake City, 125 pp.

Richins, W. D., W. J. Arabasz, G. M. Hathaway, E. McPherson, P. J. Oehmich, and L. L. Sells (1984). *Earthquake Data for the Utah Region: January 1, 1981 to December 31, 1983,* Special Publications, University of Utah Seismograph Stations, Salt Lake City, 111 p.

Richins, W.D., J.C. Pechmann, R.B. Smith, C.J. Langer, S.K. Goter, J.E. Zollweg, and J.J. King (1987). The 1983 Borah Peak, Idaho, earthquake and its aftershocks, *Bull. Seism. Soc. Am., 77,* 694-723.

Richter, C.F. (1958). *Elementary Seismology,* W.H. Freeman and Co., San Francisco, Calif., 768 pp.

Rinehart, W., H. Meyers, and C.A. von Hake (1985). *Summary of Earthquake Data Base,* National Geophysical Data Center, National Oceanic and Atmospheric Administration, Boulder, Colorado, 70 pp.

Rogers, A. M., D. L. Carver, W. W. Hays, K. W. King and R. D. Miller (1984). Preliminary estimates of geographic variation in relative ground shaking in the Wasatch front urban corridor, in Proceedings of Conference XXVI, A Workshop on "Evaluation of Regional and Urban Earthquake Hazards and Risk in Utah, W. W. Hays and P. L. Gori, Editors, *U.S. Geol. Surv. Open-File Rept. 84-763,* 547-556.

Ryall, A. S., and J. D. Van Wormer (1980). Estimation of maximum magnitude and recommended seismic zone changes in the western Great Basin, *Bull. Seism. Soc. Am., 70,* 1573-1581.

Savage, J. A., and L. M. Hastie (1966). Surface deformation associated with dip-slip faulting, *J. Geophys. Res., 71,* 4897-4904.

Schnabel, P., and H. B. Seed (1973). Acceleration in rocks for earthquakes in the western United States, *Bull. Seism. Soc. Am., 63,* 501-516.

Schwartz, D. P., and K. J. Coppersmith (1984). Fault behavior and characteristic earthquakes: Examples from the Wasatch and San Andreas fault zones, *J. Geophys. Res., 89,* 5681-5698.

Schwartz, D. P., F. H. Swan III, and L. S. Cluff (1984). Fault behavior and earthquake recurrence along the Wasatch fault, in Proceedings of Conference XXVI, A Workshop on "Evaluation of Regional and Urban Earthquake Hazards and Risk in Utah," W. W. Hays and P. L. Gori, Editors, *U.S. Geol. Surv. Open-File Rept. 84-763,* 113-125.

Schwartz, D.P. (1987). Earthquakes of the Holocene, *Reviews of Geophysics,* in press.

Seed, H. B., and I. M. Idriss (1982). *Ground Motions and Soil Liquefaction During Earthquakes,* Earthquake Engineering Research Institute, Berkeley, Calif., 134 pp.

Shenon, P. J. (1936). The Utah earthquake of March 12, 1934 (extracts from unpublished report), in F. Neumann, *United States Earthquakes, 1943,* U.S. Coast and Geodetic Survey, serial 593, 43-48.

Shimizu, Y. (1987). Earthquake clustering in the Utah region, *M.S. Thesis,* Mass. Inst. of Tech., Cambridge, Mass., 149 pp.

Singh, S.K., E. Bazan, and L. Esteva (1980). Expected earthquake magnitude from a fault, *Bull. Seism. Soc. Am., 70,* 903-914.

Slemmons, D.B., A.E. Jones, and J.I. Gimlett (1965). Catalog of Nevada earthquakes, 1852-1960, *Bull. Seism. Soc. Am., 55,* 537-583

Slemmons, D.B (1980). Design earthquake magnitudes for the western Great Basin, in Proceedings of Conference X, Earthquake Hazards Along the Wasatch Sierra-Nevada Frontal Fault Zones, *U.S. Geol. Surv. Open-File Rept. 80-801,* 62-85.

Slemmons, D.B. (1982). Determination of design earthquake magnitudes for microzonation, in *3rd International Earthquake Microzonation Conference Proceedings,* v. I, 119-130.

Smith, R.B. (1978). Seismicity, crustal structure, and intraplate tectonics of the interior of the western Cordillera, in *Cenozoic Tectonics and Regional Geophysics of the Western*

Cordillera, R.B. Smith and G.P. Eaton, Editors, *Geol. Soc. Am. Memoir 152*, 111-144.

Smith, R. B., and R. L. Bruhn (1984). Intraplate extensional tectonics of the eastern Basin-Range: Inferences on structural style from seismic reflection data, regional tectonics, and thermal-mechanical models of brittle-ductile deformation, *J. Geophys. Res., 89*, 5733-5762.

Smith, R. B., and W. D. Richins (1984). Seismicity and earthquake hazards of Utah and the Wasatch Front: Paradigm and paradox, in Proceedings of Conference XXVI, A Workshop on "Evaluation of Regional and Urban Earthquake Hazards and Risk in Utah," W. W. Hays and P. L. Gori, Editors, *U.S. Geol. Surv. Open-File Rept. 84-763*, 73-112.

Smith, R. B., and M. L. Sbar (1974). Contemporary tectonics and seismicity of the western United States with emphasis on the Intermountain seismic belt, *Geol. Soc. Am. Bull., 85*, 1205-1218.

Stein, R. S., and S. E. Barrientos (1985). Planar high-angle faulting in the Basin and Range: Geodetic analysis of the 1983 Borah Peak, Idaho, earthquake, *J. Geophys. Res., 90*, 11355-11366.

Stickney, M.C. and M.S. Bartholomew (1987). Seismicity and late Quaternary faulting of the northern Basin and Range province, Montana and Idaho, *Bull. Seism. Soc. Am., 77*, in press.

Stokes, W.L. (1977). Subdivisions of the major physiographic provinces in Utah, *Utah Geology, 4*, no. 1, 1-17.

Stokes, W.L. (1986). *Geology of Utah*, Utah Mus. of Nat. Hist. and Utah Geol. and Min. Surv., Salt Lake City, 312 pp.

Stover, C.W., B.G. Reagor, and S.T. Algermissen (1986). Seismicity map of the State of Utah, *U.S. Geol. Surv. Misc. Field Studies Map MF-1856*, scale 1:1,000,000.

Sullivan, J. T., A. R. Nelson, R. C. LaForge, C. K. Wood and R. A. Hansen (1986). Regional seismotectonic study for the back valleys of the Wasatch Mountains in northeastern Utah, Technical Summary Document, Seismotectonic Section, U.S. Bureau of Reclamation, Denver, Colorado, 317 pp.

Swan, F. H. III, D. P. Schwartz, and L. S. Cluff (1980). Recurrence of moderate to large magnitude earthquakes produced by surface faulting on the Wasatch fault zone, Utah, *Bull. Seism. Soc. Am., 70*, 1431-1462.

Veneziano, D., and J. Van Dyck (1986). Statistical analysis of earthquake catalogs for seismic hazard, in *Proceedings, Int. Symp. on Engineering Geology Problems in Seismic Areas,* Bari, Italy.

Vetter, U.R., and E.J. Corbett (1987). *Bulletin of the Seismological Laboratory for the Period January 1 to December 31, 1982,* Mackay School of Mines, University of Nevada-Reno, Reno, Nevada, 45 pp.

Viveiros, J. J. (1986). Cenzoic tectonics of the Great Salt Lake from seismic reflection data, *M.S. Thesis,* University of Utah, Salt Lake City, Utah, 81 pp.

Wallace, R.E. (1970). Earthquake recurrence intervals on the San Andreas Fault, California, *Geol. Soc. Am. Bull. 81,* 2875-2890.

Wallace, R.E. (1981). Active faults, paleoseismology, and earthquake hazards in the western United States, in *Earthquake Prediction: An International Review,* D.W. Simpson and P.G. Richards, Editors, Maurice Ewing Series 4, American Geophysical Union, Washington, D.C., 209-216.

Wallace, R.E. (1987). Grouping and migration of surface faulting and variations in slip rates on faults in the Great Basin Province, *Bull. Seism. Soc. Am., 77,* 868-876.

Weichert, D.H. (1980). Estimation of the earthquake recurrence parameters for unequal observation periods for different magnitudes, *Bull. Seism. Soc. Am., 70,* 1337-1346.

Williams, J.S. and M. L. Tapper (1953). Earthquake history of Utah, 1850-1949, *Bull. Seism. Soc. Am., 43,* 191-218.

Witkind, I. J. (1964). Reactivated faults north of Hebgen Lake, *U.S. Geol. Surv. Prof. Pap. 435-G,* 37-50.

Witkind, I.J. (1975). Preliminary map showing known and suspected active faults in Idaho, *U.S. Geol. Surv. Open File Rept. 75-278,* 71 pp.

Wyss, M. (1979). Estimating maximum expectable magnitude of earthquakes from fault dimensions, *Geology, 7,* 336-340.

Youngs, R.R., F.H. Swan, M.S. Power, D.P. Schwartz and R.K. Green (1987). Probabilistic analysis of earthquake ground-shaking hazard along the Wasatch front, Utah, submitted to Assessment of Regional Earthquake Hazards and Risk Along the Wasatch Front, Utah, *U.S. Geol. Surv. Prof. Pap.*

Zoback, M L. (1983). Structure and Cenozoic tectonism along the Wasatch fault zone, Utah, *Geol. Soc. Am. Memoir 157,* 3-27.

APPENDICES

Explanation

The purpose of the following appendices is to provide documentation of the seismicity data base that was specially compiled for this site-evaluation study and which forms the basis of analyses described in the main body of this report. The database consists of three important files of seismic events:

(1) *Appendix A* -- A compilation of all identified earthquakes of esimated magnitude 2.6 and greater within 160 km of the proposed SSC sites (study area, Figure 3.2) that are included in the historical and instrumental earthquake record. Epicenters for these earthquakes are plotted in Figure 3.6.

(2) *Appendix B* -- A listing of seismic events located within the near-site region of the proposed SSC sites (see Figures 3.2 and 3.5) and included in the University of Utah earthquake catalog--but which have been identified in this study as *artificial seismic events* by special investigation. None of these events are included in the listings of either Appendix A or Appendix C.

(3) *Appendix C* -- A listing of all seismic events included in the University of Utah earthquake catalog and located within the near-site region defined in Figure 3.2. Artificial seismic events tablulated in Appendix B have been removed. The events listed here are believed to be genuine earthquakes. Their epicenters are plotted in Figure 3.7.

Data Explanation For Pre-July 1962 Earthquake Listing
(Adapted From Page 119 of Arabasz, et al, 1979)

This listing includes all earthquakes in the study area in the University of Utah historic catalog and additional events from the University of Nevada and NOAA catalogs. The following data are listed for each event:

1. Year (yr), date, and origin time (orig time) in Universal or Greenwich Mean Time (GMT). Origin time given in hours and minutes for non-instrumental locations, and in hours, minutes, and seconds for instrumental locations.
2. Earthquake location coordinates in degrees and minutes of north latitude (lat-n) and west longitude (long-w). For non-instrumental locations, epicenter is assumed; in most cases, assigned coordinates correspond to location of town or city where felt effects were strongest. Epicentral accuracy $\cong \pm$ 25-50 km.
3. MAG, estimated Richter magnitude determined in one of four ways, as indicated by a suffix: (1) I implies estimate from maximum Modified Mercalli Intensity (INT) assuming the Gutenberg-Richter relation (Gutenberg and Richter, 1956, *Bull. Seism. Soc. Am. 46,* 105-145): MAG = 1 + 2/3 (INT); (2) M implies magnitude determined by Seismological Laboratory in Pasadena, (3) N implies magnitude estimated by University of Nevada (Reference 5, see below); and (4) X implies value arbitrarily assumed for event of unidentified size; X = 2.3 for non-instrumental locations, and 3.0 for instrumental locations.
4. INT, maximum Modified Mercalli Intensity. Unless otherwise noted, intensity is from Reference 1 (see below) for earthquakes through 1949, and from Reference 8 (see below) thereafter. Where sources disagree on maximum intensity, range is indicated a a comment and a maximum value has been interpreted. For events of unidentified size (X suffix in MAG column), intensity II arbitrarily assumed for non-instrumental locations--and no intensity assigned for instrumental locations.
5. Comments: Compilation of the 1850-1962 catalog has involved the careful checking and correlation of numerous sources--and extensive annotation. For convenience, several abbreviations and numbered references have been used, as outlined below. Earthquakes without comments generally are from Reference 1 for 1850-1949, and from either Reference 6 (instrumental) or Reference 8 (non-instrumental) for 1950-1962.

Abbreviations

LOC: location
INT: intensity (Modified Mercalli)
PAS: Pasadena, Seismological Laboratory
NEV: University of Nevada, Reno
ID: Idaho
UT: Utah
NOAA: event from NOAA catalog
ASSGN: assigned
A'SHOCK: aftershock
F'SHOCK: foreshock
SALT LK: Salt Lake
MAG: magnitude
UNR: event from NEV catalog

References and Footnotes

(1) Williams, J. S. and M. L. Tapper (1953). Earthquake history of Utah, 1850-1949 *Bulletin of the Seismological Society of America, 43,* 191-218.

(2) U.S. Geological Survey (1976). A study of earthquake losses in the Salt Lake City, Utah area, *U.S. Geological Survey Open-File Report 76-89,* 357 p.

(3) Townley, S. D. and M. W. Allen (1939). Descriptive catalog of earthquakes of the Pacific Coast of the United States, 1769 to 1928, *Bulletin of the Seismological Society of America, 29,* (1), Ch. 4,5,6.

(4) Coffman, J. L. and C. A. von Hake, editors (1973). *Earthquake History of the United States,* Publ. 41-1, U.S. Dept. Commerce, 208 p.

(5) Jones, A. E. (1975). Recording of earthquakes at Reno, 1916-1951, *Bulletin of the Seismological Laboratory, University of Nevada, Reno,* 199 p.

(6) NOAA earthquake data file, National Geophysical and Solar-Terrestrial Data Center, Boulder, Colorado.

(7) Pack, F. J. (1921). The Elsinore earthquakes in central Utah, September 29 and October 1, 1921, *Bulletin of the Seismological Society of America, 11,* 155-165.

(8) U.S. Department of Commerce. *United States Earthquakes,* annual publication, U.S. Government Printing Office, Washington, D.C.

(9) Gutenberg, B. and C. F. Richter (1954). *Seismicity of the Earth,* 2nd ed., Princeton Univ. Press, Princeton, N.J.

(10) Berg, J. W. Jr. and R. C. Resler (1958). Investigation of local earthquakes February 13, 1958, near Wallsburg, Utah, *Utah Acad. Sci., Arts, Lett. Proc. 35,* 113-117.

(11) Hardy, C. T. and G. Gaeth (1959). Field investigation of Utah earthquake, May 23, 1953, *Utah Acad. Sci., Arts, Lett. Proc. 36,* 137-140.

(12) Hardy, C. T. (1959). Field investigation of Utah earthquake, February 4, 1955, *Utah Acad. Sci. Arts, Lett. Proc. 36,* 141-143.

(13) Berg, J. W. Jr. (1960). Earthquakes near Nephi, Utah, on November 28, 1958, and December 1, 1958, *Utah Acad. Sci. Arts, Lett. Proc. 37,* 77-79.

(14) Algermissen, S. T. and K. L. Cook (1962). The Ephraim, Utah, earthquake of April 15, 1961, *Utah Acad. Sci. Arts, Lett. Proc. 39,* 106-110.

(15) Cook, K. L.. and R. B. Smith (1967). Seismicity in Utah, 1850 through June 1965, *Bulletin of the Seismological Society of America, 57,* 689-718.

(16) Carr, S. L. (1972). *The Historical Guide to Utah Ghost Towns,* Western Epics, Salt Lake City, Utah, 166 p.

(17) University of Utah (1952). *Gazeteer of Utah Localities and Altitudes,* Division of Biology, University of Utah, Salt Lake City, 216 p.

(18) Stansbury, H. (1852). *An Expedition to the Valley of the Great Salt Lake of Utah,* Lipincott, Grambo and Co., 487 pp (see pp. 149-150).

Data Explanation for Post-July 1962 Earthquake Listing

The following data are listed for each event:

1. Year (YR), date and origin time in Universal Coordinated Time (UTC). Subtract seven hours to convert to Mountain Standard Time (MST).
2. Earthquake location coordinates in degrees and minutes of north latitude (LAT-N) and west longitude (LONG-W), and depth in kilometers. "*" indicates poor depth resolution: no recording stations within 10 km or twice the depth.
3. MAG, computed local magnitude for each earthquake. "W" indicates Wood-Anderson records were used.
4. NO, number of P and S readings used in solution.
5. GAP, largest azimuthal separation in degrees between recording stations used in the solution.
6. DMN, epicentral distance in kilometers to the closest station.
7. RMS, root-mean-square error in seconds of the travel-time residuals:

$$RMS = [\Sigma_i(W_i R_i)^2)/\Sigma_i(W_i)^2]^{1/2}$$

where:

R_i is the observed minus the computed arrival time for the i-th P or S reading,

W_i is the relative weight given to the i-th P or S arrival time (0.0 for no weight through 1.0 for full weight).

APPENDIX A.

Earthquake Listings for Events 160 km from SSC Sites

1) Pre-Network Earthquakes (Pre-July 1962)

2) Post-Network Earthquakes (July 1962 - March 1987)

Historical Earthquakes 160 km From SSC Sites

yr	date	orig time	lat-n	long-w	mag	int	comments
1850	222	2200	40-44.94	111-50.95	3.7I	4	(18)
1853	1201	1815	39-42.36	111-49.90	4.3I	5	(1)
1853	1201	1845	40-14.35	111-39.33	4.3I	5	(1)
1868	1017	1030	39-21.67	111-35.26	3.0I	3	THREE SHOCKS (1)
1873	1218	1400	42-13.62	111-24.00	3.7I	4	ASSGN PARIS,ID (1)
1873	1227	0300	40-58.75	111-53.08	3.7I	4	
1874	618	0600	40-44.94	111-50.95	3.7I	4	
1874	618	0700	40-44.94	111-50.95	3.7I	4	(1)
1876	322		39-31.64	111-34.89	5.0I	6	THREE SHOCKS (1)
1878	821	1200	40-44.94	111-50.95	3.0I	3	
1878	907	1900	40-44.94	111-50.95	3.0I	3	
1880	712	0500	41-58.58	112-13.80	4.3I	5	INT=5-6,TWO SHOCKS (1)
1880	917	0627	40-44.94	111-50.95	3.7I	4	INT=4-5
1880	1227		41-42.00	113- 6.60	3.0I	3	TWO SHOCKS,LATE PM (1)
1881	1016	0700	39-32.54	111-27.35	3.0I	3	
1883	928	1100	39-54.60	112- 7.80	3.7I	4	
1884	1110	0850	42- 0.	111-16.00	6.3I	8	LOC ASSUMED (1,3)
1884	1208		41-13.45	111-57.55	3.0I	3	
1889	1207	1100	39-15.83	111-38.23	3.7I	4	
1893	830	2330	41-58.25	112-43.19	3.7I	4	
1894	108	1800	39-45.60	113-23.40	4.3I	5	(4) HAS WRONG DATE
1894	718	2250	41-13.45	111-57.55	5.0I	6	INT=5-7
1895	727	2225	39-32.54	111-27.35	3.7I	4	
1896	607	0530	39- 9.19	111-49.10	3.0I	3	
1896	913	0130	39-42.36	111-49.90	3.7I	4	
1896	1003	1550	41-44.26	111-49.85	3.0I	3	
1899	1213	1350	40-44.94	111-50.95	3.7I	4	
19 0	801	0745	39-57.15	112- 6.84	5.7I	7	
19 1	811	1600	40-44.94	111-50.95	3.0I	3	
19 1	811	1800	40-14.35	111-39.33	3.0I	3	
19 2	105	0114	42-13.62	111-24.00	3.0I	3	LOC ASSUMED (1)
19 3	723	0834	41- 5.00	111-55.00	3.0I	3	LOC ASSUMED (1)
19 5	1111	2300	41-58.25	112-43.15	4.3I	5	SHOSHONE,ID SHOCK? (1)
19 6	524	2110	41-13.45	111-57.55	4.3I	5	THREE SHOCKS (1)
19 6	1019	200	42-18.00	111-18.00	4.3I	5	NOAA
19 9	1006	0250	41-46.00	112-40.00	6.3I	8	INT=7-9
19 9	1117	0630	41-44.66	112- 9.72	4.3I	5	
1910	522	1428	40-44.94	111-50.95	5.7I	7	
1910	523	1545	40-44.94	111-50.95	3.0I	3	A'SHOCK (1)
1913	412	0825	42-18.00	112- 0.	4.3I	5	ASSGN SWAN LAKE,ID (1,2)

Historical Earthquakes 160 km From SSC Sites

yr	date	orig time	lat-n	long-w	mag	int	comments
1914	408	1606	40-59.00	111-55.00	4.3I	5	LOC ASSUMED (1)
1914	513	1715	41-13.45	111-57.55	5.7I	7	INT=6-7
1915	315	325	42-18.00	111-18.00	4.3I	5	NOAA
1915	715	2200	40-14.35	111-39.33	5.0I	6	
1915	730	1850	41-44.66	112- 9.72	4.3I	5	ASSGN GARLAND,UT (1)
1915	811	1020	40-30.00	112-39.00	4.3I	5	INT=5-8,LOC ASSUMED (1)
1915	920	0128	39-59.58	111-29.40	3.0I	3	TWO SHOCKS (1)
1915	1003	0150	40-44.94	111-50.95	3.0I	3	(1)
1915	1003	656	42- 0.	111-30.00	5.0I	6	NOAA
1915	1004	1200	41-55.19	112- 3.25	3.0I	3	
1915	1005	0800	40- 6.00	114- 0.	4.3I	5	INT=5-7,LOC FROM (4)
1916	205	0625	39-58.37	111-46.87	4.3I	5	ASSGN SANTAQUIN,UT (1,3)
1918	1016	1145	41-55.19	112- 3.25	3.0I	3	
1919	507	2230	39-31.64	111-34.89	3.7I	4	
1920	918	2010	41-30.61	112- 0.95	4.3I	5	INT=5-6
1920	919	1350	41-30.61	112- 0.95	4.3I	5	INT=5-6
1920	1120	0435	41-30.61	112- 0.95	4.3I	5	INT=5-6
1920	1217	0955	41-30.61	112- 0.95	3.7I	4	A'SHOCK? (1)
1923	607	0415	41-44.26	111-49.85	4.3I	5	
1923	907	1839	41-55.26	111-48.41	3.7I	4	
1925	1201	0730	40-44.94	111-50.95	3.0I	3	
1926	728	0425	41-58.22	111-52.72	3.0I	3	
1926	729	1850	41-58.22	111-52.72	3.0I	3	
1926	1219	0330	39-57.00	111-57.60	3.7I	4	
1928	905	536	42- 6.00	115-12.00	5.2I	6	UNR
1932	1111	1000	40-31.04	111-28.27	3.7I	4	
1932	1221	0613	40-44.94	111-50.95	3.0I	3	
1934	130	2021	40-44.94	111-50.95	3.0I	3	
1934	312	1505 48.00	41-42.00	112-48.00	6.6M	9	INT=8-9,PAS (5,8,9)
1934	312	1820 12.00	41-42.00	112-48.00	6.1N	7	A'SHOCK,PAS (5,8,9)
1934	315	1202	41-42.00	112-48.00	5.1N	6	INT ASSUMED,A'SHOCK (5)
1934	315	1347	41-42.00	112-48.00	4.8N	5	INT ASSUMED,A'SHOCK (5)
1934	317	2240	41-46.50	112- 5.70	3.0I	3	
1934	407	216	40-30.00	111-30.00	3.0I	3	NOAA
1934	414	2126 32.00	41-30.00	112-30.00	5.6N	7	A'SHOCK (1,5,6,8,9)
1934	506	0809 42.00	41-42.00	112-48.00	5.6N	6	A'SHOCK,PAS (5,8,9)
1934	506	830	42- 6.00	112- 6.00	3.7I	4	NOAA
1934	704	0030	41-58.25	112-43.15	3.7I	4	
1935	709	1059	40-44.94	111-50.95	3.7I	4	INT=4-5
1935	709	1205	40-30.00	111-36.00	3.0I	3	NOAA

Historical Earthquakes 160 km From SSC Sites

yr	date	orig time	lat-n	long-w	mag	int	comments
1937	1118	2350	42- 6.00	113-54.00	5.4N	6	NEV (1,2,5)
1938	318		39-59.58	111-29.40	3.0I	3	
1938	630	1337	40-44.94	111-50.95	4.3I	5	SALT LK VALLEY? (1)
1939	331	0640	40-44.94	111-50.95	3.7I	4	
1940	1123	1300	39-15.83	111-38.23	3.7I	4	
1940	1125	1425	39-15.83	111-38.23	3.7I	4	A'SHOCK?
1941	620	1520	41-44.26	111-49.85	3.0I	3	
1942	418	0545 42.00	41-30.00	112-18.00	4.3I	5	HANSEL VALLEY? (1,6,8)
1942	418	1615	42-12.00	112-18.00	3.7I	4	NOAA
1942	604	2204	39-34.80	111-39.00	4.3I	5	TWO SHOCKS (1)
1943	222	1420	40-42.00	112- 4.80	5.0I	6	W. SALT LK VALLEY (1,6,8)
1943	312	1245	39-21.67	111-35.26	3.7I	4	
1943	410	2242	40-42.00	112- 4.80	4.3I	5	W. SALT LK VALLEY (1,8)
1943	411	1932	40-42.00	112- 4.80	3.0I	3	A'SHOCK
1946	506	0230	41-43.80	112- 7.80	4.3I	5	LOC ASSUMED (1)
1946	1025	1653	40-42.60	112- 6.30	3.0I	3	
1947	307	1414	40-44.94	111-50.95	3.0I	3	
1947	328	1102	40-39.90	111-53.40	3.7I	4	INT=4-5
1948	1104	1318	39-15.83	111-38.23	4.3I	5	
1949	307	0650	40-44.94	111-50.95	5.0I	6	
1949	307	0709	40-44.94	111-50.95	3.7I	4	INT=4-6,A'SHOCK (1,4)
1949	1118	1911	40-30.00	111-36.00	3.7I	4	NOAA
1949	1119	1845	41- 6.00	111-36.00	3.7I	4	NOAA
1950	102	1953 04.00	41-30.00	112- 0.	4.3N	4	(5,6,8)
1950	220	1459	40- 2.32	111-43.76	3.7I	4	
1950	225	1337 37.00	40- 0.	112- 0.	3.0X	0	(6)
1950	508	2235	40- 2.32	111-43.76	4.3I	5	
1950	721	1923	41-44.26	111-49.85	3.7I	4	TWO SHOCKS (8)
1951	123	1333	39-42.36	111-49.90	3.7I	4	
1951	812	0026	40-14.35	111-39.33	4.3I	5	
1952	721	0100	39-58.37	111-46.87	3.7I	4	
1952	723	1928	40-44.94	111-50.95	3.7I	4	
1952	928	2000	40-23.81	111-51.64	4.3I	5	
1953	524	0254 29.00	40-30.00	111-30.00	4.3I	5	INT=4-6 (4,6,8,11)
1953	816	1600	40-46.80	111-57.00	3.7I	4	
1954	1101	0745	41-44.26	111-49.85	3.7I	4	
1955	202	1923	40-47.00	111-56.00	4.3I	5	INT=4-5,FEB 4? (4,8,12)
1955	512	2257	40-54.82	111-52.64	4.3I	5	LOC ASSUMED (8)
1955	625	0500	41- 2.51	111-40.49	3.7I	4	
1957	721	1730 02.00	41-30.00	113- 0.	3.0X	0	(6)

Historical Earthquakes 160 km From SSC Sites

yr	date	orig time	lat-n	long-w	mag	int	comments
1957	1025	1626 47.00	40- 0.	111- 0.	3.0X	0	(6)
1957	1026	0146 41.00	40- 0.	111- 0.	3.0X	0	A'SHOCK? (6)
1958	105	1700 04.00	41- 0.	112-30.00	3.0X	0	(6)
1958	213	2252	40-20.50	111-26.40	5.0I	6	(6,8,10)
1958	217	1157 30.00	39-30.00	113- 0.	3.0X	0	(6)
1958	1128	1330	39-42.70	111-50.00	4.3I	5	INT=4-5 (4,8,13)
1958	1201	2050 41.00	39-42.70	111-50.00	4.3I	5	INT=4-5 (4,8,13)**
1958	1201	2230 08.00	39-42.70	111-50.00	3.7I	4	INT=3-4,A'SHOCK(4,6,8,13)
1958	1202	0323 08.50	39-42.70	111-50.00	4.3I	5	INT=4-5,A'SHOCK(4,6,8,13)
1958	1211	0930	39-31.80	111- 1.20	3.7I	4	(8)
1959	104	0022	42-18.00	111-24.00	4.3I	5	LOC ASSUMED (8)
1960	506	2028 42.00	39-30.00	111- 0.	3.0X	0	(6)
1960	709	2136 40.00	41-30.00	112- 0.	3.0X	0	(6)
1960	820	0801 54.30	42-18.00	111-18.00	4.3I	5	SWARM
1961	416	0502 39.30	39-20.40	111-39.60	5.0I	6	INT=4-6 (4,6,8,14)
1961	525	1828 03.20	42-12.00	111-54.00	3.0X	0	(6)
1961	1015	2105 02.00	39-12.00	111-24.00	3.0X	0	(6)
1961	1016	1913 06.50	39-12.00	111-30.00	3.0X	0	A'SHOCK? (6)
1961	1017	0059 41.80	39-12.00	111-30.00	3.0X	0	A'SHOCK? (6)
1961	1017	0354 46.70	40- 0.	112-30.00	3.0X	0	(6)

number of earthquakes = 140

Earthquakes 160 km From SSC Sites

yr	date	orig time	lat-n	long-w	depth	mag	no	gap	dmn	rms
62	709	703 5.47	40-19.19	111-50.14	7.0*	2.9	4	133	49	0.20
62	830	1335 24.41	42- 2.12	111-44.46	7.0*	5.7W	7	221	141	0.37
+62	831	100 0.	41-30.00	111-30.00	0.	3.7	0	0	0	0.
+62	831	1030 0.	41-30.00	111-30.00	0.	3.7	0	0	0	0.
+62	905	300 0.	41-30.00	111-30.00	0.	4.3	0	0	0	0.
62	905	1604 27.78	40-42.92	112- 5.33	7.0*	5.2W	9	188	21	0.41
+62	907	847 20.00	41-36.00	111-30.00	0.	4.3	0	0	0	0.
62	909	1438 8.92	41-50.80	111-46.17	7.0*	3.1	8	214	120	0.44
62	914	1316 54.94	42- 7.07	111-42.78	7.0*	2.8	7	253	150	0.23
63	707	1920 39.59	39-31.96	111-54.51	7.0*	4.4W	9	89	95	0.33
63	709	1520 40.85	39-31.71	111-54.29	7.0*	3.1	5	229	94	0.11
63	709	2025 25.80	40- 1.70	111-11.41	7.0*	4.0W	6	92	57	0.78
63	710	1832 49.76	40- 1.20	111-14.95	7.0*	3.7W	7	93	59	0.39
63	814	1230 2.44	41-37.30	112- 4.24	7.0*	3.2	7	267	97	0.15
63	816	321 4.23	39-28.57	111-59.31	7.0*	3.3	4	237	102	0.
63	816	700 58.87	41-39.66	112- 9.82	7.0*	3.0	6	236	103	0.49
63	817	509 7.42	41-33.75	112- 7.95	7.0*	2.8	8	232	91	0.54
63	817	1023 8.61	40-24.03	111- 1.56	7.0*	2.7	7	127	80	0.44
+63	828	13 12.90	40-54.00	111-54.00	33.0	2.6	6	0	0	0.
+63	1215	1136 23.60	39-12.00	114-12.00	33.0	2.7	8	0	0	0.
63	1221	302 19.43	39-20.06	114-12.01	7.0*	2.7	6	137	152	0.41
63	1225	2355 14.31	39-26.33	114-13.66	7.0*	2.9	6	143	147	0.08
+63	1226	155 14.50	39-12.00	114-12.00	0.	2.8	0	0	0	0.
63	1229	406 9.50	39- 9.45	114- 7.84	7.0*	2.7	8	103	161	0.42
63	1229	415 0.20	39- 8.39	114-17.44	7.0*	3.9W	6	219	172	0.20
64	107	1155 31.72	39- 9.33	114- 6.05	7.0*	2.9	6	121	159	0.51
64	107	1253 45.45	39- 8.81	114-10.43	7.0*	2.9	8	122	159	0.95
64	121	2331 39.75	39- 9.39	114-10.20	7.0*	2.8	6	122	159	0.45
64	220	2019 48.20	39-24.79	114-13.06	7.0*	3.2W	7	141	148	0.44
64	302	729 19.74	39-29.73	111-52.38	7.0*	2.7	5	232	92	0.25
64	305	1240 50.06	39- 8.36	114- 9.83	7.0*	2.9	9	121	160	0.37
64	812	504 47.09	39- 8.87	112- 9.81	7.0*	2.9	6	166	127	0.31
64	906	1903 33.75	39-10.93	111-27.81	7.0*	3.1	10	223	73	0.74
64	1018	1833 20.80	41-43.55	111-43.77	7.0*	4.1W	7	207	7	0.36
65	511	150 25.41	40-57.98	111-31.16	7.0*	2.7W	6	241	35	0.31
65	617	1522 6.15	39-30.82	111-13.24	7.0*	2.8	6	225	37	0.16
65	705	1717 6.07	39-13.95	111-26.13	7.0*	2.7W	7	130	68	0.67
65	727	2023 57.30	40-22.12	111-20.91	7.0*	2.8	7	110	60	0.15
65	910	2147 44.60	39-25.63	111-28.33	7.0*	3.0	4	124	60	0.08
65	1001	2158 43.66	39-27.52	115- 7.07	7.0*	2.9	6	155	73	0.71

Earthquakes 160 km From SSC Sites

yr	date	orig time	lat-n	long-w	depth	mag	no	gap	dmn	rms
65	1029	1652 50.28	41-19.15	113-23.26	7.0*	3.7W	9	203	133	0.51
66	211	2036 21.99	42-15.15	111-16.63	7.0*	2.8	8	284	172	0.75
66	317	1147 47.41	41-39.66	111-33.63	7.0*	4.6W	8	199	22	0.46
66	418	47 29.51	39-17.58	112- 3.93	7.0*	2.7	7	103	114	0.58
66	424	300 1.85	39-33.79	111-33.86	7.0*	2.7	6	123	65	0.72
66	1114	1430 49.88	41-44.70	112-43.85	7.0*	3.2	8	144	76	0.46
67	216	1921 35.19	41-16.40	113-20.03	7.0*	4.0W	10	199	127	0.60
67	403	2117 12.30	39-26.57	111- 4.45	7.0*	2.7	7	137	29	0.37
67	721	1527 57.49	41-15.85	113-17.91	7.0*	3.6W	8	198	125	0.28
67	902	1004 7.17	41- 9.78	111-31.92	7.0*	2.7	8	118	51	0.25
67	922	739 53.92	41-20.75	113-21.97	7.0*	3.1	8	204	136	0.59
67	924	500 28.58	40-42.46	112- 5.90	7.0*	3.0	8	145	22	0.17
67	1207	1333 22.49	41-17.17	111-44.26	7.0*	3.7W	15	127	51	0.53
67	1209	1935 44.00	41-37.44	111-44.59	7.0*	2.7	11	152	14	0.52
68	116	858 41.53	39-18.00	112- 3.72	4.1	3.5W	7	156	113	0.25
68	116	917 50.54	39-17.40	112- 2.69	7.0*	3.4W	13	102	112	0.45
68	116	920 10.26	39-18.78	112- 2.69	7.0*	3.3W	9	155	111	0.38
68	116	941 44.38	39-16.78	112- 1.52	7.0*	3.2W	13	131	111	0.44
68	116	942 52.13	39-15.93	112- 2.28	7.0*	3.9W	7	156	112	0.27
68	307	417 6.77	42-12.32	112-46.98	7.0*	3.0	11	255	95	0.82
68	328	448 8.47	41-19.65	113-28.10	7.0*	2.7	7	206	137	0.74
68	802	707 2.49	39-30.92	111- 2.54	7.0*	2.9	10	106	22	0.50
68	1117	1433 38.19	39-31.42	110-58.16	7.0*	3.5W	13	93	16	0.42
69	730	2359 56.33	40- 1.85	111-55.29	7.0*	2.9	6	85	78	0.64
70	329	1240 40.34	41-39.74	113-50.39	7.0*	4.7W	10	203	168	0.57
+70	726	2157 58.90	39-16.68	114-58.80	5.0	2.9	5	0	0	0.
70	1025	746 42.40	39- 9.46	111-26.35	7.0*	2.7	13	113	73	0.82
70	1025	748 21.94	39-10.28	111-24.72	7.0*	3.1W	6	174	71	0.49
71	420	919 15.04	39-21.41	111-55.16	7.0*	2.7	10	134	99	0.44
71	422	2301 2.81	39-24.63	111-56.46	7.0*	3.1W	8	96	100	0.34
72	306	1333 24.92	41-52.70	111-36.65	7.0*	3.2W	10	166	22	0.46
72	427	804 55.74	39-11.86	111-26.75	7.0*	2.7	5	169	71	0.26
72	612	1302 29.31	41-36.51	111-44.76	7.0*	2.7	5	132	15	0.42
72	1001	1942 29.52	40-30.36	111-20.91	7.0*	4.3W	13	90	36	0.53
72	1016	2149 31.19	40-25.27	111- 0.97	7.0*	3.4W	9	129	65	0.53
73	206	1023 59.52	39-54.14	111-51.28	7.0*	2.7	5	182	75	0.22
73	414	645 46.52	42- 2.57	112-37.87	7.0*	4.2W	19	64	75	0.88
73	722	1235 52.76	41-55.82	112-24.93	7.0*	2.9	6	283	54	0.13
73	819	1913 4.80	40-17.04	111-26.00	7.0*	2.7	8	121	42	0.61
73	1120	2336 30.33	41-59.75	112-40.60	7.0*	3.4W	10	125	77	0.54

Earthquakes 160 km From SSC Sites

yr	date	orig time	lat-n	long-w	depth	mag	no	gap	dmn	rms
73	1120	2347 44.45	41-57.87	112-40.99	7.0*	2.7	7	286	76	0.33
73	1203	1842 47.31	42- 0.21	112-46.64	7.0*	2.7	8	289	85	0.32
73	1203	2059 58.25	42- 0.38	112-49.14	7.0*	2.9	8	290	88	0.48
74	712	836 4.72	39-25.90	112- 7.85	7.0*	2.7W	6	245	77	0.28
74	903	444 41.90	39-33.07	111- 0.42	7.0*	2.7	4	150	18	0.22
74	1228	1357 42.58	41-55.72	111-57.20	7.0*	2.8	13	310	23	0.33
75	327	448 51.71	42- 3.95	112-32.05	5.5	4.2W	11	159	34	0.12
75	328	231 5.99	42- 3.77	112-31.48	5.0	6.0W	11	159	33	0.13
75	328	259 54.11	42- 3.06	112-31.83	5.0	3.0W	10	159	33	0.14
75	328	314 29.04	42- 6.35	112-31.36	5.0	3.3W	9	159	34	0.11
75	328	330 44.40	42- 4.81	112-33.46	5.0	3.1W	11	160	36	0.10
75	328	404 58.01	42- 4.21	112-31.22	11.3	3.3W	11	159	33	0.15
75	328	518 54.11	42- 1.40	112-30.00	5.0	3.1W	10	158	31	0.08
75	328	552 15.98	42- 0.17	112-32.10	8.7	2.9W	11	160	34	0.06
75	328	652 33.33	41-53.50	111-47.03	6.7	3.0W	14	170	9	0.27
75	328	742 45.27	42- 4.35	112-31.57	9.1	2.8W	11	159	33	0.13
75	328	811 23.25	42- 4.18	112-26.76	5.0	2.7	11	155	27	0.16
75	328	1122 24.13	42- 4.80	112-31.59	10.2	3.1W	11	159	33	0.20
75	328	1126 16.07	42- 2.51	112-28.03	5.0	3.0W	11	156	28	0.06
75	328	1307 45.41	42- 1.67	112-29.18	5.0	2.8W	11	157	29	0.15
75	328	1311 16.46	42- 4.61	112-29.01	5.0	3.1W	11	157	30	0.08
75	328	1615 6.40	42- 4.96	112-34.46	9.1	3.8W	11	161	37	0.15
75	328	1642 33.94	42- 4.63	112-31.11	5.0	2.7W	11	159	33	0.14
75	328	1757 41.28	42- 6.42	112-28.07	5.0	2.8W	11	156	29	0.16
75	328	1830 7.73	42- 3.77	112-31.53	9.3	3.1W	11	159	33	0.13
75	328	1921 45.33	42- 3.04	112-31.57	5.8	3.0W	11	159	33	0.15
75	328	2132 55.90	42- 0.31	112-28.05	5.0	3.1W	11	157	28	0.07
75	328	2205 10.95	42- 2.84	112-30.57	15.8	3.2W	11	158	31	0.11
75	329	129 53.19	42- 1.14	112-29.43	5.0	3.0W	13	158	7	0.13
75	329	147 23.98	42- 3.62	112-31.97	4.5	3.1W	13	159	7	0.11
75	329	218 19.23	42- 6.80	112-27.26	5.0	3.0W	13	155	4	0.14
75	329	544 32.02	42- 7.43	112-28.48	5.0	3.3W	12	156	6	0.19
75	329	549 1.89	42- 8.85	112-29.03	5.9	2.8W	12	157	9	0.12
75	329	824 10.29	42- 2.00	112-35.81	5.0	2.8W	10	184	39	0.19
75	329	932 13.91	42- 0.14	112-32.26	5.6	3.2W	11	160	34	0.15
75	329	1301 19.89	42- 2.00	112-31.09	6.8	4.7W	13	159	7	0.15
75	329	1432 42.27	42- 4.20	112-33.16	5.0	3.0W	11	160	35	0.11
75	329	1543 43.63	42- 7.35	112-34.85	5.0	3.3W	11	161	39	0.33
75	330	514 5.11	42- 2.20	112-27.76	5.0	2.8W	8	91	4	0.04
75	330	532 29.27	41-59.92	112-29.56	5.0	2.8W	11	112	9	0.19

Earthquakes 160 km From SSC Sites

yr	date	orig time	lat-n	long-w	depth	mag	no	gap	dmn	rms
75	330	656 28.73	42- 1.99	112-34.85	7.1	4.1W	13	162	12	0.20
75	330	722 0.29	42- 3.33	112-39.18	5.0	3.0W	7	276	17	0.06
75	330	732 13.23	42- 1.49	112-34.88	5.0	3.5W	13	162	12	0.15
75	330	846 30.97	42- 1.38	112-35.81	0.2	3.2W	10	122	3	0.20
75	330	854 51.36	42- 2.66	112-35.38	4.3	2.9W	7	182	3	0.18
75	330	1006 48.95	42- 1.08	112-36.11	5.0	2.8	8	134	3	0.17
75	330	1217 59.83	42- 3.29	112-32.06	5.0	2.7	10	103	7	0.13
75	330	1256 33.49	42- 2.00	112-35.89	5.0	3.3W	8	102	3	0.12
75	330	1402 26.52	42- 1.54	112-36.26	5.8	3.6W	16	106	2	0.17
75	330	1653 28.55	42- 1.42	112-35.64	5.0	2.7W	7	140	3	0.13
75	330	2123 12.63	41-58.65	112-30.00	5.0	2.7W	7	161	11	0.04
75	330	2343 50.88	42- 6.05	112-29.98	5.0	2.7W	8	147	9	0.09
75	331	155 36.06	42- 3.80	112-32.57	10.6	3.6W	15	86	8	0.19
75	331	822 54.46	42- 1.26	112-30.00	5.0	2.9W	6	162	11	0.13
75	331	842 46.89	42- 2.78	112-30.68	5.0	2.7W	8	160	6	0.19
75	331	852 12.69	42- 0.91	112-29.24	5.0	2.9W	8	103	7	0.16
75	331	1030 56.40	42- 4.62	112-29.87	6.2	3.5W	13	67	4	0.17
75	331	1322 57.60	42- 0.84	112-28.90	5.6	2.7W	7	103	7	0.13
75	331	1323 58.41	42- 0.35	112-30.01	7.1	3.1W	8	110	8	0.12
75	331	1345 51.87	41-59.58	112-29.05	5.0	3.3W	8	114	9	0.16
75	331	1444 23.89	42- 4.71	112-25.44	5.0	2.9W	7	148	1	0.14
75	331	2043 31.98	42- 0.58	112-29.14	5.0	2.8W	6	155	1	0.11
75	331	2326 35.97	42- 0.82	112-29.34	3.0	3.0W	6	153	0	0.15
75	401	1229 34.61	42- 1.75	112-30.00	6.4	2.7W	8	79	1	0.08
75	401	1847 56.41	42- 2.77	112-29.55	8.1	2.8W	9	70	3	0.12
75	402	2106 46.16	42- 5.43	112-26.54	6.1	3.3W	7	165	2	0.05
75	402	2345 17.59	41-59.31	112-29.39	5.7	2.9W	8	122	3	0.15
75	403	114 29.53	42- 0.84	112-28.56	6.0	3.0W	8	193	1	0.09
75	403	122 10.16	42- 0.06	112-29.32	5.9	2.9W	8	122	2	0.05
75	404	522 33.98	41-59.36	112-29.74	5.0	3.0W	10	92	3	0.08
75	404	652 26.57	42- 6.12	112-30.27	9.0	2.9W	11	67	2	0.06
75	404	1346 3.52	42- 1.00	112-28.42	5.8	2.9W	9	116	1	0.05
75	405	108 16.50	42- 2.38	112-30.20	7.0	3.2W	9	75	2	0.05
75	405	644 35.67	42- 0.96	112-28.30	5.7	2.7W	9	117	1	0.04
75	406	2105 34.13	42- 1.55	112-29.30	6.3	3.3W	9	77	0	0.10
75	407	822 44.18	42- 2.00	112-30.46	6.2	2.9W	9	80	2	0.08
75	407	1342 34.59	42- 3.18	112-29.45	6.2	3.2W	9	77	3	0.06
75	407	1401 42.20	42- 9.44	112-35.10	3.9	3.1W	9	186	1	0.07
75	407	1443 54.35	42- 2.93	112-29.61	5.4	3.1W	9	73	3	0.04
75	408	348 3.61	41-51.64	112-22.39	8.7	3.0W	6	241	14	0.01

Earthquakes 160 km From SSC Sites

yr	date	orig time	lat-n	long-w	depth	mag	no	gap	dmn	rms
75	409	520 11.01	42- 2.45	112-30.98	7.2	3.0W	9	78	3	0.06
75	410	1021 0.72	42- 1.07	112-33.24	5.7	3.2W	7	110	5	0.08
75	414	1824 24.60	42- 6.16	112-26.66	8.3	2.8W	10	78	3	0.14
75	414	2032 16.94	42- 6.39	112-27.91	5.3	2.8W	9	141	4	0.15
75	420	856 27.00	41-58.85	112-26.17	7.0*	3.1W	6	253	26	0.14
75	420	1923 24.61	41-58.35	112-26.77	7.0*	2.9W	6	255	27	0.15
75	420	2210 27.87	41-59.37	112-27.54	7.0*	2.7W	7	258	27	0.12
75	423	428 33.81	42- 0.37	112-31.75	7.0*	2.7W	5	286	33	0.07
75	426	152 4.39	42- 0.23	112-28.20	7.0*	3.2W	6	260	28	0.13
75	503	154 32.06	42- 5.53	112-27.74	7.0*	2.7W	6	145	7	0.16
75	512	517 13.69	41-58.88	112-29.58	2.2	3.1W	12	178	18	0.11
#75	512	941 30.50	41- 1.56	114-52.32	0.	3.1	7	0	0	0.56
75	519	2137 28.05	42- 0.25	112-30.35	1.0	2.9	6	181	15	0.27
75	529	1229 52.37	41-58.69	112-30.45	7.0*	2.9W	7	179	18	0.19
75	613	1609 56.58	41-44.39	112-20.73	7.0*	2.7	7	201	36	0.19
#75	616	2330 54.90	40-52.38	114-48.18	0.	3.9	0	0	0	0.
#75	627	147 3.90	40-56.04	114-52.38	0.	3.2	8	0	0	0.95
75	629	1859 28.45	42- 0.90	112-29.70	7.0*	2.7W	6	196	14	0.27
75	630	326 45.89	42- 8.56	112-32.56	14.8	3.0W	5	277	2	0.08
75	707	133 25.03	41-58.54	112-28.34	7.0*	2.7	7	190	19	0.29
75	816	2120 53.76	42- 5.02	112-26.91	4.1	3.7W	16	142	9	0.19
75	912	1826 6.80	42- 6.50	112-27.25	8.2	3.3	13	140	6	0.12
75	914	413 24.57	41-53.57	112-22.79	7.0*	2.8	16	147	25	0.17
75	922	1042 36.28	42- 5.77	112-27.00	6.2	3.6W	6	144	8	0.20
75	1006	1550 48.44	39- 9.13	111-30.22	7.0*	2.8	11	170	62	0.39
75	1011	9 56.31	40-33.31	111-11.65	3.2	2.7W	14	208	13	0.16
75	1011	2155 1.22	41-49.54	111-32.33	7.0*	2.9	15	90	18	0.53
#75	1012	947 3.90	40-52.74	114-53.76	0.	3.2	0	0	0	0.
75	1013	659 25.63	41-58.96	112-30.88	7.0*	2.7	17	172	18	0.22
75	1117	821 11.15	41-57.36	112-32.15	7.0*	3.2	25	177	21	0.32
76	220	1512 29.90	39-18.63	111- 8.17	7.0*	2.7W	9	185	43	0.32
76	221	1412 46.85	41-59.90	112-33.26	0.5	3.0	14	184	16	0.17
76	227	718 16.47	41-15.83	111-15.76	7.0*	2.7W	17	201	30	0.28
76	307	723 10.94	42- 3.88	112-31.54	3.5	2.8	15	177	9	0.17
#76	313	2120 31.30	40-48.60	114-58.56	0.	2.9	7	0	0	1.03
76	322	918 45.28	42- 5.83	112-37.31	2.0	3.3	14	233	10	0.18
76	614	937 57.83	42- 6.99	112-29.08	6.2	3.6W	17	134	4	0.19
76	615	208 10.79	41-53.67	112-25.78	7.0*	2.8W	20	156	29	0.42
76	711	1242 55.33	42- 9.80	112-37.46	4.7	2.7	11	270	8	0.13
76	712	1644 37.68	42-11.56	112-38.59	5.5	2.9W	15	273	11	0.26

Earthquakes 160 km From SSC Sites

yr	date	orig time	lat-n	long-w	depth	mag	no	gap	dmn	rms
76	712	2032 42.04	42-10.34	112-30.13	5.0	2.7W	10	201	10	0.12
76	721	101 6.00	42- 6.19	112-37.77	2.0	3.0	14	238	10	0.16
76	819	1329 53.91	39-18.32	111- 6.68	1.0	2.9W	20	139	42	0.52
76	1105	115 7.06	41-49.35	112-41.65	7.0*	3.3W	21	199	38	0.22
76	1105	248 55.59	41-48.59	112-41.88	7.0*	4.0W	15	199	40	0.19
76	1105	554 0.92	41-48.94	112-41.77	7.0*	3.4W	21	199	39	0.25
76	1105	1058 3.62	41-48.83	112-41.91	7.0*	2.8W	13	199	39	0.19
76	1106	316 26.96	41-48.81	112-42.87	7.0*	2.8W	21	201	40	0.25
76	1106	1958 46.11	39-28.14	111-18.44	7.0*	2.8W	17	215	62	0.56
76	1126	2226 29.43	39-30.79	111-15.72	7.0*	3.1W	15	248	40	0.40
76	1203	205 38.51	41-54.78	112-21.87	7.0*	2.9	12	87	23	0.16
77	209	42 16.13	39-17.55	111- 6.69	7.0*	3.2W	16	187	43	0.52
+77	609	459 55.40	40- 7.80	115-15.54	2.0	3.0	6	0	0	0.
77	1128	223 11.16	41-21.09	111-42.33	6.8	2.7W	23	98	20	0.20
78	228	20 6.50	40-44.66	112-12.17	10.6	2.7W	15	85	30	0.35
78	309	630 51.88	40-45.82	112- 5.27	8.8	3.2W	18	70	13	0.26
78	313	1335 43.70	40-45.28	112- 5.46	8.3	2.7W	18	71	7	0.23
78	603	842 45.80	40-43.35	112- 3.30	6.3	2.7W	11	107	10	0.29
78	623	454 29.46	41-41.71	111-29.62	7.0*	2.8	25	196	25	0.49
78	729	1404 3.36	41-50.92	112- 7.84	4.2	3.1W	27	63	18	0.23
78	923	820 7.41	39-19.27	111- 5.67	7.0*	2.7	18	102	44	0.53
78	1130	653 40.21	42- 6.08	112-29.48	2.5	4.6W	32	123	5	0.33
78	1130	1155 9.60	42- 7.07	112-30.01	4.4	3.4W	24	124	3	0.29
78	1202	230 37.42	42- 6.67	112-28.75	6.4	2.8W	15	107	5	0.23
78	1205	1124 57.49	42- 6.46	112-29.69	3.0	3.8W	24	124	4	0.27
78	1205	1156 27.85	42- 6.35	112-29.71	2.8	3.0W	24	125	5	0.26
78	1210	1459 7.18	40-48.72	111-33.91	6.9	2.7W	29	129	7	0.36
78	1216	110 55.90	39-17.18	111-58.83	7.0*	2.7	26	120	26	0.34
78	1220	1346 22.58	42- 7.03	112-29.73	5.7	3.9W	23	119	3	0.26
78	1220	1544 31.82	42- 6.51	112-30.33	6.1	2.8	18	135	4	0.13
79	220	2152 37.55	39-34.31	111-32.97	7.0*	2.8	24	124	25	0.47
79	224	1243 41.17	41-43.02	111- 8.90	90.5	3.8W	29	129	41	0.30
79	325	1900 37.73	41-19.92	113-17.58	7.0*	2.7W	22	218	65	0.31
79	325	1913 42.17	41-23.02	113-22.75	7.0*	2.9W	25	229	66	0.46
79	325	2141 55.74	41-20.59	113-17.07	7.0*	3.2W	24	218	64	0.30
79	515	220 22.09	41-59.45	112-34.10	4.1	2.9	18	157	17	0.21
79	1018	3 32.24	39-18.65	111- 6.91	7.0*	2.7	11	116	45	0.46
80	106	2147 24.30	41-40.40	111-40.21	8.5	2.7	22	60	16	0.31
80	206	203 6.80	42- 6.27	112-29.71	4.0	2.8W	23	125	5	0.31
80	403	1422 9.25	41-20.00	113-19.97	7.0*	2.9W	22	236	68	0.30

Earthquakes 160 km From SSC Sites

yr	date	orig time	lat-n	long-w	depth	mag	no	gap	dmn	rms
80	404	45 4.50	41-20.19	113-17.17	7.0*	3.1W	23	213	65	0.30
80	404	56 9.03	41-20.49	113-20.15	7.0*	2.7	15	264	67	0.24
80	406	1045 4.03	39-56.86	111-58.46	4.4	3.5W	28	70	16	0.25
80	517	903 38.64	39-42.55	112- 1.59	7.0*	3.0	9	121	67	0.29
80	524	1003 36.47	39-56.21	111-57.59	7.0*	4.4W	17	113	60	0.37
80	524	2212 14.28	39-55.78	111-57.39	7.0*	2.7	13	114	61	0.31
80	603	2159 5.47	39-50.76	111-58.89	2.3	2.9	16	105	16	0.35
80	705	1936 11.30	39-15.70	111-54.32	7.0*	2.7W	14	101	86	0.35
80	801	116 22.86	41-26.16	113- 9.62	7.0*	2.8W	21	208	49	0.24
80	815	625 23.72	41-39.74	111-41.10	7.0*	3.1W	20	106	34	0.35
80	1022	926 34.42	42- 8.85	112-29.13	6.0	2.8	16	291	27	0.22
80	1029	730 54.58	41-46.08	111-41.72	8.0	2.7	22	72	7	0.30
81	220	913 1.19	40-19.33	111-44.11	0.7	3.9W	32	110	19	0.29
81	331	2040 45.51	41-41.42	111- 2.60	0.1	3.1W	37	143	32	0.29
81	411	519 48.65	41-51.43	112-40.81	3.3	3.0W	26	137	11	0.19
81	411	808 2.32	41-51.53	112-40.58	0.4	3.1W	32	137	12	0.24
81	514	511 4.34	39-28.86	111- 4.72	0.7	3.5W	27	133	58	0.51
81	609	1912 19.35	39-30.76	111-15.37	1.1	2.8W	18	123	49	0.24
81	1229	403 4.33	41-53.85	112-33.62	6.4	2.8W	29	133	19	0.20
81	1229	1139 21.22	41-53.42	112-33.46	2.1	3.1W	33	130	19	0.27
82	129	1209 49.19	39-29.69	112-10.88	5.9	2.7W	32	66	30	0.30
82	215	1952 30.52	39-12.02	111-59.30	1.3	2.8	19	62	27	0.50
82	323	2249 2.63	39-28.03	112- 0.40	0.2	2.7	11	96	43	0.32
82	829	1207 54.32	40-52.73	111-40.04	5.2	2.7W	33	81	11	0.31
82	1115	1659 59.23	39-30.26	111- 4.24	0.4	2.8	16	120	28	0.36
82	1209	1444 20.43	39-18.47	111- 9.22	4.5	2.8	22	93	33	0.45
82	1224	1511 21.09	42- 8.57	112-29.43	0.7	3.3W	11	157	32	0.36
83	212	1257 40.48	39-18.68	111- 9.75	0.5	2.7	10	92	32	0.38
83	306	1053 35.65	41- 8.42	111-40.32	8.9	2.8W	38	122	18	0.28
83	609	1657 15.00	39-51.23	111-58.75	5.9	2.9W	23	49	13	0.35
83	829	1253 11.45	41- 4.99	111-25.60	9.8	3.0W	12	165	50	0.24
83	1008	1157 53.83	40-44.88	111-59.56	5.5	4.3W	30	66	15	0.33
83	1119	350 46.93	42- 0.33	112-29.96	4.8	3.8W	18	229	16	0.24
84	225	704 44.94	41-44.65	114-54.01	7.0	3.5	15	236	176	0.21
84	318	944 59.84	39-28.78	115-13.19	1.7	3.2	20	257	158	0.41
84	321	1119 30.58	39-20.64	111- 6.53	0.1	2.9W	24	102	37	0.51
84	512	1520 4.41	42- 0.15	112-33.11	3.6	3.0W	38	130	20	0.28
84	610	1410 30.92	40-45.21	112- 4.08	1.2	2.7	27	66	14	0.32
84	806	2230 38.66	41-52.53	112-22.38	2.1	3.0W	26	92	7	0.35
84	816	1419 21.71	39-23.50	111-56.16	6.1	3.7W	12	95	34	0.33

Earthquakes 160 km From SSC Sites

yr	date	orig time	lat-n	long-w	depth	mag	no	gap	dmn	rms
84	829	909 30.57	39-19.22	111- 9.69	0.1	2.7	28	116	5	0.42
84	930	2046 31.74	41-27.32	112-24.57	0.0	2.8W	37	116	7	0.32
84	1015	2323 56.53	41-48.27	112-24.10	4.1	3.4W	25	81	15	0.17
85	126	1508 6.71	41-53.43	112-31.80	2.0	3.6W	30	109	17	0.24
85	127	1046 49.60	41-53.40	112-32.21	1.5	3.3W	33	109	18	0.25
85	208	107 57.77	40-18.27	114- 1.38	6.4	2.7W	28	101	84	0.45
85	611	721 45.12	39- 9.93	111-28.21	0.1	3.0	8	169	15	0.42
85	728	2319 7.07	41-56.26	112-36.37	1.4	2.7W	21	132	22	0.26
85	807	710 33.25	42- 6.48	112-19.32	0.5	2.8W	28	90	16	0.25
85	1203	1755 36.17	39-42.09	111-10.28	1.3	2.7	22	73	16	0.34
86	113	1232 4.68	41-42.88	111-39.91	5.3	3.2W	21	64	12	0.27
86	123	1929 1.21	41-21.04	111-37.80	3.3	2.7W	31	116	16	0.27
86	221	2320 12.60	41-44.51	112-48.89	4.7	3.6W	33	161	5	0.25
86	324	2233 41.38	39-13.35	112- 0.38	0.1	3.3W	23	106	22	0.32
86	324	2240 23.48	39-14.17	112- 0.54	0.8	4.4W	32	87	21	0.36
86	325	249 6.33	39-13.79	112- 0.35	0.4	2.8W	14	95	21	0.42
86	325	253 1.24	39-13.40	112- 0.65	0.3	3.9W	21	90	22	0.31
#86	403	541 1.67	40-22.92	115-12.89	0.0	3.1	10	334	227	1.92
86	528	17 54.40	39-46.47	112-47.41	1.4	2.8W	29	118	46	0.35
86	605	741 21.00	41-15.94	111-40.76	11.9	2.8W	31	155	18	0.25
86	605	805 41.77	41-16.06	111-41.16	6.9	3.6W	21	153	17	0.27
#86	704	1726 4.09	39-46.41	114-52.94	0.0	2.7	23	162	127	0.65
86	729	1048 12.27	39-56.99	115- 3.29	14.3	3.3	20	250	144	0.96
86	829	826 24.06	42- 6.33	111-39.28	0.1	3.2W	28	75	34	0.32
86	914	340 25.62	41-17.64	111-28.48	7.7	2.8	34	154	18	0.34
86	919	1041 28.25	41-27.94	111-42.21	4.8	3.4W	35	71	16	0.27
86	1001	1151 46.68	40-49.07	111-49.27	5.3	2.7W	23	78	4	0.27
86	1018	2121 28.96	42- 1.40	111-27.66	0.4	3.5W	24	149	20	0.35
86	1026	1431 56.40	41-49.69	112-19.39	0.2	3.0W	34	74	11	0.33
86	1029	2213 14.47	41-49.28	112-19.09	5.0	3.6W	19	75	12	0.14
86	1030	5 42.76	39-44.23	110-58.15	0.4	2.8W	14	195	67	0.24
86	1031	1158 27.97	41-49.51	112-19.20	0.2	3.5W	28	74	11	0.26
86	1108	448 29.39	41-49.70	112-19.01	4.2	2.7W	26	73	11	0.17
86	1231	1121 56.47	41-49.48	112-19.14	2.2	3.3W	24	73	11	0.21
87	108	1459 2.83	39-43.86	110-56.68	2.3	2.7	19	160	68	0.26
87	204	2315 45.07	39-20.36	111- 7.87	0.4	2.7	18	117	47	0.39
87	205	1117 2.62	39-19.93	111- 7.88	0.5	2.8	21	114	47	0.41
87	222	1057 16.97	39-23.50	112- 9.34	3.0	2.8	13	147	63	0.38
87	225	1230 33.48	41-49.40	112-19.48	2.6	3.7W	27	74	11	0.28
87	225	1259 40.75	39-20.05	111- 7.72	0.6	2.9	17	114	47	0.45

Earthquakes 160 km From SSC Sites

yr	date	orig time	lat-n	long-w	depth	mag	no	gap	dmn	rms
87	226	1301 22.55	41-49.61	112-19.60	2.8	2.8W	25	75	11	0.29
87	227	2210 59.02	41-49.10	112-19.23	0.3	2.9	19	75	12	0.14
87	228	2116 10.67	41-49.71	112-20.08	5.8	2.7	16	75	11	0.12
87	309	1341 23.13	40- 4.52	114-39.48	7.1	2.7W	17	210	114	0.34
87	310	128 12.18	41-52.30	112-43.08	0.2	2.8	26	150	11	0.22
#87	310	508 33.87	40-25.59	114-15.75	10.0	2.9	11	326	307	1.24
87	311	156 7.84	40- 7.49	114-19.95	5.2	3.4W	25	207	91	0.40
87	311	1311 29.47	39-14.73	111-37.75	0.8	2.7	17	82	7	0.37
87	311	1531 2.98	39-14.99	111-38.18	1.6	2.9	25	81	7	0.37
87	317	1507 58.17	41-50.22	112-20.35	0.3	2.8W	30	77	10	0.28
87	322	241 55.10	41-52.58	112-42.24	1.7	3.4W	25	164	12	0.20
87	323	318 8.08	40- 7.52	114-23.16	1.6	2.9W	19	202	95	0.32
87	323	407 0.06	40- 6.64	114-22.90	1.9	3.4W	36	184	94	0.35
#87	323	447 45.33	40- 4.05	114-13.08	10.0	2.7	6	325	304	0.63
87	323	559 12.50	40- 6.67	114-19.01	3.6	3.0W	22	199	90	0.25

number of earthquakes = 335

\+ indicates events from the NOAA cataog
\# indicates events from the University of Nevada cataog

* indicates poor depth control
W indicates Wood-Anderson data used for magnitude calculation

APPENDIX B.

Blast Listings by Blast Sites

Blasts 10 km From Dolomite Mine

yr	date	orig time	lat-n	long-w	depth	mag	no	gap	dmn	rms
74	429	2019 50.38	40-40.93	112-35.77	7.0*	1.9	3	261	57	0.
75	1103	1820 26.51	40-39.16	112-33.05	7.0*	0.7	6	165	20	0.35
76	123	54 56.48	40-40.86	112-36.86	7.0*	1.3	11	175	20	0.32
76	207	418 29.66	40-38.81	112-33.84	7.0*	1.1	12	166	31	0.21
76	224	2249 37.81	40-40.59	112-36.34	7.0*	1.1	7	174	20	0.57
76	423	1829 41.02	40-38.91	112-34.38	7.0*	1.3	10	167	21	0.47
76	520	2159 21.31	40-39.15	112-33.19	7.0*	1.3	6	165	20	0.18
76	604	2225 42.53	40-42.35	112-41.33	7.0*	1.5	7	187	22	0.55
76	628	2329 54.12	40-43.02	112-36.17	1.0	1.0	10	165	16	0.68
76	807	129 36.23	40-39.89	112-35.29	7.0*	1.8	6	175	47	0.50
76	903	2136 8.95	40-39.51	112-34.20	2.1	1.1	7	173	20	0.30
76	915	1734 41.26	40-39.36	112-33.36	7.0*	1.9	6	184	45	0.40
76	1105	2313 13.28	40-39.63	112-33.49	7.0*	1.1	14	166	27	0.45
76	1123	2354 34.84	40-41.79	112-35.08	7.0*	0.9	11	172	24	0.30
76	1204	345 38.60	40-40.61	112-40.41	7.0*	1.4	6	187	29	0.21
76	1209	313 45.18	40-39.11	112-31.83	7.0*	0.8	5	159	28	0.26
77	110	2227 45.68	40-38.42	112-31.13	7.0*	0.7	6	144	29	0.20
77	126	1307 28.01	40-39.15	112-34.73	7.0*	1.1	12	167	29	0.36
77	204	2036 12.98	40-39.81	112-34.54	7.0*	0.7	7	151	27	0.43
77	218	1443 56.27	40-40.68	112-37.50	7.0*	0.8	12	158	27	0.31
77	302	303 56.80	40-41.45	112-39.69	7.0*	0.7	8	162	27	0.37
77	309	2325 49.60	40-37.66	112-33.33	7.0*	0.5	6	163	31	0.17
77	315	1318 13.68	40-38.79	112-33.81	7.0*	1.1	8	165	29	0.25
77	331	359 23.12	40-39.05	112-34.17	7.0*	0.8	13	150	29	0.28
77	405	232 22.78	40-37.21	112-32.29	7.0*	0.9	8	145	32	0.17
77	420	2053 28.01	40-42.76	112-36.36	7.0*	0.8	12	156	23	0.41
77	429	624 28.33	40-39.44	112-33.28	7.0*	1.2	11	148	28	0.33
77	504	2307 6.95	40-37.36	112-34.21	7.0*	1.2	15	149	32	0.29
77	623	2221 6.30	40-39.49	112-33.06	7.0*	0.7	5	164	28	0.33
77	707	1233 47.19	40-39.95	112-37.80	7.0*	0.8	6	176	28	0.10
77	713	2234 17.03	40-42.23	112-32.90	7.0*	0.9	4	167	23	0.12
77	801	2242 51.02	40-41.98	112-37.65	7.0*	1.5	10	178	58	0.44
77	810	1328 46.35	40-40.10	112-36.40	7.0*	1.4	7	155	55	0.22
77	817	2246 46.42	40-39.39	112-36.00	7.0*	1.1	5	184	29	0.10
77	930	2211 22.88	40-39.96	112-37.81	7.0*	1.0	10	158	28	0.36
77	1013	232 11.12	40-41.05	112-39.01	7.0*	1.0	8	177	27	0.38
78	116	2153 57.02	40-39.85	112-38.57	7.0*	0.1	7	159	29	0.50
78	124	1436 30.48	40-39.66	112-33.60	7.0*	0.7	7	169	27	0.28
78	510	2308 7.34	40-42.87	112-35.25	1.1	1.1	6	210	13	0.40

number of events = 39

Blasts 10 km From Ireco

yr	date	orig time	lat-n	long-w	depth	mag	no	gap	dmn	rms
75	225	1614 22.40	40-15.21	112-22.32	7.0*	1.7	5	241	31	0.58
78	428	1650 36.70	40-18.02	112-21.90	7.0*	2.2	8	171	27	0.25

number of events = 2

* indicates poor depth control
W indicates Wood-Anderson data used for magnitude calculation

Blasts 10 km From Lakeside

yr	date	orig time	lat-n	long-w	depth	mag	no	gap	dmn	rms
75	218	1851 24.24	41-12.42	112-48.94	7.0*	1.3	10	212	63	0.17
75	724	1908 48.64	41-13.41	112-51.68	7.0*	1.1	10	198	37	0.15
75	814	1617 59.85	41- 8.74	112-54.30	7.0*	1.5	8	200	43	0.27
75	1231	2116 13.77	41-13.97	112-53.40	7.0*	1.2	13	200	44	0.31
76	116	1537 58.83	41-13.35	112-52.32	7.0*	1.2	13	198	43	0.21
76	213	2105 31.26	41-13.57	112-52.78	7.0*	1.1	7	199	43	0.22
76	324	1747 39.51	41-14.15	112-54.53	7.0*	1.2	12	202	45	0.26
76	330	1953 16.68	41- 8.82	112-55.76	7.0*	1.1	11	202	51	0.51
76	409	2228 25.31	41-13.32	112-52.77	7.0*	1.3	7	199	43	0.05
76	525	1658 57.97	41-12.88	112-52.31	7.0*	1.6	8	217	43	0.22
76	608	1746 48.69	41-13.82	112-53.18	7.0*	1.2	11	200	43	0.24
76	624	1502 33.52	41-13.43	112-50.70	7.0*	1.1	9	196	41	0.42
76	708	2004 29.99	41-13.18	112-52.31	7.0*	1.4	12	198	43	0.19
76	730	1954 5.93	41-13.69	112-53.39	7.0*	1.2	8	200	44	0.25
76	910	1624 9.89	41-13.27	112-52.17	7.0*	1.2	7	198	57	0.21
76	929	2227 1.53	41-13.76	112-52.49	7.0*	1.2	10	199	43	0.18
76	1029	1555 19.89	41-13.37	112-51.50	7.0*	1.4	11	197	42	0.19
76	1111	1959 17.22	41-13.33	112-52.73	7.0*	1.0	10	225	43	0.27
76	1119	2000 2.99	41-13.35	112-52.58	7.0*	1.4	12	190	43	0.20
76	1208	1617 43.28	41-12.74	112-54.18	7.0*	0.9	8	234	45	0.17
76	1215	2213 28.41	41- 8.68	112-54.01	7.0*	1.6	13	192	42	0.26
77	107	1720 3.33	41-12.17	112-45.76	7.0*	1.2	8	189	39	0.62
77	125	2048 6.46	41-13.71	112-54.45	7.0*	0.8	10	202	45	0.17
77	127	1749 17.52	41-13.30	112-54.04	7.0*	0.5	7	193	45	0.27
77	302	1808 40.25	41-13.05	112-51.80	7.0*	0.8	11	189	42	0.18
77	329	2220 47.21	41-12.93	112-53.31	7.0*	0.6	9	226	44	0.13
77	404	2041 30.19	41-13.42	112-52.05	7.0*	0.6	9	189	42	0.25
77	427	2011 46.47	41-13.08	112-54.76	7.0*	1.2	9	195	46	0.13
77	510	1515 29.08	41-12.66	112-50.58	7.0*	1.1	8	186	41	0.32
77	601	1529 43.73	41-13.67	112-51.83	7.0*	1.1	9	189	42	0.14
77	729	1600 58.80	41-13.45	112-54.76	7.0*	1.1	11	202	46	0.28
77	1018	2209 47.39	41- 8.96	112-50.16	7.0*	1.2	9	252	38	0.20
78	627	2017 42.40	41-14.46	112-52.23	7.2	1.4	7	190	42	0.18
83	1203	42 47.33	41-13.89	112-54.07	7.3	1.3	18	193	44	0.35
86	1112	2204 18.41	41-12.81	112-54.35	1.8	1.1	10	232	46	0.20

number of events = 35

* indicates poor depth control
W indicates Wood-Anderson data used for magnitude calculation

Blasts 10 km From Lakeside Mountain

yr	date	orig time	lat-n	long-w	depth	mag	no	gap	dmn	rms
74	209	2055 10.87	40-49.52	112-50.84	7.0*	2.2	4	289	70	0.31
76	528	42 39.85	40-53.57	112-49.89	7.0*	1.8	13	192	31	0.37
76	702	2045 41.26	40-54.68	112-52.68	7.0*	1.9	11	196	79	0.24
76	1013	2048 13.60	40-54.70	112-51.38	7.0*	2.2	13	209	29	0.34
77	115	2156 16.03	40-54.13	112-48.96	7.0*	1.3	6	190	26	0.20
77	228	2159 1.38	40-54.07	112-49.33	7.0*	1.0	9	191	26	0.20
77	401	1700 10.27	40-54.32	112-51.56	7.0*	1.8	7	187	29	0.20
77	425	1935 30.18	40-54.40	112-50.03	7.0*	1.3	9	192	27	0.24
77	525	2046 14.38	40-55.28	112-51.26	7.0*	1.7	9	186	29	0.35
77	622	2051 16.86	40-55.35	112-50.31	7.0*	1.9	11	193	28	0.41
77	831	2052 32.93	40-53.05	112-53.02	7.0*	2.0	12	190	31	0.31
78	206	2257 28.94	40-54.67	112-54.46	7.0*	1.3	10	192	79	0.33
78	424	2200 15.96	40-55.03	112-50.17	7.0*	1.7	6	192	80	0.05
78	606	2059 12.55	40-55.47	112-48.11	7.0*	1.5	8	204	24	0.43

number of events = 14

* indicates poor depth control
W indicates Wood-Anderson data used for magnitude calculation

Blasts 10 km From Mercur Mine

yr	date	orig time	lat-n	long-w	depth	mag	no	gap	dmn	rms
80	214	2120 41.62	40-18.62	112-13.75	2.2	1.0	7	199	18	0.37
80	417	1957 29.25	40-18.42	112-13.70	2.4	0.9	7	182	18	0.47
80	930	1953 27.94	40-20.09	112-15.73	7.0*	0.8	9	144	18	0.76

number of events = 3

* indicates poor depth control
W indicates Wood-Anderson data used for magnitude calculation

Blasts 10 km From Promontory Point

yr	date	orig time	lat-n	long-w	depth	mag	no	gap	dmn	rms
65	925	57 11.72	41-12.40	112-23.21	7.0*	2.3	5	300	66	0.58
75	610	2104 47.52	41-12.80	112-25.94	1.4	1.0	8	177	10	0.26
83	608	1802 19.92	41-12.96	112-25.17	0.0	1.0	16	168	19	0.31
83	627	157 24.46	41-12.14	112-24.27	2.5	1.0	12	197	21	0.28
83	1023	16 17.86	41-12.50	112-24.42	1.2	0.7	23	138	20	0.27
83	1209	2017 35.61	41-14.94	112-24.54	0.8	0.9	15	158	15	0.33
83	1217	2226 24.32	41-15.35	112-23.60	1.3	1.1	18	159	15	0.36
84	314	2301 20.97	41-15.64	112-21.94	1.9	0.8	13	164	14	0.34

number of events = 8

* indicates poor depth control
W indicates Wood-Anderson data used for magnitude calculation

Blasts 20 km From Tooele Army Depot

yr	date	orig time	lat-n	long-w	depth	mag	no	gap	dmn	rms
62	914	30 1.32	40-28.14	112-14.48	7.0*	1.5	7	154	46	0.39
74	227	1835 10.59	40-36.18	112-30.53	7.0*	1.6	4	243	52	0.14
74	315	2019 39.48	40-27.15	112-28.92	7.0*	1.6	4	213	40	0.21
74	429	2023 28.69	40-32.41	112-39.81	7.0*	1.8	4	220	40	0.05
74	429	2026 35.79	40-23.97	112-27.87	7.0*	1.8	4	163	37	0.34
74	429	2029 15.11	40-30.36	112-29.46	7.0*	1.8	4	187	44	0.11
74	429	2032 6.75	40-29.57	112-29.43	7.0*	1.8	4	222	43	0.43
74	429	2034 49.53	40-27.37	112-28.79	7.0*	1.8	4	213	40	0.39
74	429	2037 42.67	40-30.52	112-31.09	7.0*	1.8	3	228	42	0.
74	1206	1946 35.18	40-34.37	112-30.55	7.0*	1.6	3	261	37	0.
74	1206	1951 36.64	40-32.06	112-29.54	7.0*	1.5	3	251	34	0.
74	1224	1858 18.09	40-38.07	112-29.84	7.0*	1.7	3	259	55	0.
75	225	1717 48.97	40-30.90	112-29.57	7.0*	1.2	7	224	30	0.29
75	1103	1820 26.51	40-39.16	112-33.05	7.0*	0.7	6	165	20	0.35
76	207	418 29.66	40-38.81	112-33.84	7.0*	1.1	12	166	31	0.21
76	302	1947 55.48	40-30.81	112-29.55	7.0*	1.1	7	146	30	0.24
76	302	2038 56.60	40-30.52	112-29.53	7.0*	1.2	7	145	30	0.32
76	423	1829 41.02	40-38.91	112-34.38	7.0*	1.3	10	167	21	0.47
76	520	2159 21.31	40-39.15	112-33.19	7.0*	1.3	6	165	20	0.18
76	903	2136 8.95	40-39.51	112-34.20	2.1	1.1	7	173	20	0.30
76	915	1734 41.26	40-39.36	112-33.36	7.0*	1.9	6	184	45	0.40
76	1105	2313 13.28	40-39.63	112-33.49	7.0*	1.1	14	166	27	0.45
76	1209	313 45.18	40-39.11	112-31.83	7.0*	0.8	5	159	28	0.26
77	110	2227 45.68	40-38.42	112-31.13	7.0*	0.7	6	144	29	0.20
77	126	1307 28.01	40-39.15	112-34.73	7.0*	1.1	12	167	29	0.36
77	309	2325 49.60	40-37.66	112-33.33	7.0*	0.5	6	163	31	0.17
77	311	2244 7.22	40-29.61	112-29.03	7.0*	1.1	7	130	32	0.23
77	311	2250 46.99	40-30.77	112-28.99	7.0*	1.2	6	139	30	0.22
77	315	1318 13.68	40-38.79	112-33.81	7.0*	1.1	8	165	29	0.25
77	331	359 23.12	40-39.05	112-34.17	7.0*	0.8	13	150	29	0.28
77	405	232 22.78	40-37.21	112-32.29	7.0*	0.9	8	145	32	0.17
77	429	624 28.33	40-39.44	112-33.28	7.0*	1.2	11	148	28	0.33
77	504	2307 6.95	40-37.36	112-34.21	7.0*	1.2	15	149	32	0.29
77	623	2221 6.30	40-39.49	112-33.06	7.0*	0.7	5	164	28	0.33
77	721	2020 46.36	40-33.13	112-34.11	7.0*	1.2	5	194	39	0.18
78	124	1436 30.48	40-39.66	112-33.60	7.0*	0.7	7	169	27	0.28
78	501	2109 51.43	40-27.43	112-16.66	1.3	0.9	5	281	14	0.20
78	510	2114 36.54	40-37.61	112-27.53	7.0*	0.8	3	145	18	0.
78	906	1924 9.81	40-23.56	112-19.89	13.9	0.7	9	292	20	0.36
78	1119	1736 33.03	40-35.46	112-18.54	7.0*	1.3	5	331	13	0.17

Blasts 20 km From Tooele Army Depot

yr	date	orig time	lat-n	long-w	depth	mag	no	gap	dmn	rms
80	1114	1726 58.33	40-24.22	112-16.40	7.0*	1.6	11	216	47	0.49
81	902	2035 21.65	40-27.45	112-19.72	0.3	1.5	8	209	49	0.43
87	327	138 2.92	40-29.05	112-30.34	8.1	1.1	9	140	33	0.24

number of events = 43

* indicates poor depth control
W indicates Wood-Anderson data used for magnitude calculation

Blasts 20 km from USAF Disposal

yr	date	orig time	lat-n	long-w	depth	mag	no	gap	dmn	rms
64	627	1953 28.33	41-10.24	113-12.89	7.0*	1.9	5	259	113	0.37
75	814	1617 59.85	41- 8.74	112-54.30	7.0*	1.5	8	200	43	0.27
75	1231	2116 13.77	41-13.97	112-53.40	7.0*	1.2	13	200	44	0.31
76	116	1537 58.83	41-13.35	112-52.32	7.0*	1.2	13	198	43	0.21
76	213	2105 31.26	41-13.57	112-52.78	7.0*	1.1	7	199	43	0.22
76	324	1747 39.51	41-14.15	112-54.53	7.0*	1.2	12	202	45	0.26
76	330	1953 16.68	41- 8.82	112-55.76	7.0*	1.1	11	202	51	0.51
76	409	2228 25.31	41-13.32	112-52.77	7.0*	1.3	7	199	43	0.05
76	525	1658 57.97	41-12.88	112-52.31	7.0*	1.6	8	217	43	0.22
76	608	1746 48.69	41-13.82	112-53.18	7.0*	1.2	11	200	43	0.24
76	708	2004 29.99	41-13.18	112-52.31	7.0*	1.4	12	198	43	0.19
76	730	1954 5.93	41-13.69	112-53.39	7.0*	1.2	8	200	44	0.25
76	908	2052 41.95	40-56.45	112-58.75	7.0*	1.5	12	236	84	0.39
76	910	1624 9.89	41-13.27	112-52.17	7.0*	1.2	7	198	57	0.21
76	910	2038 29.17	41- 8.44	112-59.13	7.0*	1.9	9	207	106	0.24
76	1111	1959 17.22	41-13.33	112-52.73	7.0*	1.0	10	225	43	0.27
76	1119	2000 2.99	41-13.35	112-52.58	7.0*	1.4	12	190	43	0.20
76	1208	1617 43.28	41-12.74	112-54.18	7.0*	0.9	8	234	45	0.17
76	1215	2213 28.41	41- 8.68	112-54.01	7.0*	1.6	13	192	42	0.26
77	125	2048 6.46	41-13.71	112-54.45	7.0*	0.8	10	202	45	0.17
77	127	1749 17.52	41-13.30	112-54.04	7.0*	0.5	7	193	45	0.27
77	302	1808 40.25	41-13.05	112-51.80	7.0*	0.8	11	189	42	0.18
77	329	2220 47.21	41-12.93	112-53.31	7.0*	0.6	9	226	44	0.13
77	404	2041 30.19	41-13.42	112-52.05	7.0*	0.6	9	189	42	0.25
77	427	2011 46.47	41-13.08	112-54.76	7.0*	1.2	9	195	46	0.13
77	729	1600 58.80	41-13.45	112-54.76	7.0*	1.1	11	202	46	0.28
77	1018	2209 47.39	41- 8.96	112-50.16	7.0*	1.2	9	252	38	0.20
83	1203	42 47.33	41-13.89	112-54.07	7.3	1.3	18	193	44	0.35
85	207	2227 38.85	41- 7.86	112-54.86	4.3	1.6	17	194	51	0.26
86	422	6 24.82	41- 5.84	113- 1.12	6.8	1.4	12	191	83	0.31
86	521	1839 13.25	41- 2.51	112-50.18	0.7	1.3	8	205	52	0.42
86	611	2009 39.13	41- 5.18	113- 1.07	0.8	2.1	17	199	46	0.26
86	628	351 7.78	41- 5.34	113- 0.84	1.9	2.2	21	204	46	0.26
86	1112	2204 18.41	41-12.81	112-54.35	1.8	1.1	10	232	46	0.20
86	1114	1813 4.79	41- 5.56	113- 0.83	4.7	2.0	17	204	48	0.24

number of events = 35

* indicates poor depth control
W indicates Wood-Anderson data used for magnitude calculation

APPENDIX C.

Earthquake Listings for Events in the Near-Site Region

1) Pre-Network Earthquakes (Pre-July 1962)

2) Post-Network Earthquakes (July 1962 - March 1987)

Historical Earthquakes 70 km From SSC Site Midpoint

yr	date	orig time	lat-n	long-w	mag	int	comments
1915	811	1020	40-30.00	112-39.00	4.3I	5	INT=5-8,LOC ASSUMED (1)
1958	105	1700 04.00	41- 0.	112-30.00	3.0X	0	(6)

number of earthquakes = 2

* indicates poor depth control
W indicates Wood-Anderson data used for magnitude calculation

Earthquakes 70 km From SSC Side Midpoint

yr	date	orig time	lat-n	long-w	depth	mag	no	gap	dmn	rms
64	326	2201 47.41	40-50.60	113-49.50	7.0*	2.4	5	223	112	0.78
64	627	2310 39.15	41-15.84	113-10.09	7.0*	2.4	7	259	122	0.44
65	1029	1851 51.49	41- 1.24	113-28.43	7.0*	2.5	6	189	107	0.05
66	417	958 51.34	41-16.97	113-27.35	7.0*	2.0	7	203	132	0.52
67	216	1921 35.19	41-16.40	113-20.03	7.0*	4.0W	10	199	127	0.60
67	721	1527 57.49	41-15.85	113-17.91	7.0*	3.6W	8	198	125	0.28
70	1008	601 59.76	40-50.27	112-15.58	7.0*	2.1	8	234	35	1.10
75	104	850 8.30	40-39.61	112-46.14	7.0*	1.2	5	315	61	0.12
75	204	1540 29.56	40-19.42	113- 6.52	7.0*	1.7	5	321	28	0.16
75	610	933 48.25	40-32.45	112-51.90	7.0*	1.2	11	210	38	0.16
75	616	2001 4.02	40-41.89	112-18.45	7.0*	0.9	6	134	9	0.06
76	330	1500 2.26	40-29.61	112-51.96	7.0*	0.7	10	209	33	0.28
76	1019	1651 33.68	40-43.29	112-43.12	7.0*	0.8	7	213	27	0.09
76	1023	1503 22.96	40-40.34	112-49.89	7.0*	1.3	10	206	38	0.17
77	311	2246 16.30	40-21.33	112-44.38	7.0*	0.9	6	174	18	0.30
79	327	1545 49.59	40-12.76	113-17.44	7.0*	1.1	12	201	40	0.37
79	329	1017 15.75	40-28.84	113-12.55	7.0*	2.2	28	264	76	0.40
79	1115	1229 47.61	40-52.01	112-55.04	7.0*	2.0	20	193	34	0.41
80	1014	1138 59.67	40-40.10	113-47.85	7.0*	2.1	16	233	98	0.40
81	711	1120 16.81	40-27.44	113-11.71	6.1	1.7	21	181	43	0.19
81	1024	18 1.54	40-21.54	112-18.81	7.0	1.5	8	267	49	0.11
82	822	2009 27.61	40-17.19	112-46.82	3.5	2.3	23	175	10	0.36
82	1124	1757 17.17	40-44.02	112-13.68	5.1	1.9	33	90	7	0.23
82	1128	411 24.22	40-58.62	112-29.21	6.3	0.8	9	168	6	0.27
84	1119	831 15.54	40-51.48	112-31.94	9.1	0.4	16	171	7	0.29
86	1018	44 18.71	41-15.52	113- 6.89	2.2	1.3	12	219	60	0.20

number of earthquakes = 26

* indicates poor depth control
W indicates Wood-Anderson data used for magnitude calculation